THESIS

M.Sc. (PHYSICS)

LIBRARY
UNIVERSITY OF SCIENCE AND TECHNOLOGY

# RADON GAS MEASUREMENT IN DEEP GOLD MINES

DAVID NII AMOO DODOO-AMOO

(FORMER NAME: DAVID NII AMOO)

DEPARTMENT OF PHYSICS

UNIVERSITY OF SCIENCE AND TECHNOLOGY

KUMASI

FEBRUARY 1994

# RADON GAS MEASUREMENT IN DEEP GOLD MINES

A THESIS SUBMITTED TO THE

FACULTY OF SCIENCE

UNIVERSITY OF SCIENCE AND TECHNOLOGY

KUMASI

IN PARTIAL FULFILLMENT OF THE REQUIREMENT

OF THE DEGREE OF

M.Sc (PHYSICS)

LIBRARY
UNIVERSITY OF SCIENCE AND TECHNOLOGY

BY

DAVID NII AMOO DODOO-AMOO

(FORMER NAME: DAVID NII AMOO)

SUPERVISOR : DR. ABA A. BENTIL ANDAM.

FEBRUARY 1994

# ACKNOWLEDGEMENTS

It is a pleasure for me to express my profound gratitude and a special indebtedness to my project supervisor, Dr. Aba A. Bentil Andam for her assistance, instruction and critical suggestions pertinent to the selection of the project work and publication of the write up.

My personal acknowledgement and thanks to the management of Tarkwa Goldfields Limited and Prestea Goldfields Limited, for their permission into the mines. The following merit special mention and my thanks: Mr. Solomon Empeh, the underground manager of Tarkwa Goldfields and Mr. G.B. Mintah, the chief geologist of Prestea Goldfields, for their supervision into the underground.

I am also grateful to the Head of Department and all members of staff of the Department of Physics, U.S.T, Kumasi for their invaluable help and advice.

Finally, to my wife, Mrs. Regina Dodoo-Amoo, for her encouragement during the project work, and all the glory must be to the Almighty God for the completion of the work.

UNIVERSITY OF SCIENCE AND TECHNOLOGY

# ABSTRACT

Measurements of radon gas concentration in the two western region gold mines in Ghana have been carried out. The measurements were made from the alpha-track density on CR-39 solid state nuclear track detector, using the closed can technique during 1992 and 1993.

Average values of 37.5Bqm$^{-3}$ and 48.6Bqm$^{-3}$ were recorded in the offices for Tarkwa and Prestea Goldfields respectively.

There were large variations in the underground results which range from 56.4Bqm$^{-3}$ to 268.3Bqm$^{-3}$ for Tarkwa Goldfields and from 42.6Bqm$^{-3}$ to 877.7Bqm$^{-3}$ for Prestea Goldfields. These were observed to be caused by the different rock formation and the ventilation at the sites of the measurements.

Radon exposure units in Working Level (WL) and the Working Level Month (WLM) were also calculated for the mines.

These results show that the radon concentrations at the offices at Tarkwa and Prestea are below the maximum safe of 110Bqm$^{-3}$ as recommended by National Radiological Protection Board, (NRPB) UK. However, sixteen (16) out of the twenty five (25) underground locations monitored in the two gold mines have radon concentrations above the recommended limit.

# CONTENTS


| | PAGE |
|---|---|
| TITLE PAGE | 1 |
| ACKNOWLEDGEMENTS | 3 |
| ABSTRACT | 4 |
| CHAPTER ONE | |
| 1.0 GENERAL INTRODUCTION | 9 |
| 1.1 : The Natural Radiation Environment | 9 |
| 1.2 : The Natural Radioactive Series of Uranium | 13 |
| 1.3 : Radon in the Mining Environment | 16 |
| 1.4 : Detection and Measurement of Radon Gas | 18 |
| 1.5 : Radon Exposure Terms | 19 |
| 1.6 : Control of the Mine Environment | 22 |
| 1.7 : Health Effects and Standards | 24 |
| CHAPTER TWO | |
| 2.0 THEORETICAL BACKGROUND OF ETCHED NUCLEAR TRACK | 27 |
| 2.1 : Solid State Nuclear Track Detection | 27 |
| 2.1.1 : History of the Solid State Nuclear Track Detection | 27 |
| 2.1.2 : General Principles Behind Nuclear Track Formation | 28 |

2.2 : Track Formation 29

2.2.1 : Criteria for Track Formation 29

2.2.2 : The Ion-Explosion Spike Model 30

2.3 : Track Etching: — Geometry 32

2.4 : The CR-39 Polymer Track Detector 37

2.5 : Tarkwa and Prestea Goldfields 38

2.5.1 : General Geological Features of Tarkwa and Prestea Goldfields 38

2.5.2 : The Underground and Surface Environment of the Goldfields 43

CHAPTER THREE

3.0 EXPERIMENTAL PROCEDURE 48

3.1 : Measurement of Radon Gas 48

3.1.1 : Radon Gas: — Underground Measurements 48

3.1.2 : Radon Gas: — Ground Level Measurements 49

3.2 : Measurement of the Physical Parameters 68

3.2.1 : Techniques of Measuring the Air Velocity 68

3.2.2 : Temperature and Humidity Measurement 71

3.3 : Chemical Etching Process and the Counting Technique 73

3.3.1 : Etching Procedure 73

3.3.2 : The Counting Technique 75

3.4 : Experimental Errors 76

3.4.1 : Errors in the Track Counting Technique 76

3.4.2 : Errors in Measuring the Radon Gas 77

3.4.3 : Errors in Measuring the Physical Parameters 77

CHAPTER FOUR

4.0 EXPERIMENTAL RESULTS 79

4.1 : The Track Density and the Calibrated Factor for CR-39 Plastic 79

4.2 : Calculation of Radon Exposure Terms 80

4.2.1 : The Becquerel per cubic metre 80

4.2.2 : The Calculation of the Working Level, the Working Level Month and the Sievert. 81

a : Results from the Radon Measurement — Tarkwa Goldfields 82

b : Results from the Radon Measurement — Prestea Goldfields 90

4.3 : Results from the Measurement of the Physical Parameters 101

4.3.1 : Airflow Rate Results 101

a : Tarkwa Measurement 101

b : Prestea Measurement 103

4.3.2 : Temperature and Humidity Results 104

a : Tarkwa Measurement 104

b : Prestea Measurement 105

UNIVERSITY OF SCIENCE AND TECHNOLOGY LIBRARY

4.4 : Graphical Representations of the Underground Measurements 106

4.4.1 : The Variations of the Radon Concentration with the Physical Parameters 106

4.4.2 : Deductions from the Graphs 111

CHAPTER FIVE

5.0 DISCUSSION AND CONCLUSION 114

5.1 : Discussion 114

5.2 : Conclusion and Suggestions for Further Work 118

APPENDIX 121

REFERENCES 127

# CHAPTER ONE

# 1.0 GENERAL INTRODUCTION

## 1.1 THE NATURAL RADIATION ENVIRONMENT

Many people are anxious about releases of radioactive materials into the environment and their possible consequences for humanity. Yet throughout history people have lived in a changing radiation environment. Human interaction with this environment and the resulting modifications underscore the dynamic of change: today's radiation environment differs from that of yesterday, and will be continuously transformed in the future.

In fact, it is virtually impossible for people to avoid exposures to radiation from their living, and working environment, although some people are more exposed than others because of their type of dwelling, work, lifestyle and the level of medical cure they receive.

Natural sources of radiation deliver the highest radiation dose that people normally receive. (Fig.1.1.) The average annual dose from natural sources is approximately 2.4mSv [1]. This value is used here as the reference level of natural background radiation. Hidden within this

statistical average are individual doses that range from 1.0 to 5.0mSv a year, in extreme cases to 1Sv or more. [1]

The two major natural radiation sources are the cosmos, which irradiates people continuously with cosmic rays, and the earth's biosphere, comprising radionuclides that have existed mainly in the earth's crust for billions of years. The distinction is important, as terrestrial radiation is by far the largest source of natural irradiation contributing as much as 85% to the average annual dose [2]. Terrestrial radiation can be found throughout the environment at various levels, depending on the activity concentration in such natural materials as rocks, soils, water, air, food and even the human body. The most important terrestrial sources are Potassium-40, Rubidium-87 and the two series of radioactive element arising from the decay of Uranium-238 and Thorium-232. Other radionuclides, such as those in the Uranium-235 decay, series, have little effect on total radiation exposures.

LIBRARY
UNIVERSITY OF SCIENCE AND TECHNOLOGY

# NATURAL RADIATION ENVIRONMENT

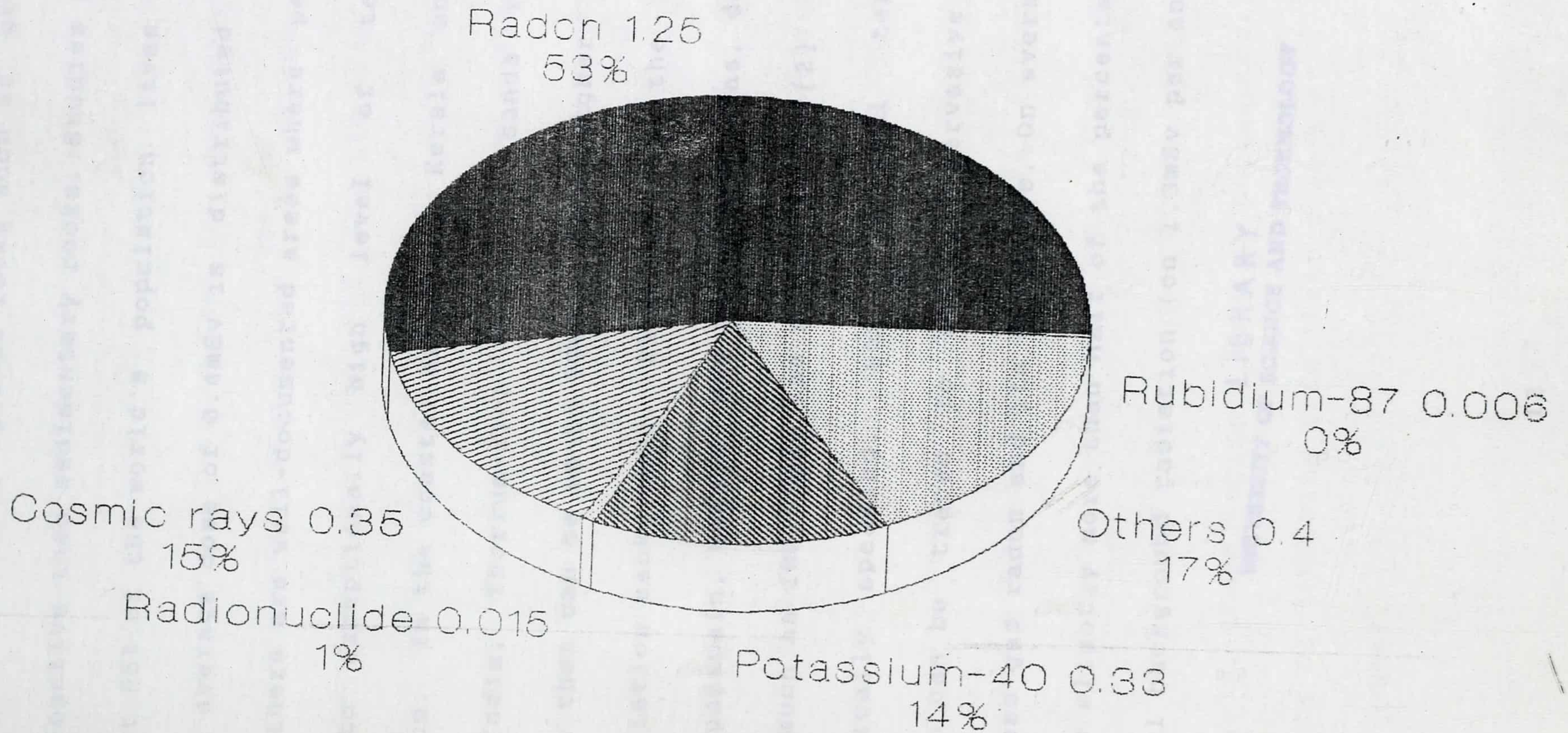


**Fig.1.1: Estimated Annual Doses Per Head From Natural Sources in millisieverts [SOURCE 2]**

The radioactivity in certain rocks and soils is the main source of terrestrial irradiation to people everywhere. Generally, igneous rocks such as granite are more radioactive than sedimentary rocks. Studies have shown that about 95% of the world's population lives in areas where the average dose of 0.4mSv is distributed normally. Even so, there are well-documented areas where people are exposed to exceptionally high level of terrestrial irradiation. In the coastal areas of Kerala and Tarnil Naolu in India, Thorium-rich menazire sands result in dose rates that can be up to 1000 times higher than the normal radiation background. Elsewhere, in the Brazilian areas of Guazapain, Meaipe, and Pocos de Caldas, dose rates can be as much as 100 times the normal level [2]

Practically speaking, most internal terrestrial irradiation can be traced to one all-pervasive source: the odourless gas radon and its daughters. On average radon constitutes slightly more than half of the percentage dose from natural background radiation (on 1.3mSv per annum).[2]

LIBRARY
UNIVERSITY OF SCIENCE AND TECHNOLOGY

## 1.2 THE NATURAL RADIOACTIVE SERIES OF URANIUM

The naturally occurring radionuclides can be divided into two types. The first type are those produced by cosmic rays and radionuclides of terrestrial origin. The second type are those elements found in natural sources and which have atomic numbers greater than 83. These belong to three distinct radioactive series: viz $^{238}U$ $^{232}Th$ and $^{235}U$. These three chains are shown in Fig 1.2 to Fig 1.4. These long-lived parent elements are widely distributed in the Earth's crust and account for much of the radioactivity to which man is exposed. In each of the three chains there is an isotope of element number 86; $^{222}Rn_{86}$, $^{220}Rn_{86}$ and $^{219}Rn_{86}$. These are radon ($t_{1/2}$ 3.82 days), thoron ($t_{1/2}$ 54sec. and actinon ($t_{1/2}$ 3.92sec.) respectively. After their formation in soils, rocks, etc. they can diffuse into the surrounding environment. Radon-222 , with the longest half-life has a greater probability to escape into the environment before undergoing decay than Thoron and Actinon. With half-life of 54sec. and 3.92sec. respectively, these isotopes have a corresponding smaller probability of diffusing from their places of origin into the environment.

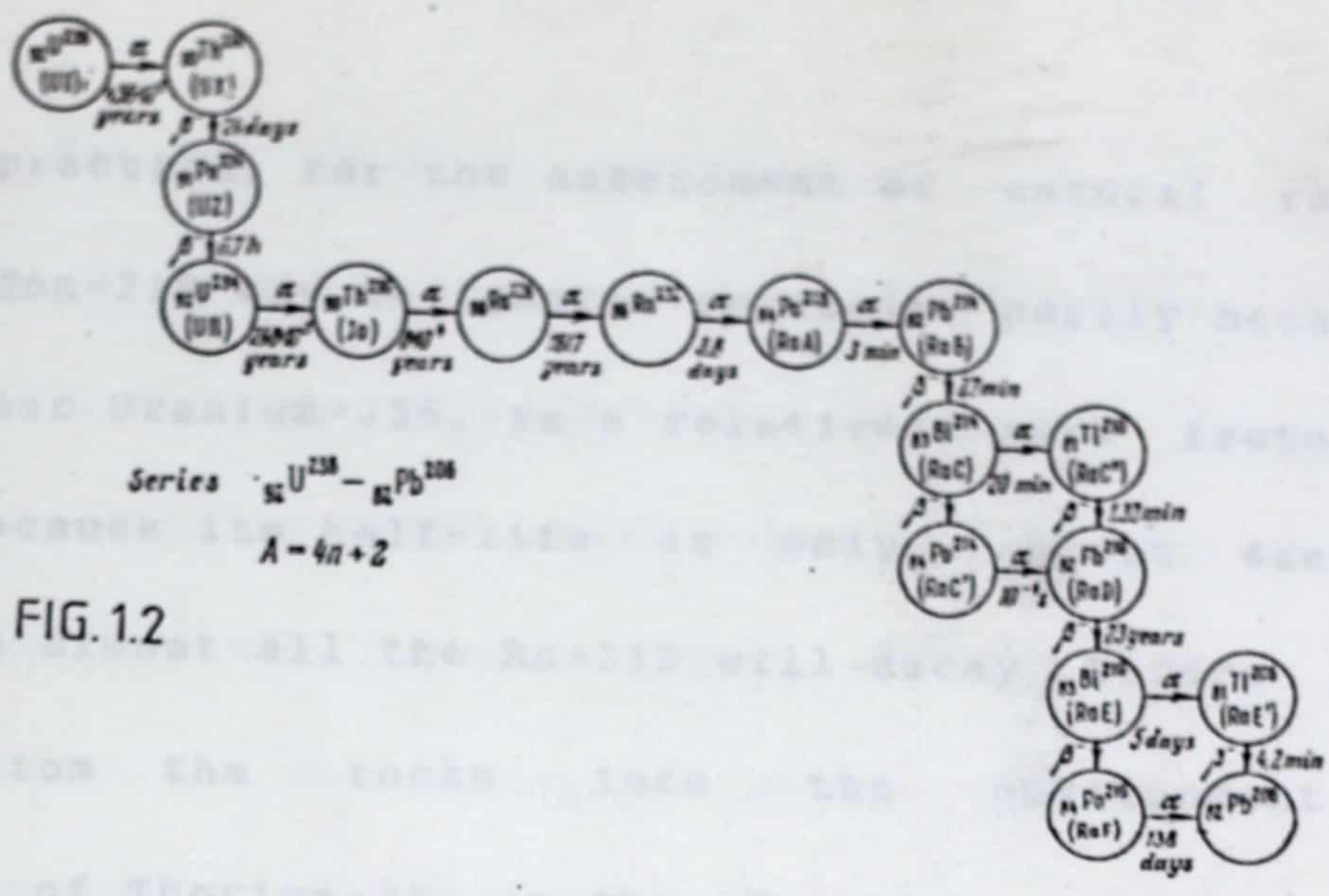


FIG. 1.2

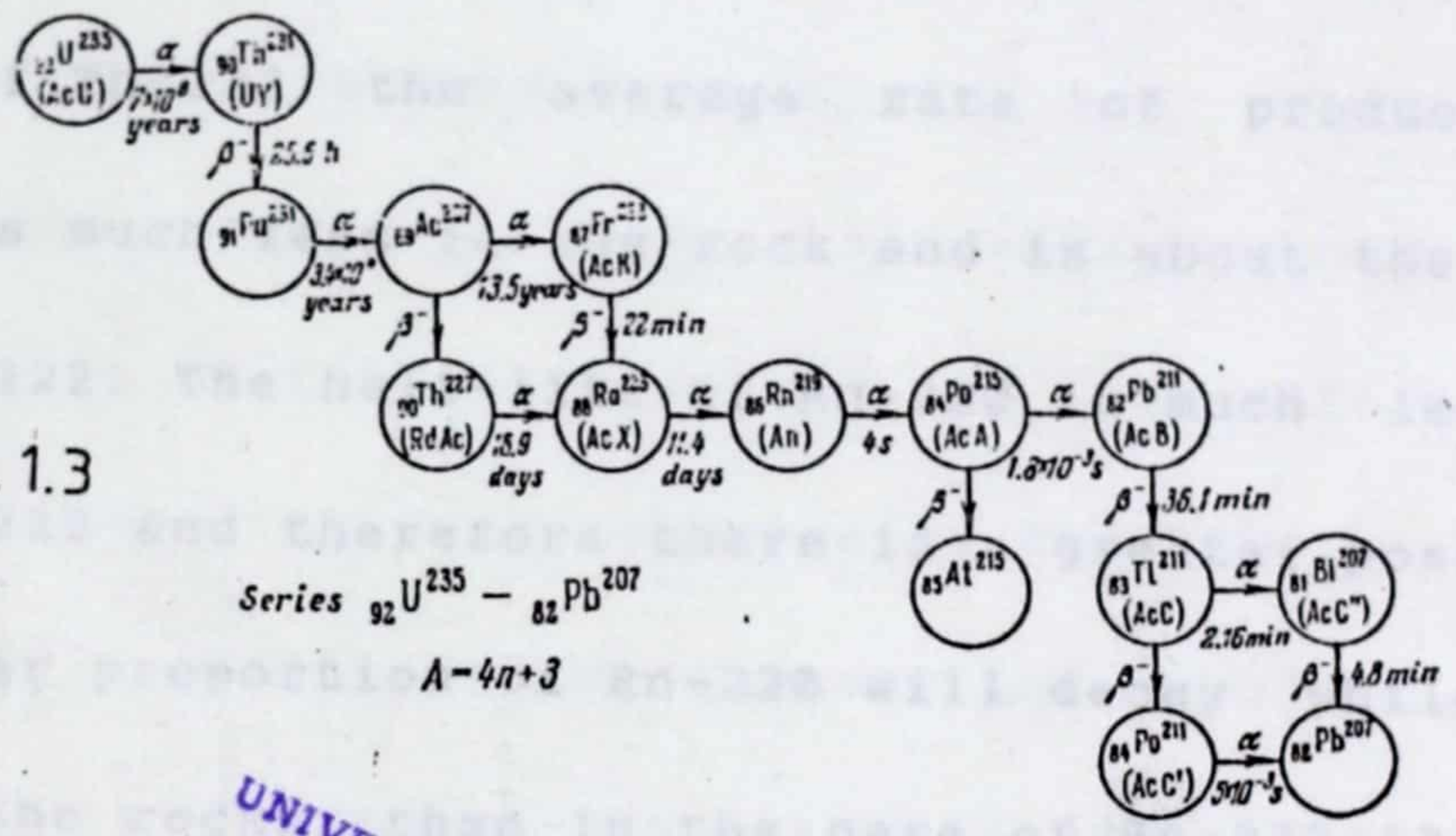


FIG. 1.3

UNIVERSITY OF SCIENCE AND TECHNOLOGY
LIBRARY

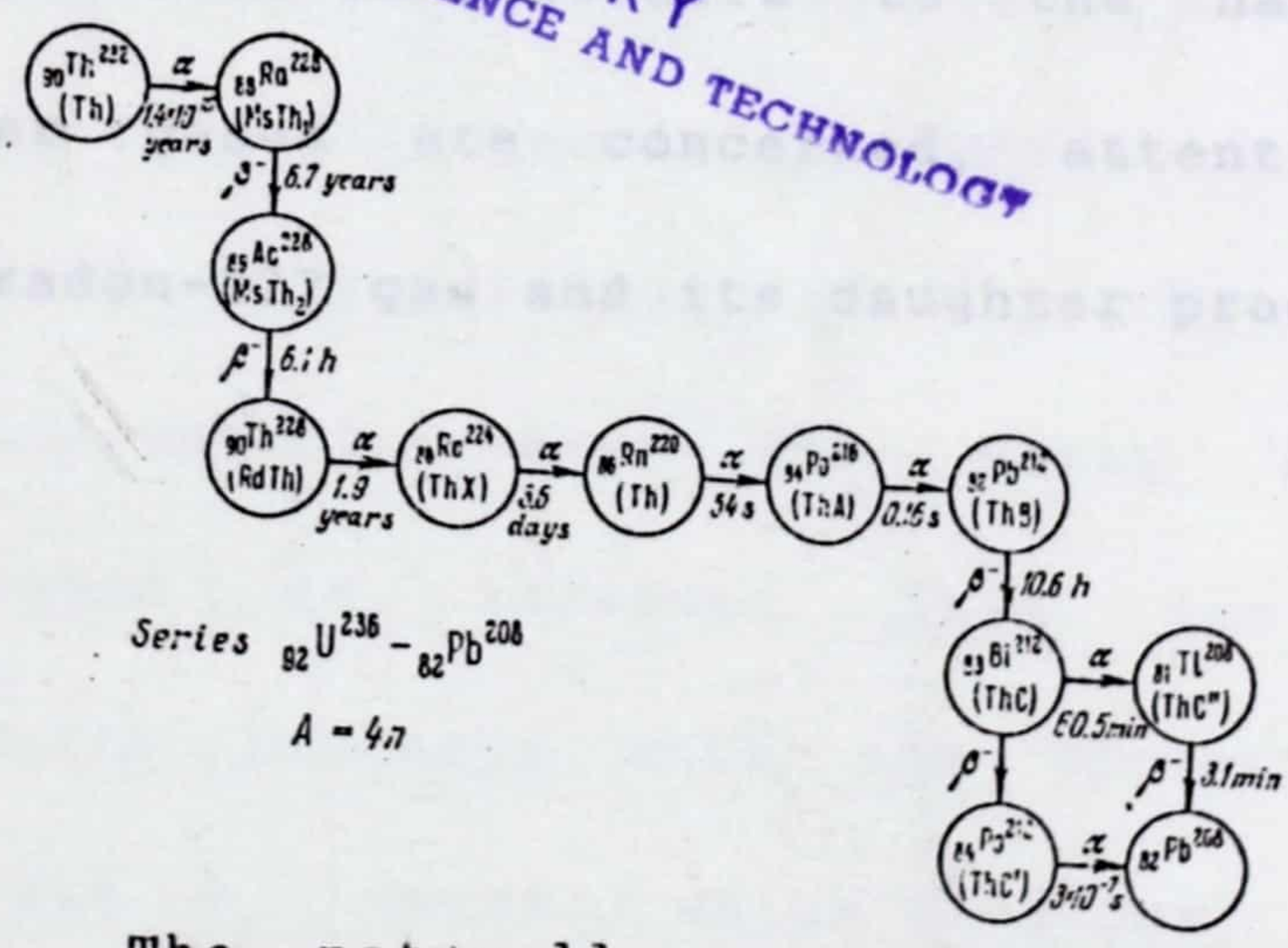


FIG. 1.4

Fig. 1.2 - Fig. 1.4, The naturally occurring radioactive chain series of Uranium-238, Uranium-235 and Thorium-232. SOURCE [17]

In practice, for the assessment of natural radiation dose, Radon-219 may be ignored entirely, partly because its fore-runner Uranium-235, is a relatively rare isotope and partly because its half-life is only about 4sec. and therefore almost all the Rn-219 will decay before it can escape from the rocks into the environment. The abundance of Thorium-232 in the Earth's crust is higher than that of uranium-238 but because of the longer half-life of Th-232 the average rate of production of radon-220 is much less in the rock and is about the same as that of Rn-222. The half-life of Rn-220 is much less than that of Rn-222 and therefore there is a greater possibility that a higher proportion of Rn-220 will decay while still trapped in the rocks, than in the case of Rn-222 [3]. Thus, as far as the exposures of mine workers to the naturally occurring $\alpha$-emitter gases are concerned, attention is focused mainly on radon-222 gas and its daughter products.

## 1.3 RADON, IN THE MINING ENVIRONMENT

Radon is a colourless, odourless radioactive material in the form of a gas at room temperature. Its density is $9.96 kgm^{-3}$, which is about seven times higher than that of air. Its melting and boiling points are $-71.0^{\circ}C$ and $-61.8^{\circ}C$ respectively. Its solubility in water is about 28% and varies inversely with temperature.

Radon is the last family in the table of the noble elements which lie between true metals and non-metals in the periodic table. These elements exhibit some characteristics of both true metals and non-metals. Radon is therefore expected to be chemically reactive.

Radon-222, which is a radioactive product of the disintegration of radium-226, is found excessively in uranium mines, and is also present in measurable amounts in other type of mines including coal, phosphate and gold mines [4]. Radon diffuses from the surrounding rock strata into the mine environment, where its decay process continues. Once radon is released into the mine surroundings, the decay proceeds with the formation of radium A (Polonium-218 $t_{1/2}$ 3mins), which produces radium C′ (Polonium-214 $t_{1/2}$ $10^{-4}$sec and so on Fig 1.2. These radon-daughter products are atoms of solid matter having

relatively short half-lives. It is the short-lived $\alpha$-particles and potential $\alpha$-emitters such as radon and its daughters (Po-218 and Po-214 ) that are of prime concern as potential health hazards.

In Ghana, as far as available records show no systematic measurement of radon gas in mines has been made in Ghana. A small pilot study was conducted at Ashanti Goldfield Corporation in 1990 and 1991 by researchers from University of Science and Technology, Kumasi. The highest of 250Bqm$^{-3}$ in a region of metavolcanic rocks at the Adansi shaft and 347Bqm$^{-3}$ in graphitic schist, graywacks and dyke rocks formation, at Ayeinm shaft were measured in that study.[5,6]

Underground water can accumulate and transport radon generated within the Earth's crust and will be a significant source of radon in the mines, if this water that is collected is held-up for a long time in the drives. Because water-bearing rock units (aquifers) are so varied in their uranium and radium concentration the radon concentration in the water is highly variable.

Environmental parameters that can influence the exhalation rate of radon into the atmosphere include:

i. wind speed (airflow rate)

ii. moisture content

iii. barometric pressure

iv. temperature and

v. relative humidity.

The influence of these parameters on the exhalation rate of radon from soil and rock is not always clear. Schery and Petschek [7] found pressure to be more important than surrounding temperature and wind speed. Parson [8] found variation in radon emanation with changes in pressure, temperature and relative humidity. Radon exhalation was found to increase linearly with increases in wind speed.[9]

The above parameters relate to surface variation of radon with no regard to underground variation.

## 1.4 DETECTION AND MEASUREMENT OF RADON GAS

Quantitative measurement of radon and its daughter product concentration is essential for the assessment and control of radiation exposure to the general public.

The following methods for the detection of radon gas are more commonly used: the cloud, the bubble and the spark chambers. These detectors have the disadvantage of being bulky. Analysing these chamber pictures is an enormous task, requiring large human and computing resources. Others

are the nuclear emulsions, and scintillation method. The simplest of all these detectors is the etchable Solid State Nuclear Track Detector (SSNTD).

The simplicity of the SSNTD technique, which goes hand in hand with the fact that it is inexpensive and is limited only by the ingenuity and resourcefulness of the researcher, has led to widespread excitement and interest in fundamental research on SSNTDs. There is hardly any branch of science and technology now where it does not have actual potential application.

The SSNTDs are very durable, pose no great handling problem, and are not fogged by exposure to light or affected by moderate degree of heating. Their simplicity and durability makes them particularly valuable for remote use, such as in high-altitude balloon exposure to cosmic rays, and their robustness enables them to be used in personnel dosimetry. They have the extra advantage of retaining their record after readout.

## .5 RADON EXPOSURE TERMS

If the total ionization produced in air by radioactivity is measured, the largest ionizing component will be radon.

Radon is considered as less important biologically than its short-lived radon daughters. To cope with this problem the concept of working level (WL) was developed. Polonium-218 and Polonium-214 are two of the immediate decay products of radon and are alpha particle emitters (Fig.1.2), which are more dangerous to health than other types of radiations such as X-ray or gamma rays. These decay products tend to adhere to dust particles (referred to as "plateout"). If these particles or the unattached progeny are inhaled, they undergo further radioactive decay and irradiate the surrounding tissue before the body's lung clearance mechanisms can remove them.

Because it is the radon daughters that pose the greatest radiological risk, it has been useful to characterize radon daughter concentration in terms of the total alpha energy emitted as a result of decay of the short-lived daughters to Lead-210. This "potential alpha energy concentration" (PAEC) is an indicator of potential dose to the lung. The conventional unit for PAEC is the working level (WL) which was introduced in 1957 by Holaday et al [16], and is defined thus;

One WL is any combination of the short-lived decay products of radon ($^{218}Po$, $^{214}Pb$, $^{214}Bi$ and $^{214}Po$)

in one litre of air that will result in the ultimate emission by them of $1.30 \times 10^5$ MeV of alpha particle energy.

The WL is defined only in terms of alpha radiation because the beta and gamma rays emitted by $^{214}Pb$ and $^{214}Bi$ make a negligible contribution to the radiation dose in the lung. Radiation dose in the lung is mainly due to alpha particles emitted by $^{218}Po$ and $^{214}Po$ (see appendix D). One WL unit is equivalent to 100pCi/l of radon only in a special case when the radon is in equilibrium with its short-lived decay products. But the unit is used for any mixture of radon daughters and is independent of their state of equilibrium. The associated exposure unit, the working level month (WLM) is the exposure that an individual would experience remaining in 1WL of the daughters for 170hours (an average working month). WLM is a cumulative measure of exposure that is calculated by multiplying the average working level of exposure during a given time period by the time of exposure and dividing by 170 (the number of working level hour per working-level month).

Sievert is the S.I unit for dose equivalent. It is the absorbed dose weighed to take into account different types

of ionizing radiation and their energies. In practice, these quantities are expressed as rate (eg μSv/hr). If the rate is summed up over time, the resulting quantity is generally called commitment. (See appendix E)

## 1.6 CONTROL OF THE MINE ENVIRONMENT

Excavation under normal circumstances can be fraught with environmental problems and hazards. In underground mining, the most critical aspect of the environment to control is the atmosphere of the working places. It is in fact the mainstay of the miner's life support system.

To the mining engineer, ventilation tends to be the environmental care-all. It is the air-conditioning process relied upon to accomplish most environmental control underground. Ventilation is the control of air movement, its amount and direction. As the principal means of airflow control, it is one of the constituent processes of total air conditioning, i.e the simultaneous control within prescribed limits of the quality, quantity, and temperature-humidity of air. Ventilation therefore is not the only total-air conditioning process, nor is it adequate alone to satisfy all mine environmental objectives.

In underground mining as in surface industry,

environmental objectives require that the air is conditioned to meet quality and temperature-humidity objective as well as quantity. Although threshold limits are based on human safety and tolerance, increasing concern is being expressed for standard of human comfort as well. Workers productivity and job satisfaction correlate closely with environmental quality.

The rate of diffusion of gas into air is inversely proportional to the square root of the ratio of the densities of the gas and air or to the square root of its specific gravity. In other words, a gas lighter than air will diffuse faster than one heavier than air, and the smaller its specific gravity, the more rapidly the diffusion. Diffusion is aided by turbulence and temperature.

In the mine atmosphere, and particularly one that is stagnant or quiescent, stratification of gaseous impurities may occur. A heavy gas e.g (radon) will stratify against the bottom and a light one (hydrogen) near the roof. Convection currents, and the ventilation airstream, however, tend to promote the diffusion of any foreign gas that is introduced into the mine atmosphere. Once the gases have diffused they will not restratify. Whether a gaseous

impurity will be found stratified or diffused is a function of the relative rates of inflow and diffusion, air movement and temperature and geometry of the mine opening.[12]

Control of radiation was originally by dilution. Effort to seal off old working areas have been generally ineffective, unless these were vented to the surface and a forced ventilation system used. Filtering of ventilating air is used in many operations (using cloth filters and electrostatic precipitators) to remove the daughters. So far, it has not been possible to remove radon gas commercially, so the longer the air is in a mine and the greater the radon concentration, the quicker the build-up of daughters and the less the effectiveness of filtering.

## .7 HEALTH EFFECTS AND STANDARDS.

The main health risk associated with radon and its daughters stems primarily from inhalation of short-lived radon daughters and secondarily from the inhalation of radon itself, although the contribution by the latter is thought to be small. It has been estimated that when both radon and its daughters are inhaled only about 5% of the α-radiation received is contributed by radon. [9]

Exposure to excessive concentration of radon and its

daughters has been linked with a high incidence of lung cancer among underground miners in the U.S.A. [10]

It has been estimated that only a small fraction of the inhaled gas will enter the blood supply by direct absorption before being exhaled and only a small amount will decay while in the lung. Radon daughters attached to large aerosols may be deposited in the nose or pharynx. At this location, the daughters can be removed by ciliary action and be swallowed into the gastrointestinal tract. Radon daughters will most likely decay at the original place of deposition. Consequently, their energy and that of their subsequent short-lived daughters is transmitted to surrounding tissue. The cell just below the surface of the bronchii receive most radiation dose from radon daughters because this is where the reparable particles tend to concentrate.

Exposure to ionizing radiation can produce various deleterious effects on human health. Acute exposure to large doses can damage organs and can produce acute gastrointestinal or nervous symptoms, bleeding, cardiac distress, and possible death.

No one knows exactly how radon specifically or radiation in general causes cancer, just as no one knows

exactly how in some cases radiation cures cancer [13]. Doctors know only that radiation damages the cell it touches. It is known radon gas itself does not interact chemically with other elements in the atmosphere or in the human body [14]. For example, it does not poison the human body by interfering with the delivery of oxygen to the lungs like carbon monoxide can. The alpha radiation emitted during the decay of radon and its daughters is believed to be the root of radon-induced cancer.

Other non cancer effects attributed to exposure of radon and its daughters include the following: excess of liver cirrhosis, small increases in various kidney diseases, excess of cataracts, growth retardation, increase in benign cartilaginous tumors of bone, spinal cord defects, and chromosomal aberration. [11]

LIBRARY
UNIVERSITY OF SCIENCE AND TECHNOLOGY

# CHAPTER TWO

## 2.0 THEORETICAL BACKGROUND OF ETCHED NUCLEAR TRACKS

### 2.1 SOLID STATE NUCLEAR TRACK DETECTION

#### 2.1.1 HISTORY OF THE SOLID STATE NUCLEAR TRACK DETECTION

In 1958, D.A. Young, [18] working in the Atomic Energy Research Establishment at Harwell in England, discovered that LiF crystal, held in contact with a Uranium foil and irradiated with thermal neutrons, revealed a number of etch pits after treatment with a chemical reagent. The number of these pits showed complete correspondence with the estimated number of fission fragments which would have recoiled into the crystal from the Uranium foil. It seemed that each pit was formed around the site of solid-state damage produced by the fission fragments. In 1959 Silk and Barnes [19] also working at AERE, Harwell, reported direct observation of these damaged regions in mica —— which appeared as hair like tracks —— using transmission electron microscopy.

During the early 1960s Fleischer et. al. [20], working at the General Electric Research Laboratories at Schenectady, New York, pioneered the extensive development of this method. In particular, they extended the etching technique of Young (whose work was unknown to them at that

time) to mica and eventually to a variety of other materials such as glasses, plastics and various mineral crystals. Early studies by Enge [21] showed that etchable tracks were:

i. produced only by heavily ionizing particles (e.g α-particles in the case of plastics and fission fragments in the case of crystals);

ii. produced only in electrical insulators or poor semiconductors;

iii. stable even when subjected to light or to high doses of X-rays, β-particles, ultraviolet radiation etc.

The durability, simplicity and markedly specific nature of the response of these detectors led to the their rapid application in a wide variety of fields.

### 2.1.2 GENERAL PRINCIPLES BEHIND NUCLEAR TRACK FORMATION

Charged particles deposit energy along their trail when they travel through matter. In organic plastic materials like Cellulose Nitrate-85 (CN-85), Lexan Resin-115 (LR-115) or Columbia Resin-39 (CR-39), this energy loss creates a submicroscopic cylinder of the order of 50 - 100Å radius of "damaged" molecules the so-called latent track. This latent track is invisible under optical microscopes. If, however,

one places the organic plastic material in a suitable chemical etching solution (e.g 6M-NaOH at 70°C for $3^1/_2$ hours, for CR-39 plastic), the volume around the latent track will be attacked preferentially, so that the trail of the nuclear particle becomes visible under an optical microscope as a cylinder or cone-shaped hole of the order of 1-30μm length [21], if we consider α-particles or fission fragments.

## 2.2 TRACK FORMATION

### 2.2.1 CRITERIA FOR TRACK FORMATION

Various models of track formation have been proposed by different workers on nuclear tracks. They have also suggested that track formation should be related to a number of different parameters, such as total energy loss rate, primary ionization, restricted energy loss, etc. A track formation criteria, may then be set up which takes the form of a statement that tracks are formed in a medium when, and only when, the chosen parameter exceeds some critical value.

Some of the models are: the thermal spike model; — threshold expected to increase with temperature required for phase change, contrary to fact and it makes no useful prediction [22]. In the Restricted Energy Loss (REL) model by Benton [23], proposed that only energy loss by delta ray are transferred to the detector material by low-energy

secondary electrons is taken into account, i.e. only a "restricted" part of the total energy loss is used for track formation. This model ignores differences between the qualitatively different defects produced by primary ionization and excitation and those produced by delta ray energy loss; etc.

By far the most satisfactory model at present for inorganic and organic detectors is the Ion-Explosion Spike model by Fleischer et al [24].

### 2.2.2 THE ION-EXPLOSION SPIKE MODEL

The passage of a heavily-ionizing particle leaves in its trail a narrow region containing a high concentration of positive ions. The process is initiated by ionization which burst to create an electrostatically unstable array of adjacent ions. These eject one another from their normal sites into interstitial position by the Coulomb energy of the ions. After which elastic relaxation diminishes the acute, local stresses by spreading the strain still further by the etchant to reveal the latent-damage trails as microscopically observable etched tracks.

From the model comes the following quantitative criteria for track formation:

For tracks to form, the "electrostatic stress" must be greater than the mechanical strength of the material. If two

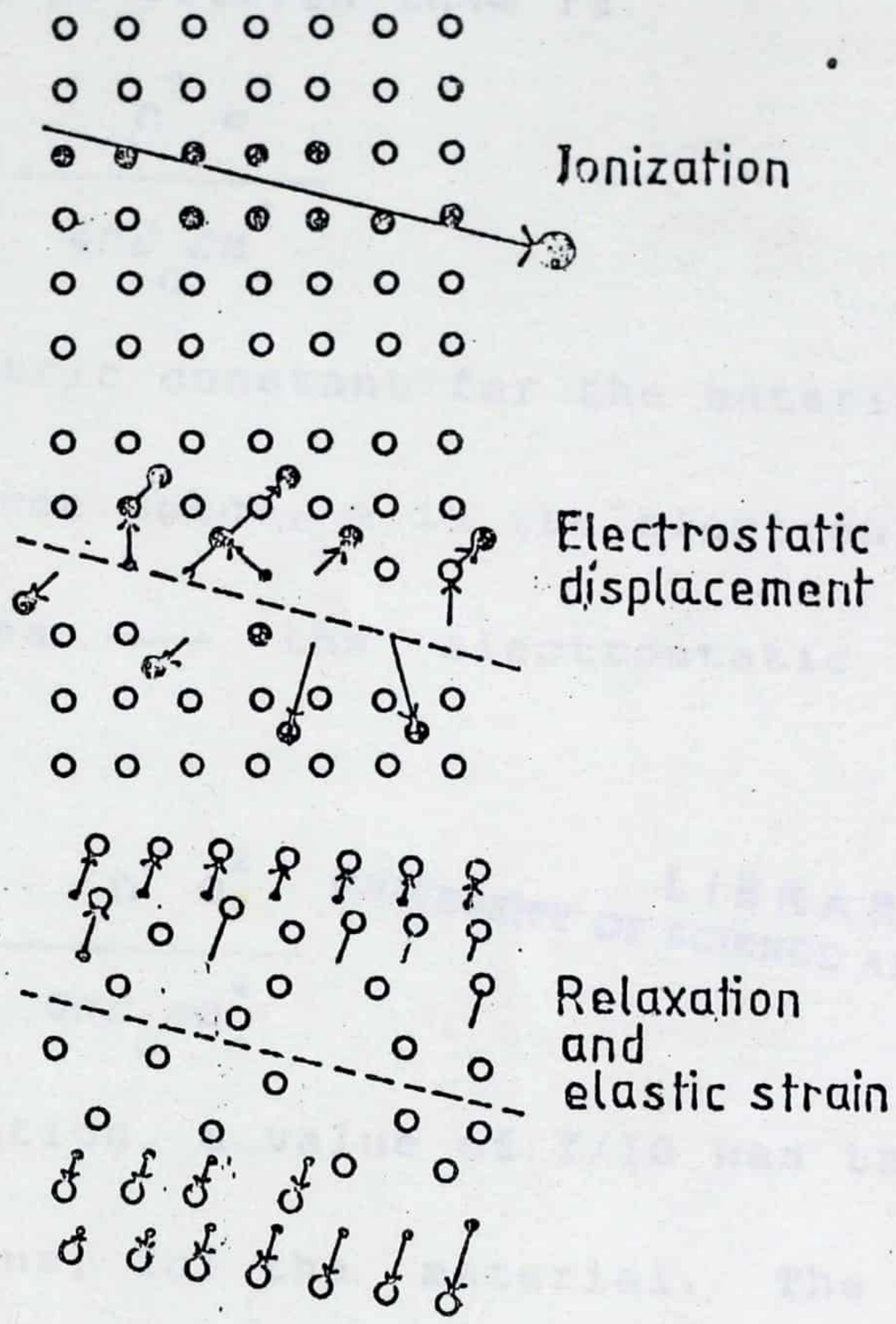


Fig.2.1, The ion explosion spike mechanism for track formation. The original ionization left by the passage of a charged particle (top) is unstable, and ejects ions into the solid, creating vacancies and interstitials (middle). Later, the stressed region relaxes elastically (bottom), straining the undamaged matrix. It is this region of extended damage that eventually enlarged still further by the etchant to reveal the latent-damage trail as microscopically observable etched tracks. Fleischer et al [24].

atoms have received an average ionization of n charges e each, and are separated by a distance $a_o$ (the inter atomic spacing), then the force between them is

$$\frac{n^2 e^2}{4\pi\varepsilon_o \varepsilon a_o^2}$$

where $\varepsilon$ is the dielectric constant for the material, $\varepsilon_o$ is the permittivity of free space, e is the electronic charge. The force per unit area —— the electrostatic stress is then

$$\frac{n^2 e^2}{4\pi\varepsilon_o \varepsilon a_o^4}$$

LIBRARY
UNIVERSITY OF SCIENCE AND TECHNOLOGY

as a working approximation, a value of Y/10 was taken, where Y is the Young's modulus, for the material. The criterion for track formation may thus be expressed as

$$n^2 > \frac{4\pi\varepsilon_o \varepsilon a_o^4 Y}{10e^2}$$

To conclude, the ion-explosion model seems to be favoured by most workers in the field of solid-state nuclear track detection at present.

## 2.3 TRACK ETCHING: —— GEOMETRY

Chemical etching is the most widely used method of "fixing" and enlarging the image of the latent damage trail on a solid state track detector. Essentially, etching takes

place via rapid dissolution of the disordered region of the track core which exists in a state of higher free energy than the undamaged bulk material.

For a plastic detector there are two kinds of etching rate: first, the bulk or the material etching rate $V_B$ ($\mu mh^{-1}$) for the undamaged material; and second, the track etching rate $V_T$ ($\mu mh^{-1}$) at which the etching solution proceeds along the latent track. (See Fig.2.3). Now, the track etching rate attack down the track so that in an etching time t the etch pit will extend to a distance L from them point of origin, where $L = V_T t$ .However, the surface is also being removed at a rate $V_B$; so that the length of the etch pit is

$$L_e = V_T t - V_B t \qquad 1.$$

Any point at a distance y from the beginning of the track is reached by the etchant at a time $t(y) = y/V_T$ ; and there is a residual $t - t(y)$ available for the etchant to attack radially outwards from the point at y to a distance $V_B \times [t - t(y)]$ in the medium. The three-dimensional pit wall is then formed by the locus of all the sphere of radius

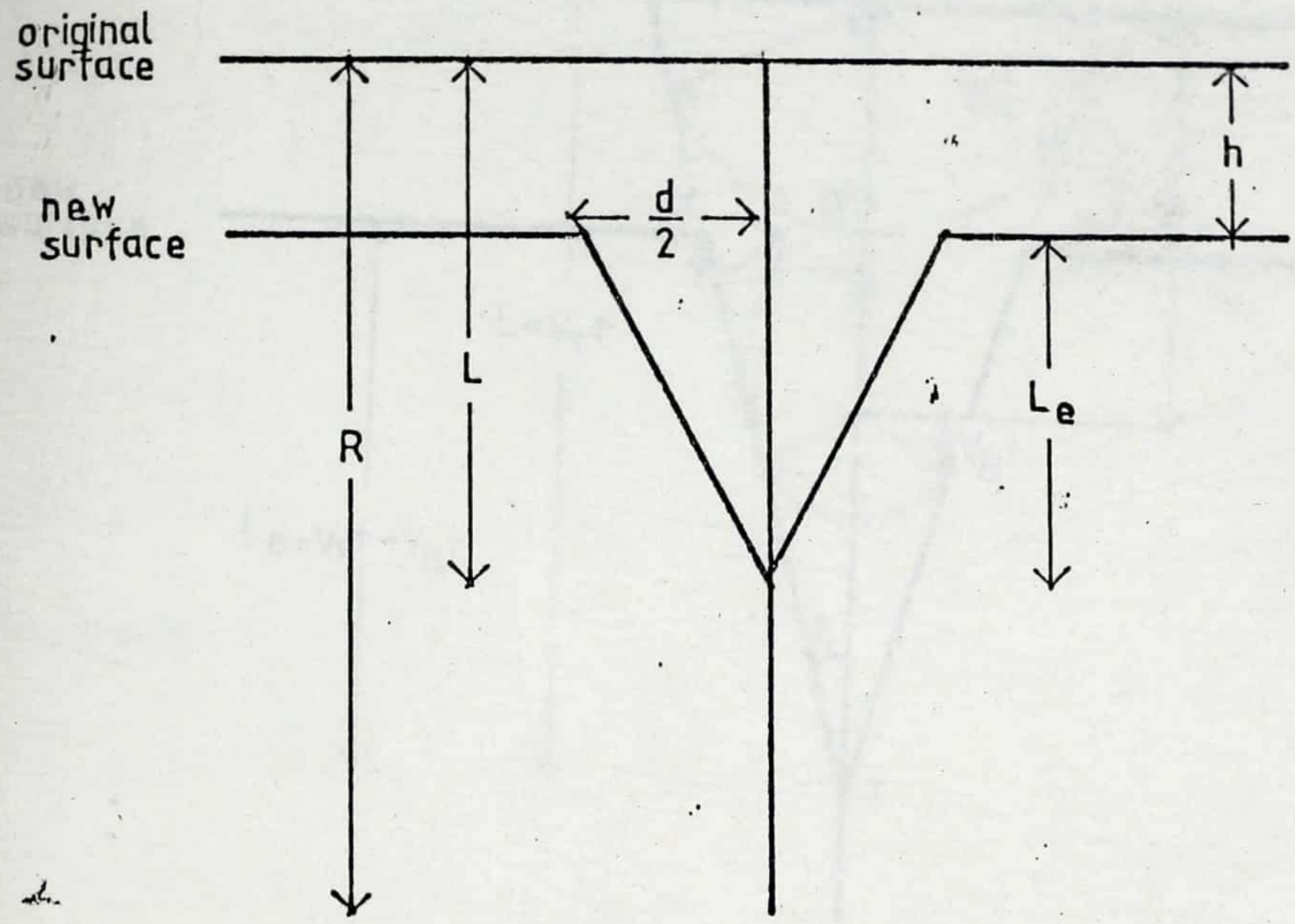


LIBRARY
UNIVERSITY OF SCIENCE AND TECHNOLOGY

Fig.2.2 Some parameters used to describe the geometry of etched tracks. R, full length of the latent (unetched) track; L, the length of track attacked by the etchant up to a given moment; $L_e$, the observed length of the etched track; h, the thickness of the surface removed by etching (= $V_B t$, where t is the duration of etching) and d is the diameter of the etch-pit opening.

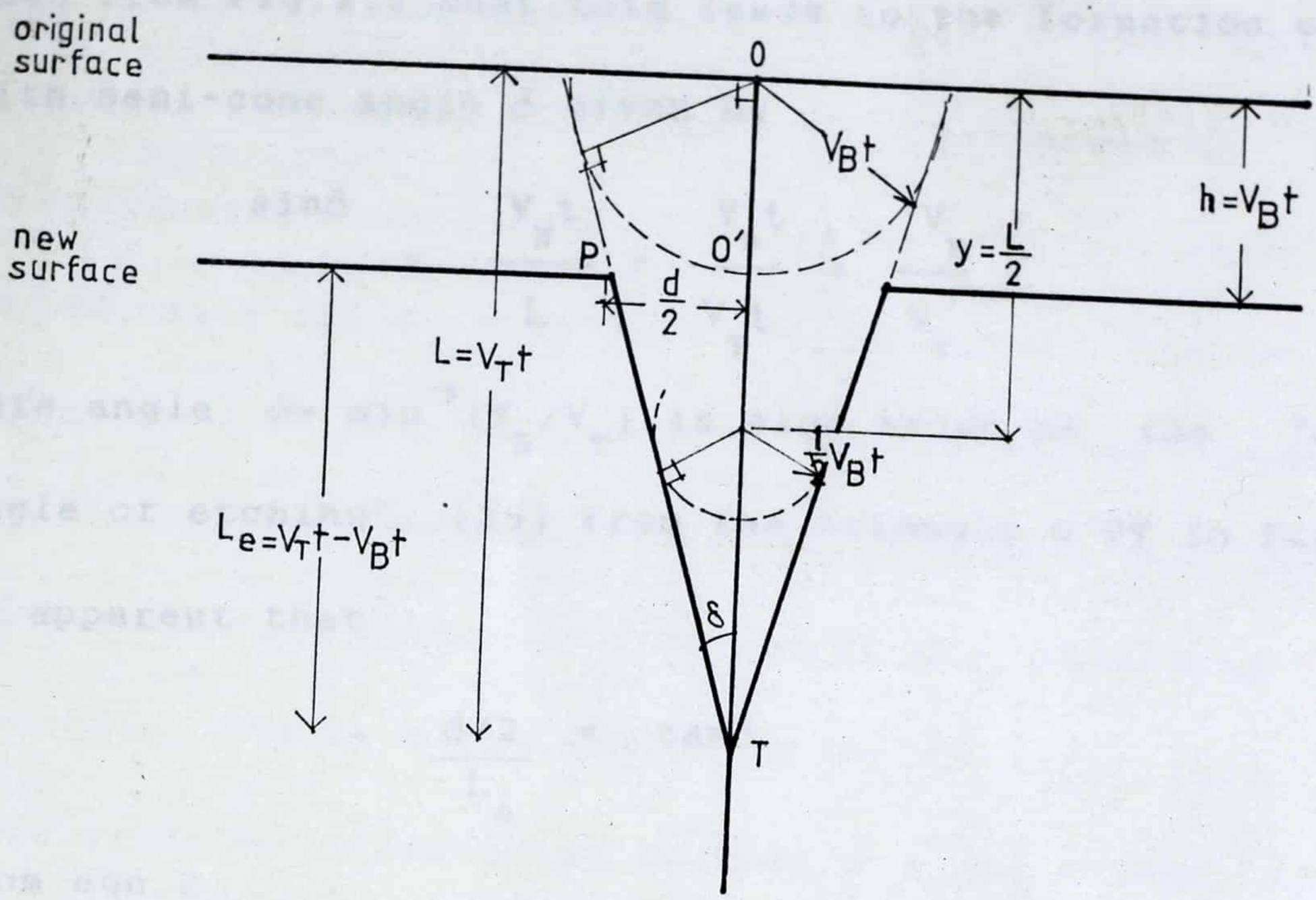


Fig.2.3, Construction for the calculation of etched-track parameters for a track of constant $V_T$, lying normally to the detector surface. The semi-cone-angle is denoted by δ.

$V_B \times [t - t(y)]$, where $t(y)$ is the variable. It will be seen from Fig.2.5 that this leads to the formation of a cone with semi-cone angle $\delta$ given by

$$\sin\delta = \frac{V_B t}{L} = \frac{V_B t}{V_T t} = \frac{V_B}{V_T} \qquad 2.$$

This angle $\delta = \sin^{-1}(V_B/V_T)$ is also known as the "critical angle of etching". [25] From the triangle O'PT in Fig.2.3 it is apparent that

$$\frac{d/2}{L_e} = \tan\delta \qquad 3.$$

from eqn.2

$$\tan\delta = \frac{V_B}{\left[V_T^2 - V_B^2\right]^{1/2}}$$

so that from eqn.3

$$d = \frac{2V_B L_e}{\left[V_T^2 - V_B^2\right]^{1/2}}$$

and from eqn.1

$$d = \frac{2V_B(V_T - V_B)t}{\left[V_T^2 - V_T^2\right]^{1/2}}$$

or

$$d = 2V_B t\left[\frac{V_T - V_B}{V_T + V_B}\right]^{1/2}$$

## 2.4 THE CR-39 POLYMER TRACK DETECTOR

CR-39 track detector is an organic polymer called allyl diglycol carbonate. It is a thermosetting plastic, cross-linked, amorphous extremely transparent and mechanically rigid. However, it is very fragile. It is widely used in the manufacture of eye-glass lenses. Its sensitivity for ionizing radiation is higher than any other track-recording solid. It can record all $\alpha$-energies without threshold. Unlike Lexan Resin-115 or LR-115, this plastic could register $\alpha$-particles between 0.5 and 4.3MeV. [3]

Beth, et al [26] investigated some aspects on etching of the CR-39 plastic detector by analyzing the bulk and track etch rate of NaOH etchant solution at various concentrations (4M - 8M), temperatures (30°C - 80°C) and the calculated value. They found that $V_B$ increases with temperature, concentration of NaOH solution and at 70°C, the experimental value obtained equal the calculated value.

## 2.5 TARKWA AND PRESTEA GOLDFIELDS.

### 2.5.1 GENERAL GEOLOGICAL FEATURES OF TARKWA AND PRESTEA GOLDFIELDS

Ghana geologically lies within the Pre-Cambrian Guinea shield of West Africa. The oldest rocks belong to the Birrimain system which is mainly argillaceous sediments, metamorphosed lavas and intrusive igneous rocks with bands of phyllite and grey-wacke related to the Dixcove Granite [29].

The rocks of the Birrimian age cover about one-sixth of the total area of Ghana and are of far more economic importance than any of the geological systems. The Birrimian may be sub-divided into lower and upper series. The lower series consist of slates, phyllites and schists (usually grey or black in colour), greywackes and ashes. The upper series comprises of greenstones (mainly metamorphosed basic and acidic lavas with some pyroclastic rocks and intercalated bands of phyllite and greywacke) [29]. The Birrimian rocks are isoclinally folded with transverse faults and fractures running diagonally from north-east down to south-west [29].

The Tarkwaian rock system is next to the Birrimian which are arenaceous in character. At the base is a conglomeratic member termed the Kawere conglomerate. This is

succeeded in turn by (a) quartzites and grits; (b) an argillaceous formation (Tarkwa Phyllite) containing porphyroblasts of chloritoid and/or magnetite, and (c) the Huni Sand-stone, or Abotenten Quartzite, a relatively fine-grained felspathic quartzite containing chlorite and epidote. [29] The Tarkwaian rocks are preserved in synclinal troughs and near Tarkwa the beds have been overturned and faulted, but not so intense as in the Birrimian rocks. The rocks of the Prestea belt are steeply inclined Birrimian sediments and lavas which have been over folded with the formation of over thrust fault and shear zones. They are intruded by granite and porphyry of the Dixcove type as well as by basic sills and dykes, younger arenace Tarkwaian sediments and basic igneous rocks which are not highly folded as the Birrimian. [27] Tables 2.1 and 2.2 show the geological information of the locations where the measurements took place.

LIBRARY
UNIVERSITY OF SCIENCE AND TECHNOLOGY

The radon-emanating properties of rocks depend on geologic type, although there may be large variation in radon emanation within a geologic type. Weiffenbach [14] identified geological regions for the State Maine in United States and compared rock types with the results of a survey of radon concentrations in wells. He found that the radon concentrations in areas of granitic bedrocks were highest.

Hess, et al [28] pointed out that, the physical conduction of the rock matrix appears to play a greater role in radon release into the drives of the mine than does the concentration of radium. Also experimental and theoretical consideration indicate that diffusion along micro-crystalline imperfections, fissure zones, fault lines etc. dominates the. release of radon into the surrounding air underground.

Table 2.1; Location of the mounted can and the geological information at Tarkwa goldfields

| LOCATION OF CANS IN THE DRIVES | | GEOLOGICAL INFORMATION |
|---|---|---|
| 10 LEVEL | Gangway | Quartzite |
| | Tramming drive (Bin) | Quartzite |
| 12 LEVEL | Gangway | Quartzite |
| | Level cross-cut | Quartzite |
| 14 LEVEL | Gangway Transformer S'tn | Quartzite/Dike and GABBRO |
| | Level cross-cut | Quartzite, Green Dike and GABBRO |
| 17 LEVEL | Gangway | Quartzite, Green Dike and GABBRO |
| | Winder house | Quartzite |
| 18 LEVEL | Gangway | Quartzite |
| | Level drive | Quartzite Reef |
| 20 LEVEL | Gangway | Quartzite |
| | Winder house | Quartzite |
| 24 LEVEL | 2416 incline | Quartzite |
| 25 LEVEL | 2525 subdrive 2 north | Quartz Reef(Conglomerate) Dike (Green)Quartz |
| | 2525 subdrive 1 south | Quartz Reef |

Table 2.2 Location of the mounted cans and the geological information at Prestea Goldfields.

| LOCATION OF CANS IN THE DRIVES | | GEOLOGICAL INFORMATION |
|---|---|---|
| 6 LEVEL | Gangway | Carbon Phyllite and Quartz |
| | 258 south cross-cut | |
| 9 LEVEL | Gangway | Carbon Phyllite and Smoky Quartz |
| | 252 south cross-cut | Carbon Phyllite and Metavolcanic Rock |
| 12 LEVEL | Gangway | Carbon & Siliceous Phyllite and Quartz |
| | 224 south cross-cut | Carbonaceous Phyllite and Siliceous Phyllite |
| 15 LEVEL | Gangway | Carbonaceous Phyllite & Schiztose (Metasediments) |
| | 235 south cross-cut | Sulphidic, Carbonated Phyllites & Quartz Reef |
| 23 LEVEL | Gangway | Phyllite and Quartz Metavolcanic |
| | 224 south cross-cut | Arsenopyrite, Carbonated Metavolcanic & Phyllites |
| 30 LEVEL | Gangway | Quartz and Phyllite |
| | Number 4 shaft | Quartz and Phyllite |

### 2.5.2 THE UNDERGROUND AND THE SURFACE ENVIRONMENTS OF THE GOLDFIELDS.

In the underground mine there is a vertical shaft as entry into the mines and horizontal drives numbered as the "levels". Each level is separated by an interval of 150 feet or 45 metres as shown Fig 2.4. In Prestea the levels are directly below each other, but not exactly so at Tarkwa. The drives can be about three kilometres long away from the shaft station or the shaft gangway, (i.e where one can enter the drives from the shaft). In the drives along the sidewalls at 75 feet or 22.5 metre intervals is the cross-cut sometimes used to link other drives in situations where there are many vertical shafts.

Various environmental conditions have been found to affect the rate of radon exhalation. Straden et al [30] measured increased radon exhalation from concrete sample with increases in temperature. However, Auxier et al [31] found that within the temperature range 23°C to 43°C, the temperature of concrete is not a sensitive parameter and has negligible effects on the exhalation rate. Temperatures underground are nearly static, i.e change within only a small range of approximately ±2°C.

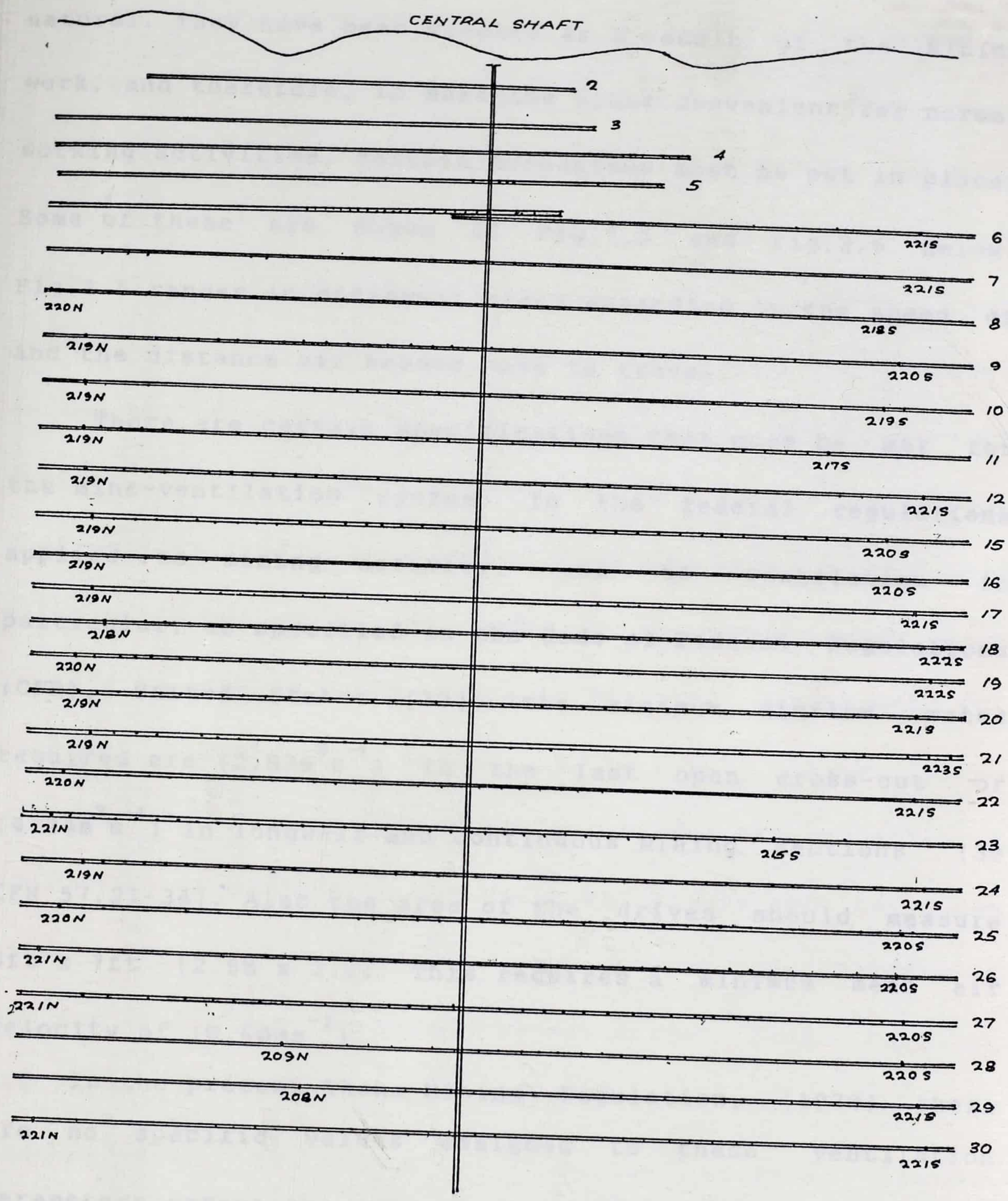


Fig.2.4, Outline of the central shaft of the State Goldmining corporation, Prestea gold mine showing the location of the various levels.

The environmental conditions underground are not natural. They have been created as a result of the mining work, and therefore, to make the place convenient for normal working activities, certain mechanisms must be put in place. Some of these are shown in Fig.2.5 and Fig.2.6 below. Fig.2.5 ranges in different sizes depending on the speed of and the distance air needed have to travel.

There are certain specifications that must be met for the mine-ventilation system. In the federal regulations applied to mining activity, and to ventilation in particular, as specified in the Code of Federal Regulations (CFR), United States [33], the minimum airflow rates required are ($2.83m^3s^{-1}$) in the last open cross-cut or ($4.24m^3s^{-1}$) in longwall and continuous mining sections (30 CFR 57.21-34). Also the area of the drives should measure 8ft x 7ft (2.5m x 2.1). This requires a minimum mean air velocity of ($0.60ms^{-1}$).

In the present Ghana Mining Regulation, (1970) there are no specific values assigned to these ventilation parameters except the general statement in section 142 of the regulation which states that "the ventilation in every mine shall be such that the air in all workings that are in use or are to be used by workmen or others shall be free from dangerous amounts of noxious impurities and shall contain sufficient oxygen to obviate danger to the health of

any one employed in any such mine.[34]

The radon concentration in indoor air( i.e. offices, laboratories etc.) is influenced by the use of the room. Human activities which affect the air exchange rate (opening and closing of door and windows, use of air conditioning, fans, etc) will cause radon levels to vary, and people can unknowingly be exposed to the gas. In Prestea for example, in the office of the chief geologist, all kinds of rock chunks have been exposed around, in the assay department rock samples from underground are grinded into powdered form which makes the whole place dusty and in crusher room, where the ore is crushed before going to the mill department for chemical treatment. These places will have radon concentration different from the background concentration if Radium-226 is present in the rocks or the ore sent to these places. The slime and tailing dumps of the two Goldfields are far from the offices and laboratories. These tailings are known to contain some radon,. the highest recorded concentration is about $1172Bqm^{-3}$ from Tarkwa Goldfields.[32]

LIBRARY
UNIVERSITY OF SCIENCE AND TECHNOLOGY

Note: Winder house is the place where the lift(cage) inside the vertical shaft is controlled. There some on the ground surface and some underground.

Fig.2.5, Picture showing an electric fan being used to ventilate the 17Level winder house at the State Goldmining Corporation Tarkwa deep gold mine

Fig.2.6 Picture showing a ventilating duct passing through the 17Level gangway to an active working area at the State Goldmining Corporation Tarkwa deep gold mine

# CHAPTER THREE

# 3.0 EXPERIMENTAL PROCEDURE

## 3.1 MEASUREMENT OF RADON GAS

### 3.1.1 UNDERGROUND MEASUREMENTS

Measurement of the radon gas underground was done using the closed-can technique. Soft-drink cans, cut into 5cm x 6cm cylinders with a volume of $160cm^3$ each, were covered with perspex lids and sealed as shown in Fig.3.1. A 2cm x 2cm piece of the CR-39 plastic detector with one face marked to identify the exposed face from the unexposed, was attached to a filter paper and placed on the topside of the lid as shown in Fig.3.2. The filter paper serves as an intervening barrier or membrane to cut out Thoron (Rn-220, half life 56s) and ensure that the alpha tracks registered are due to Radon gas (Rn-222, half life 3.82 days) and its plateout alpha-emitter daughters namely Polonium-218 (half life 3.1 min) and Polonium-214 (half life $1.6 \times 10^{-6}$s).

Measurements were made in the main central shafts in Tarkwa and Prestea Goldfields. The CR-39 exposed in the cans were mounted one at the shaft gangway and another along the drives or cross-cuts in the drives (mostly in Prestea) for a period of three and half months. The measurements were

then repeated for another three and half months making total exposure time of seven months. Passive time-integrated measurements were thus made of the radon which diffuses into the can over the exposure period. Figures 3.3 to figure 3.13 show the sectional plan of some of the locations where the cans were mounted and figures 3.14 to figure 3.25 shows photographs of how the cans were mounted in the drives. See (tables 4.1 and 4.2) and (Tables 4.9 and 4.10) for the results at Tarkwa and Prestea Goldfields respectively

### 3.1.2 RADON GAS: MEASUREMENTS AT GROUND LEVEL

The measurement of radon gas on the surface was done using the can technique as described above. The cans were placed in some selected offices and laboratories. The measurements were made twice at three and half months of exposure each. See (Tables 4.3 and 4.4) and (tables 4.11 and 4.12) for the results at Tarkwa and Prestea Goldfields respectively.

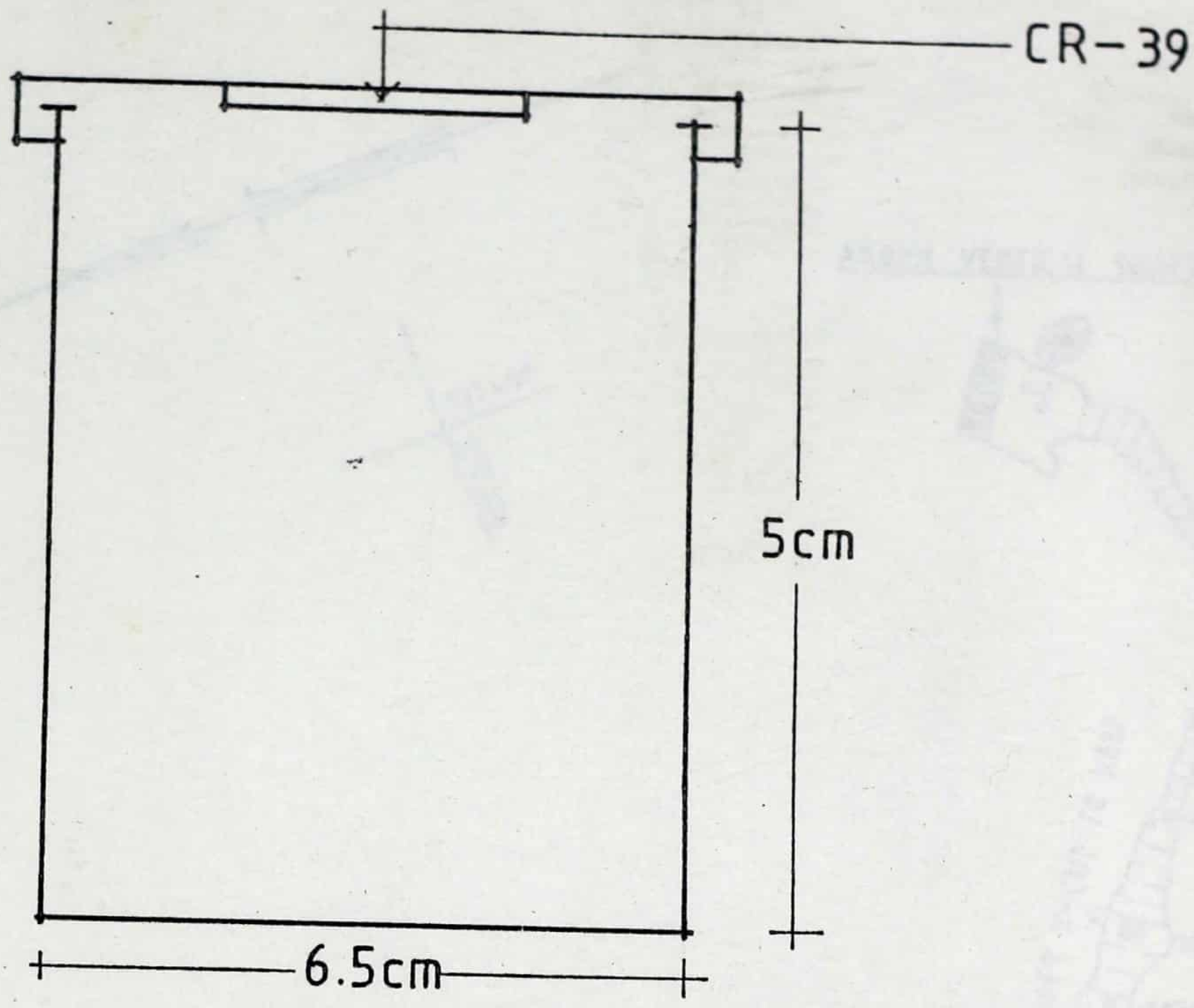


**FIG. 3.1** A 5cm. x 6.5 cm. soft-drink can with CR-39 detector placed on the topside of the lid of the can – side view

UNIVERSITY OF SCIENCE AND TECHNOLOGY
LIBRARY

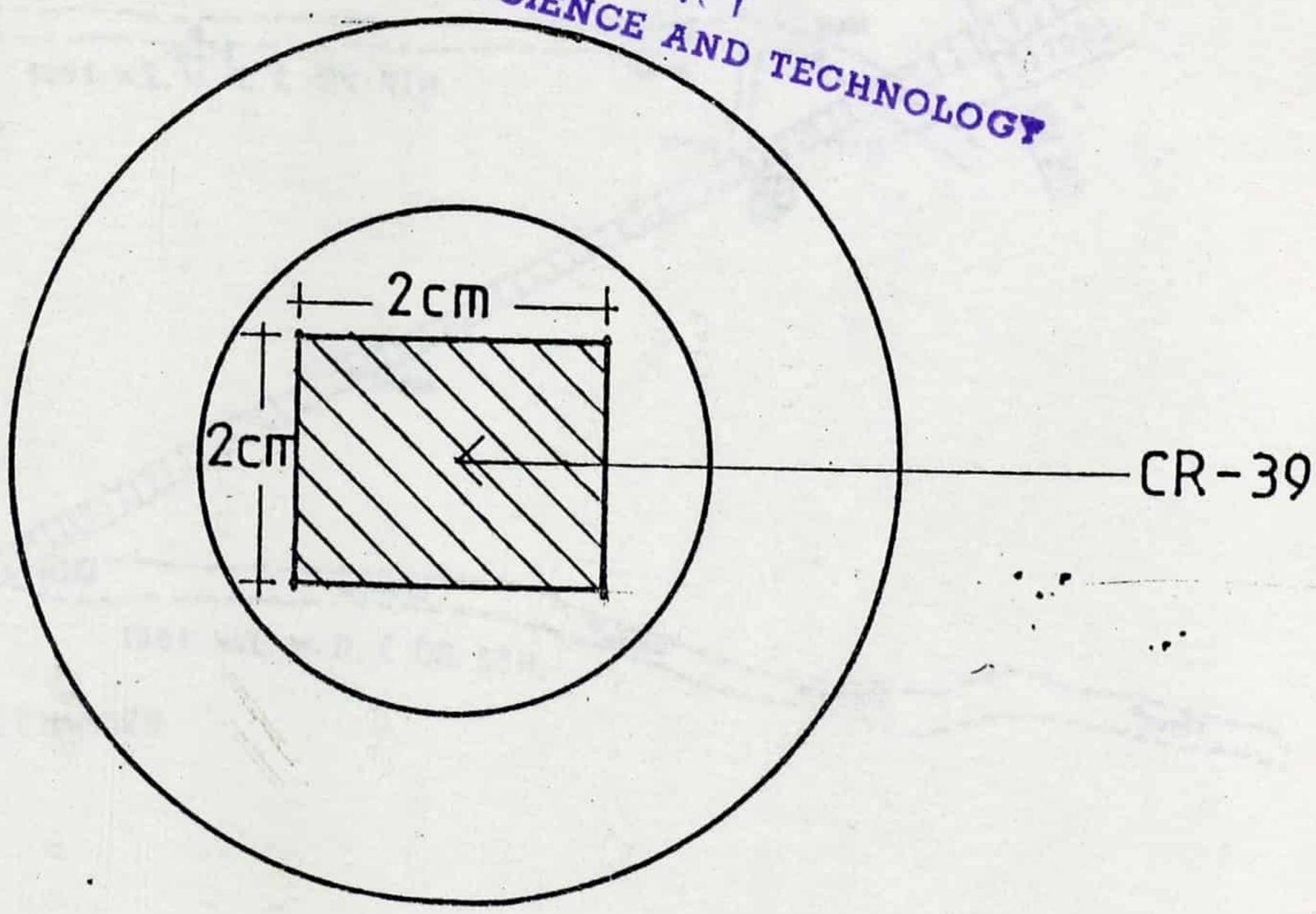


**FIG. 3.2** The lid used for covering the can with CR-39 attached to a white filter paper – top view

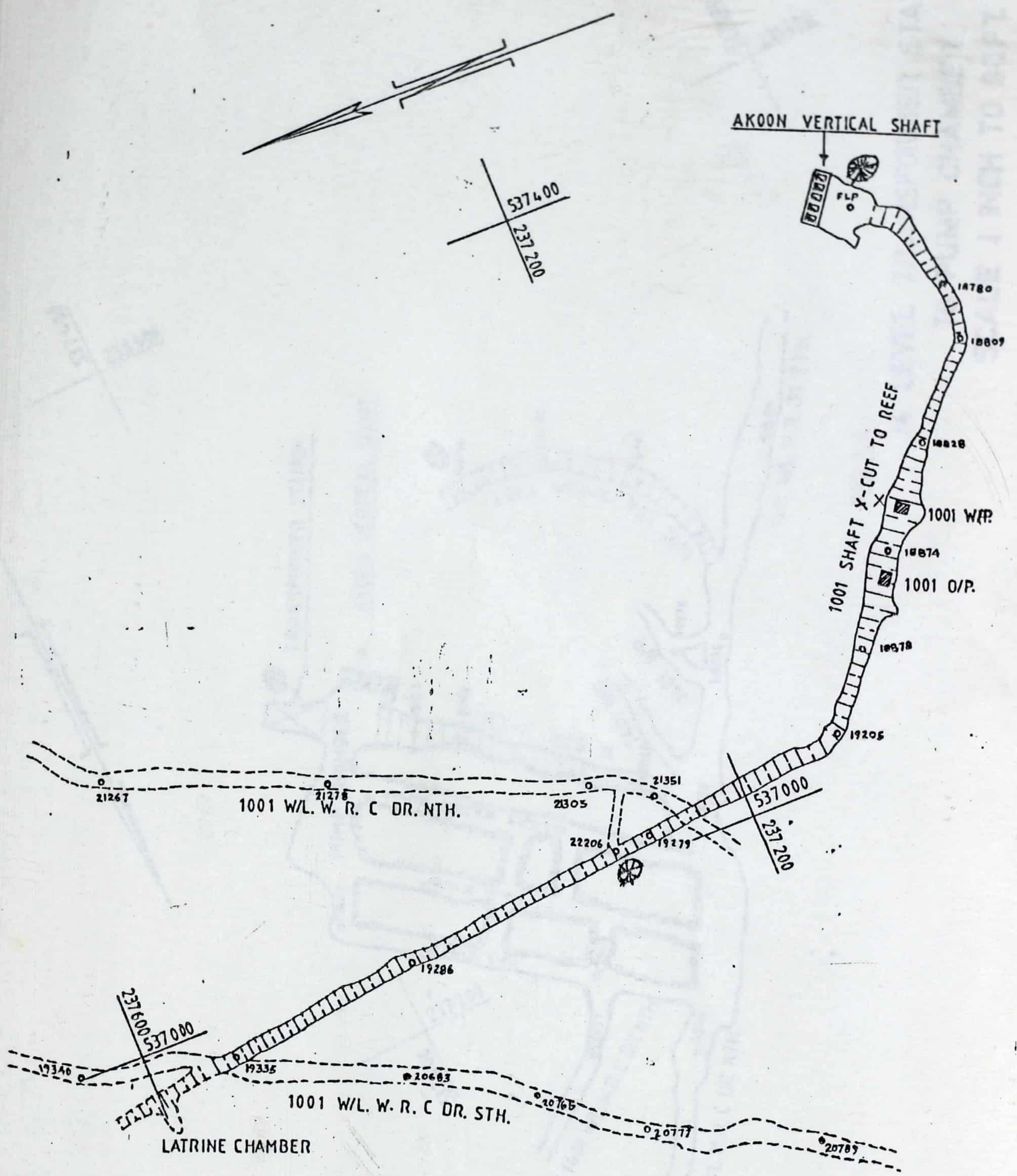


FIG. 3.3

10 LEVEL GANGWAY TO TRAMMING DRIVE BIN

SCALE 1 INCH TO 80 FT.

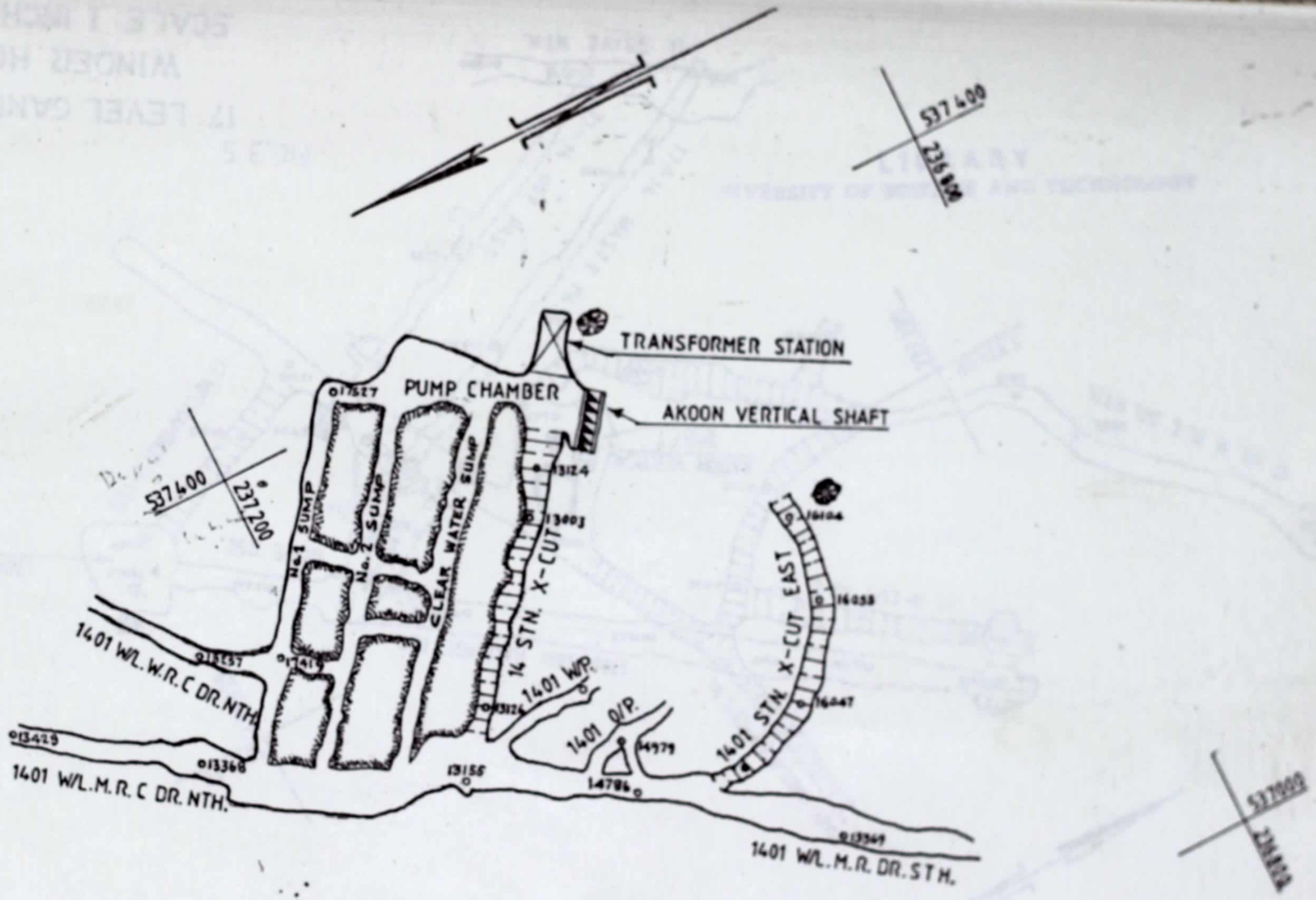


FIG 3.4

14 LEVEL TRANSFORMER STATION
TO PUMP CHAMBER
SCALE 1 INCH TO 80 FT.

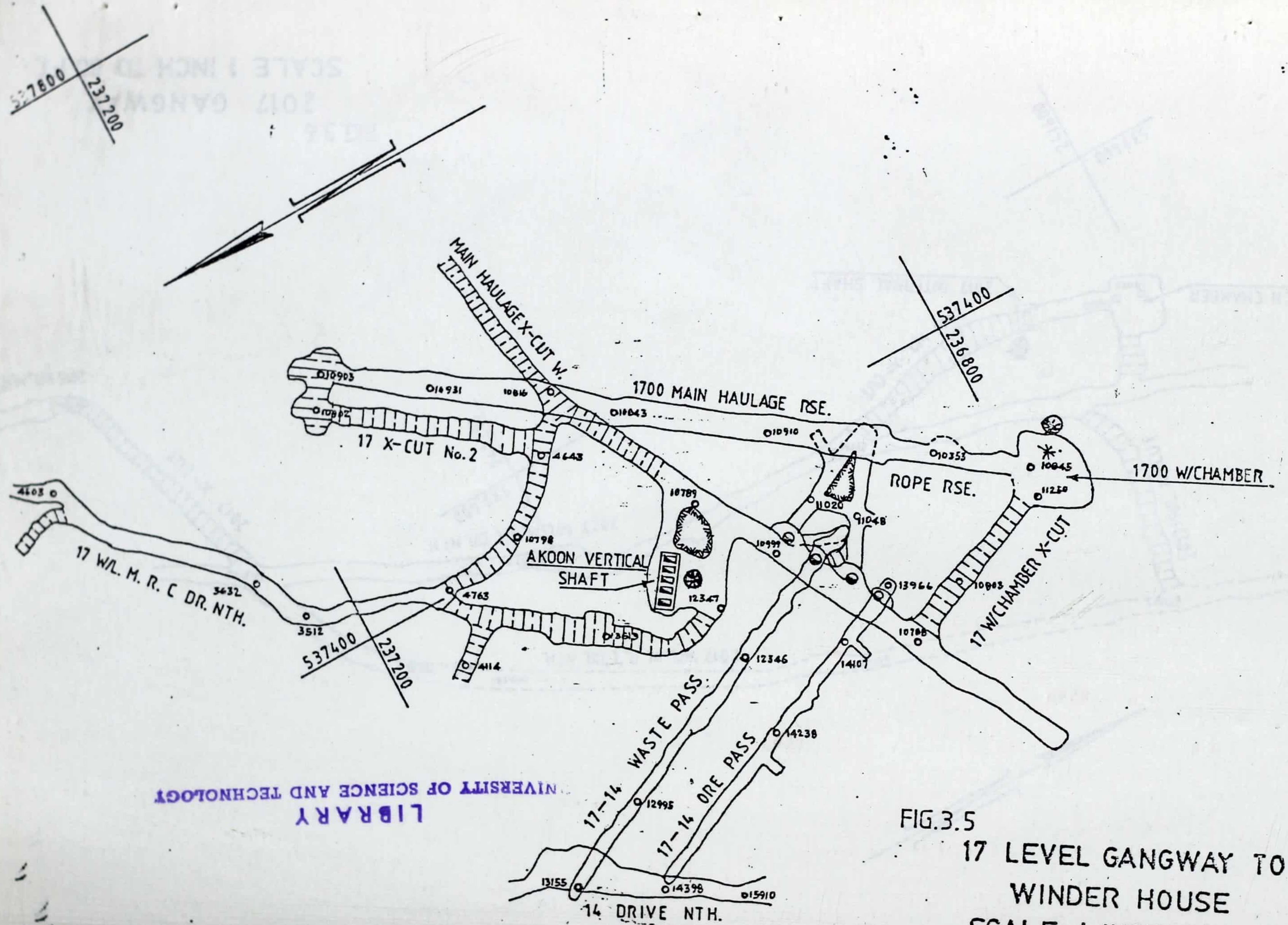


FIG.3.5

17 LEVEL GANGWAY TO WINDER HOUSE

SCALE 1 INCH TO 80 FT.

LIBRARY
UNIVERSITY OF SCIENCE AND TECHNOLOGY

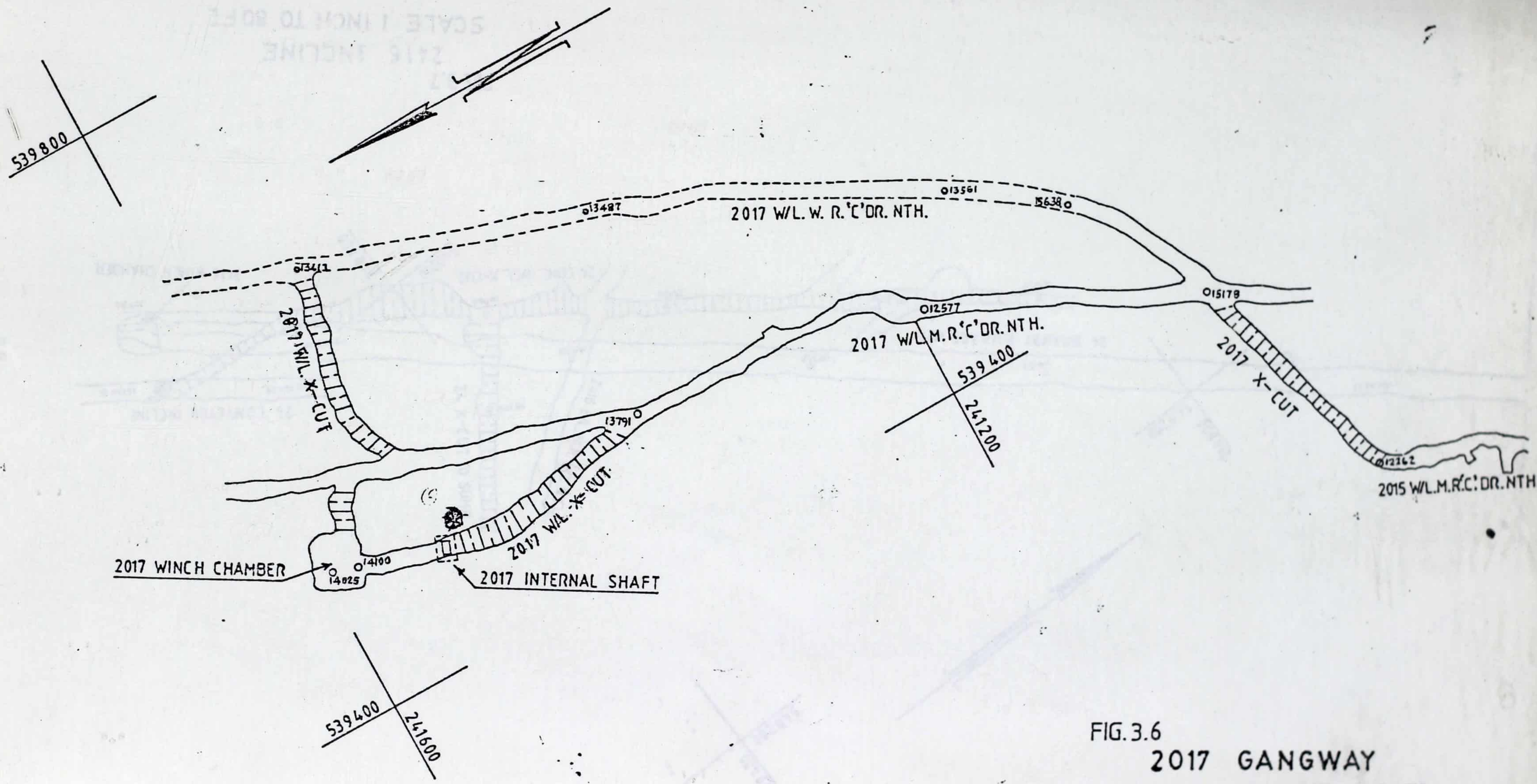


FIG. 3.6
2017 GANGWAY
SCALE 1 INCH TO 80 FT.

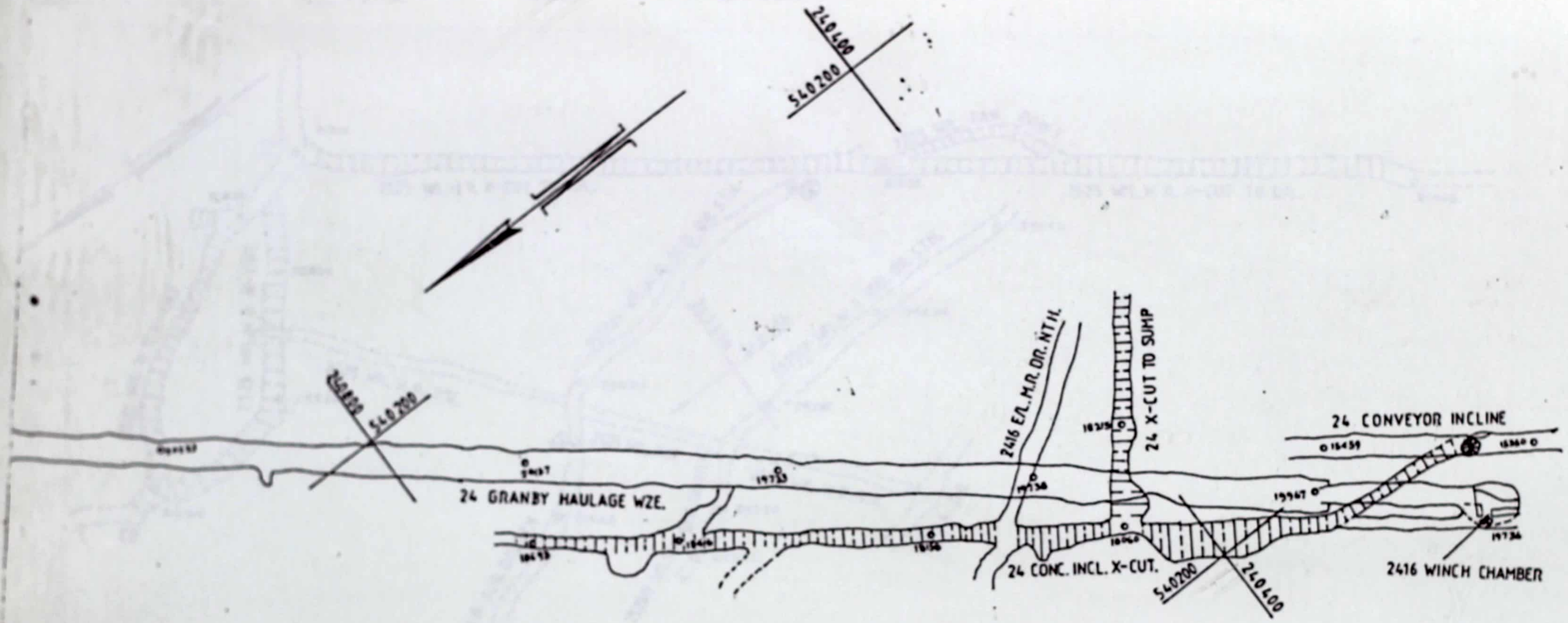


FIG. 3.7
2416 INCLINE
SCALE 1 INCH TO 80 FT.

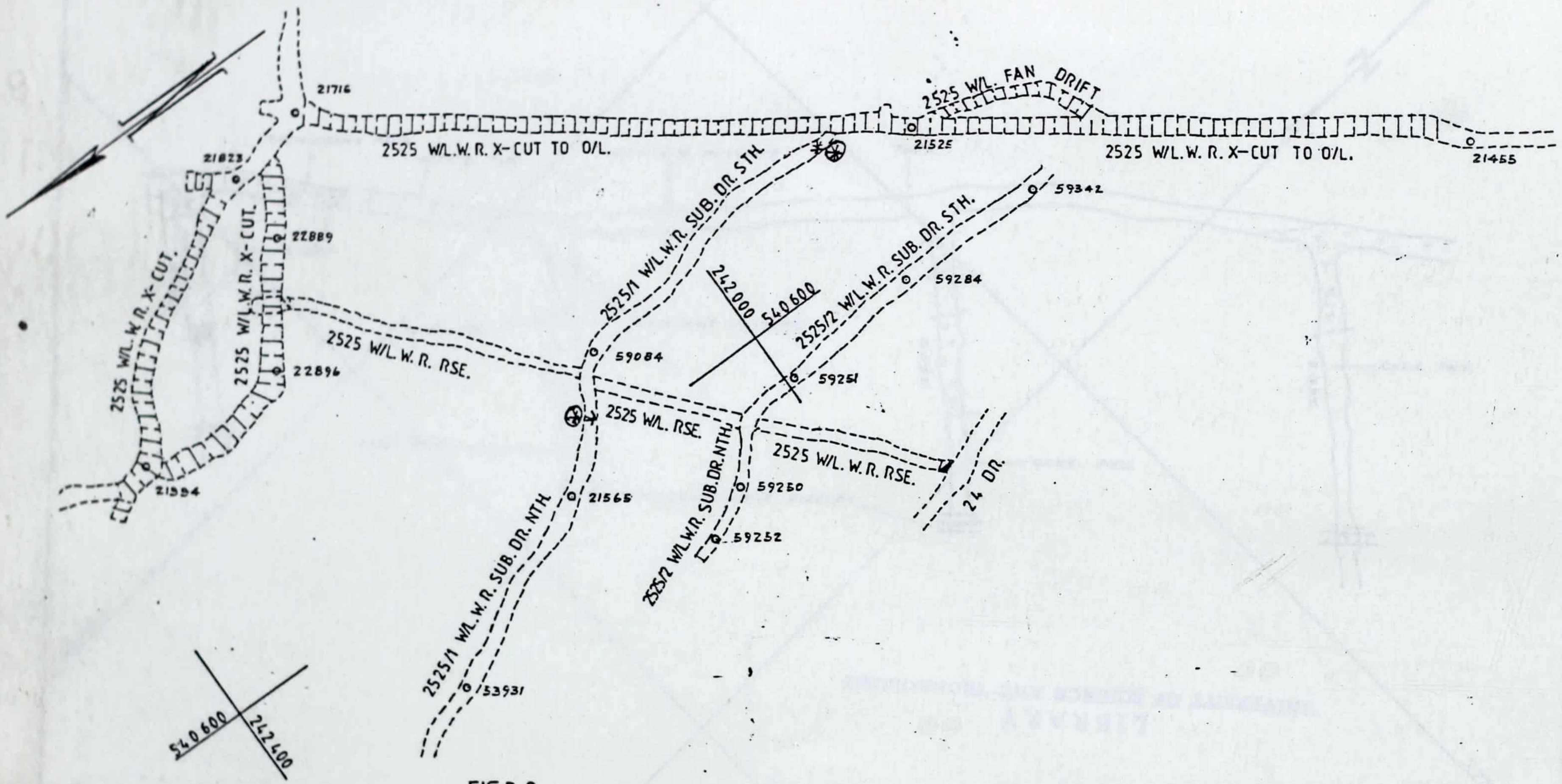


FIG.3.8

2525 SUB. DRIVE 2 NORTH
TO THE DEAD END AND
2525 SUB. DRIVE 1 NORTH
SCALE 1 INCH TO 80FT.

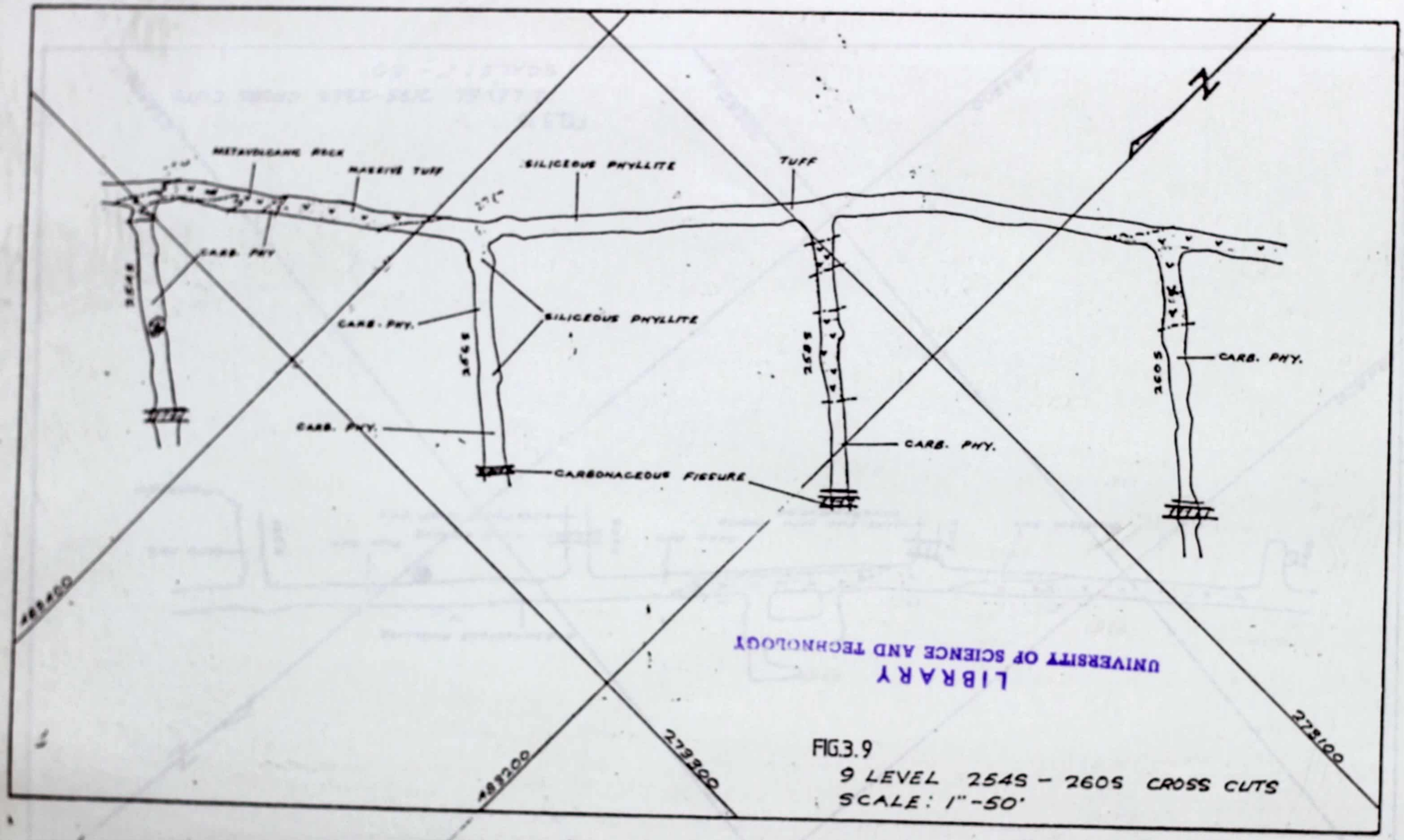


LIBRARY
UNIVERSITY OF SCIENCE AND TECHNOLOGY

FIG.3.9
9 LEVEL 254S - 260S CROSS CUTS
SCALE: 1"-50'

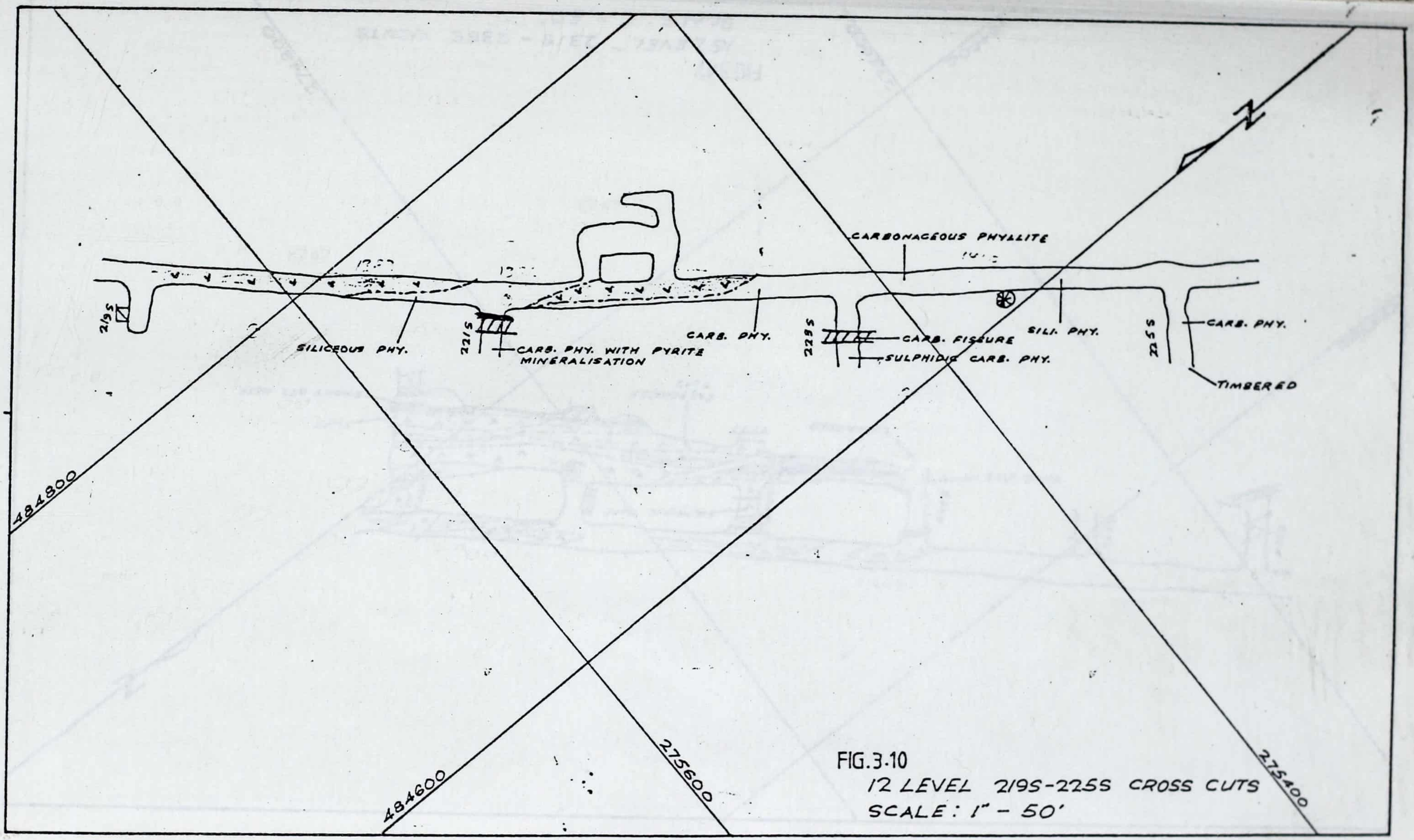


FIG. 3.10
12 LEVEL 2195-2255 CROSS CUTS
SCALE: 1" - 50'

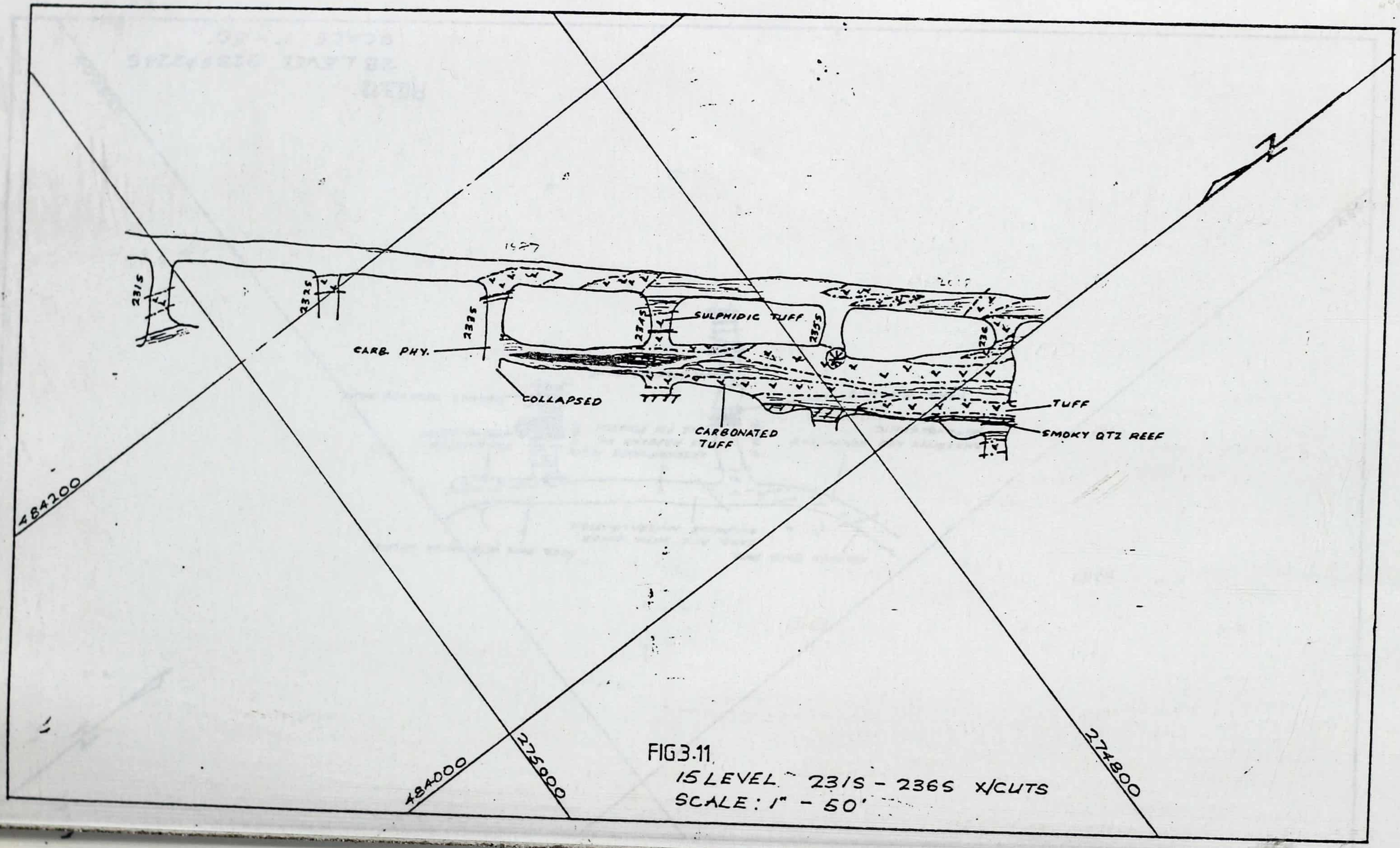


FIG 3.11
15 LEVEL ~ 231S - 236S X/CUTS
SCALE: 1" - 50'

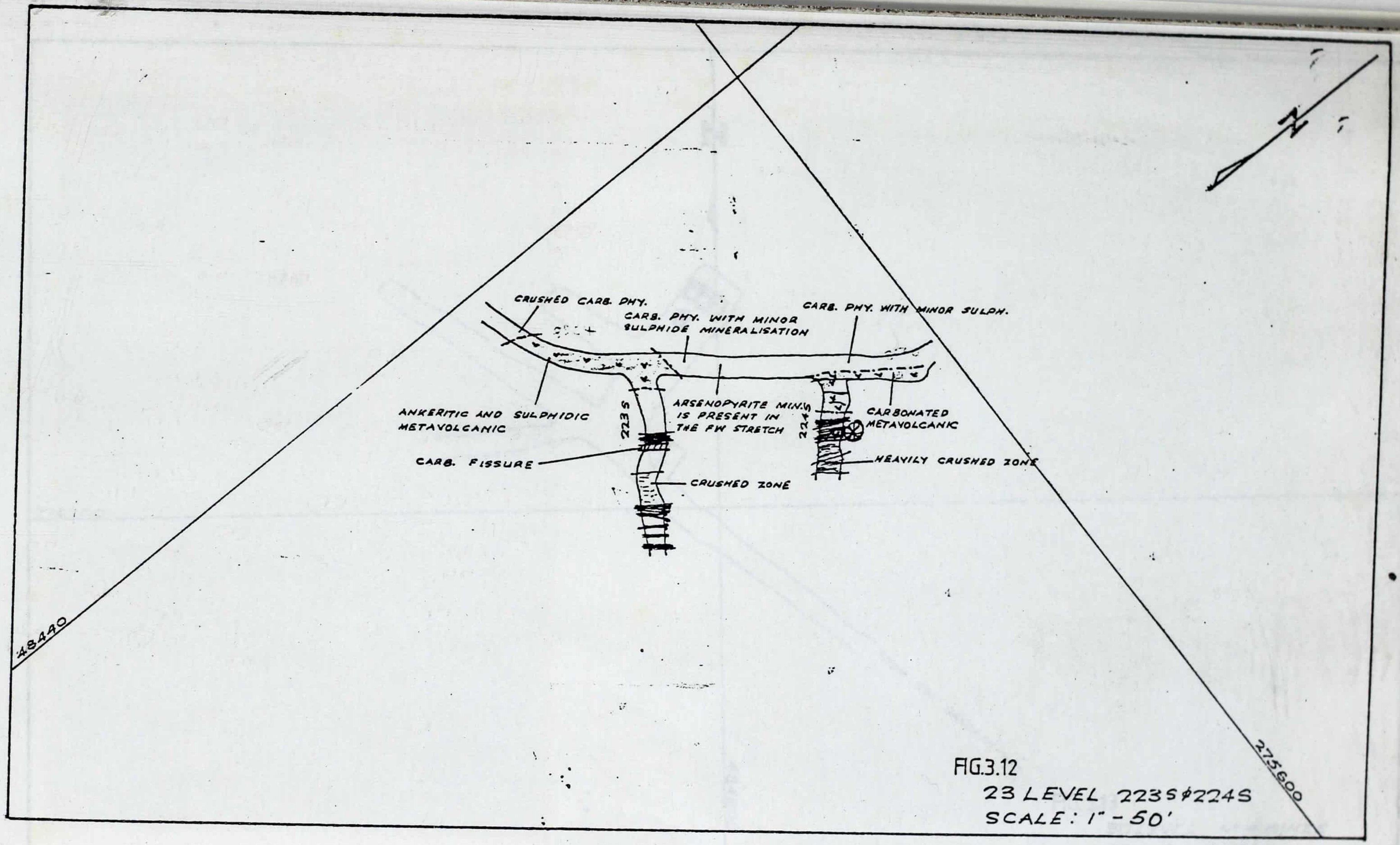


FIG.3.12
23 LEVEL 223S & 224S
SCALE: 1" - 50'

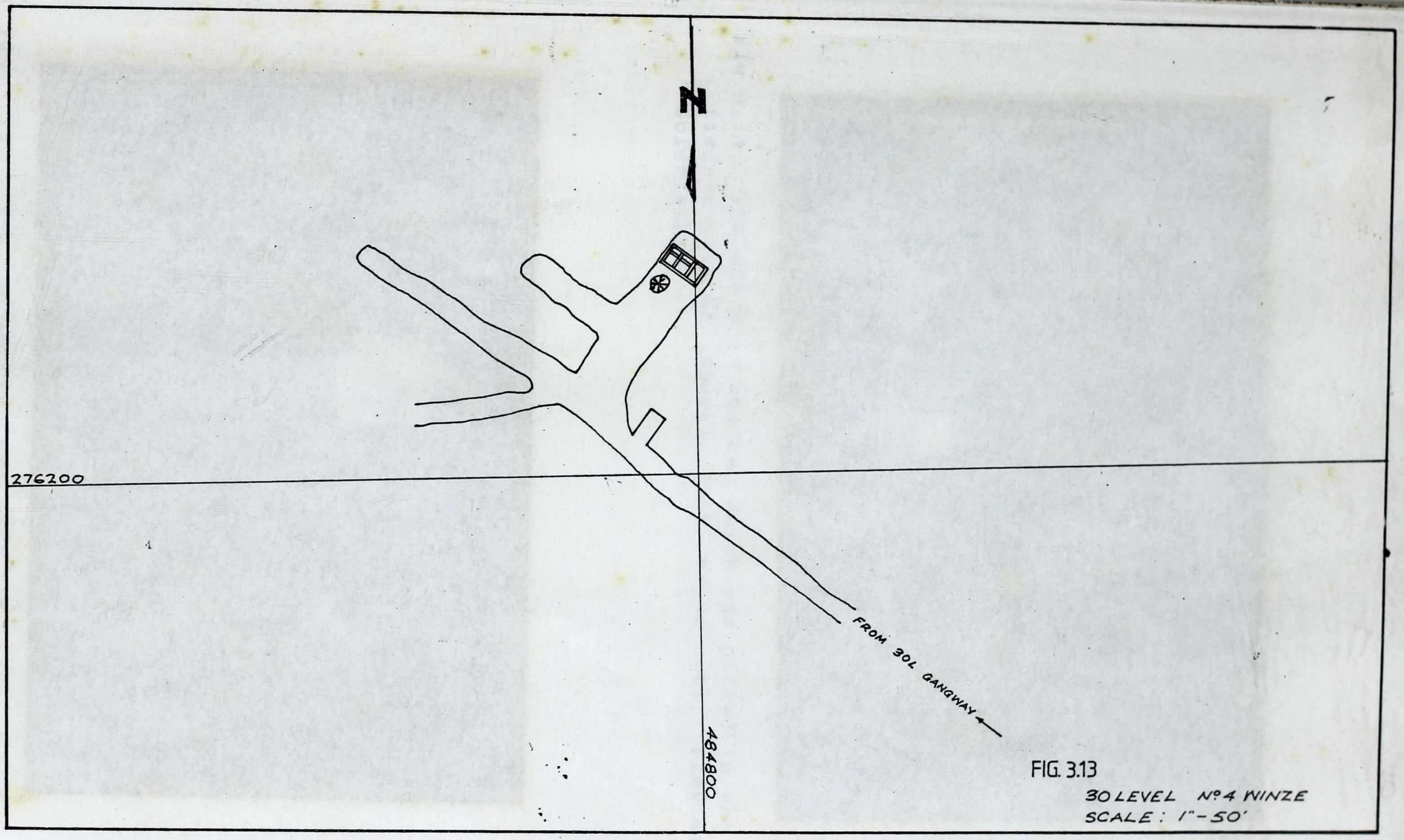


FIG. 3.13

30 LEVEL Nº 4 WINZE
SCALE : 1" - 50'

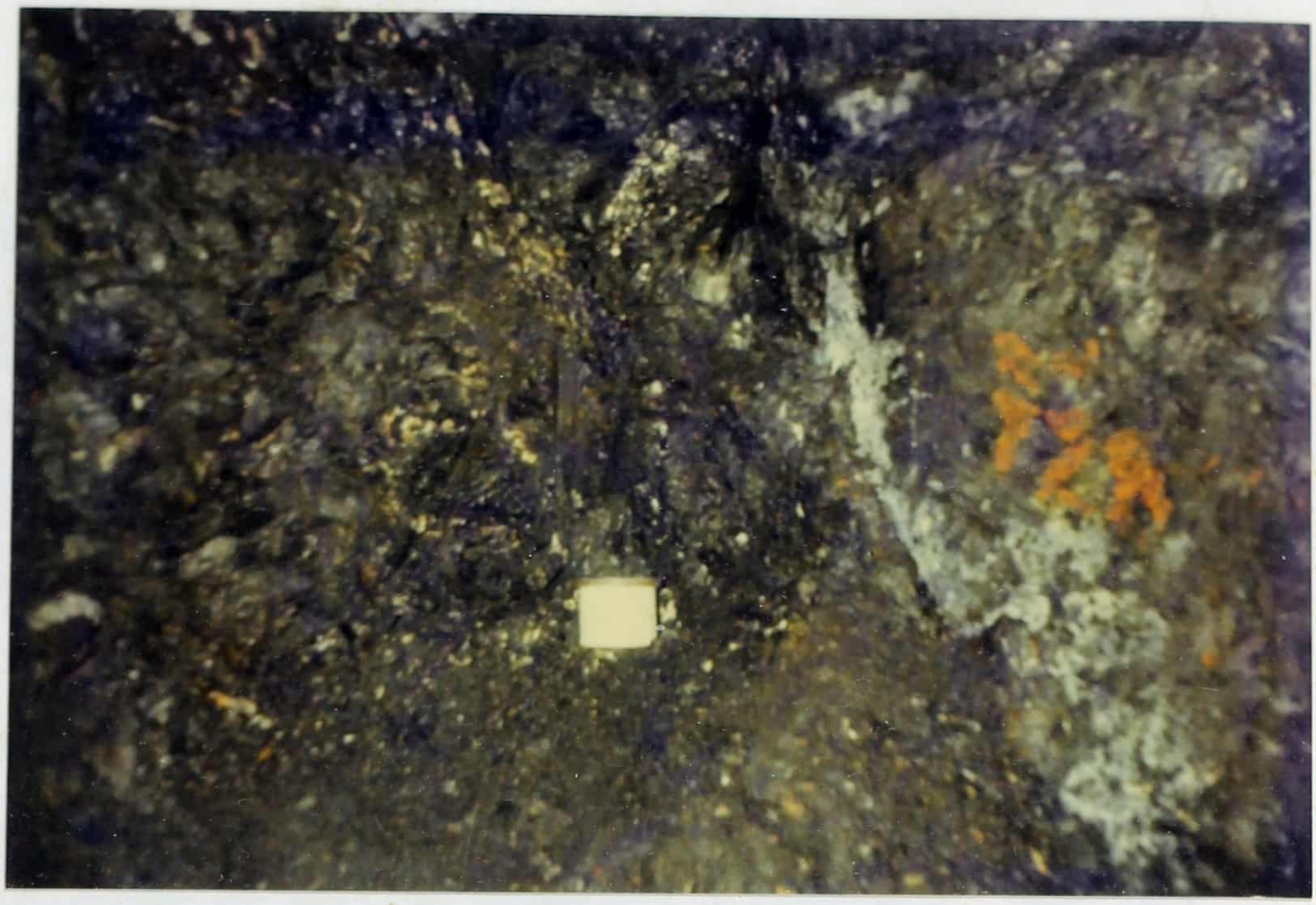

Fig.3.14, The CR-39 in the can which was placed in the fissure zone at 6Level (258 cross-cut), Prestea Goldfields.

Fig.3.15, The CR-39 in the can at the 6Level (258 cross-cut) after $3^{1}/2$ months of exposure. (i.e at the time of collection).

Fig.3.16, The CR-39 in the can which was placed at the side wall at 9Level (254 cross-cut), Prestea Goldfields.

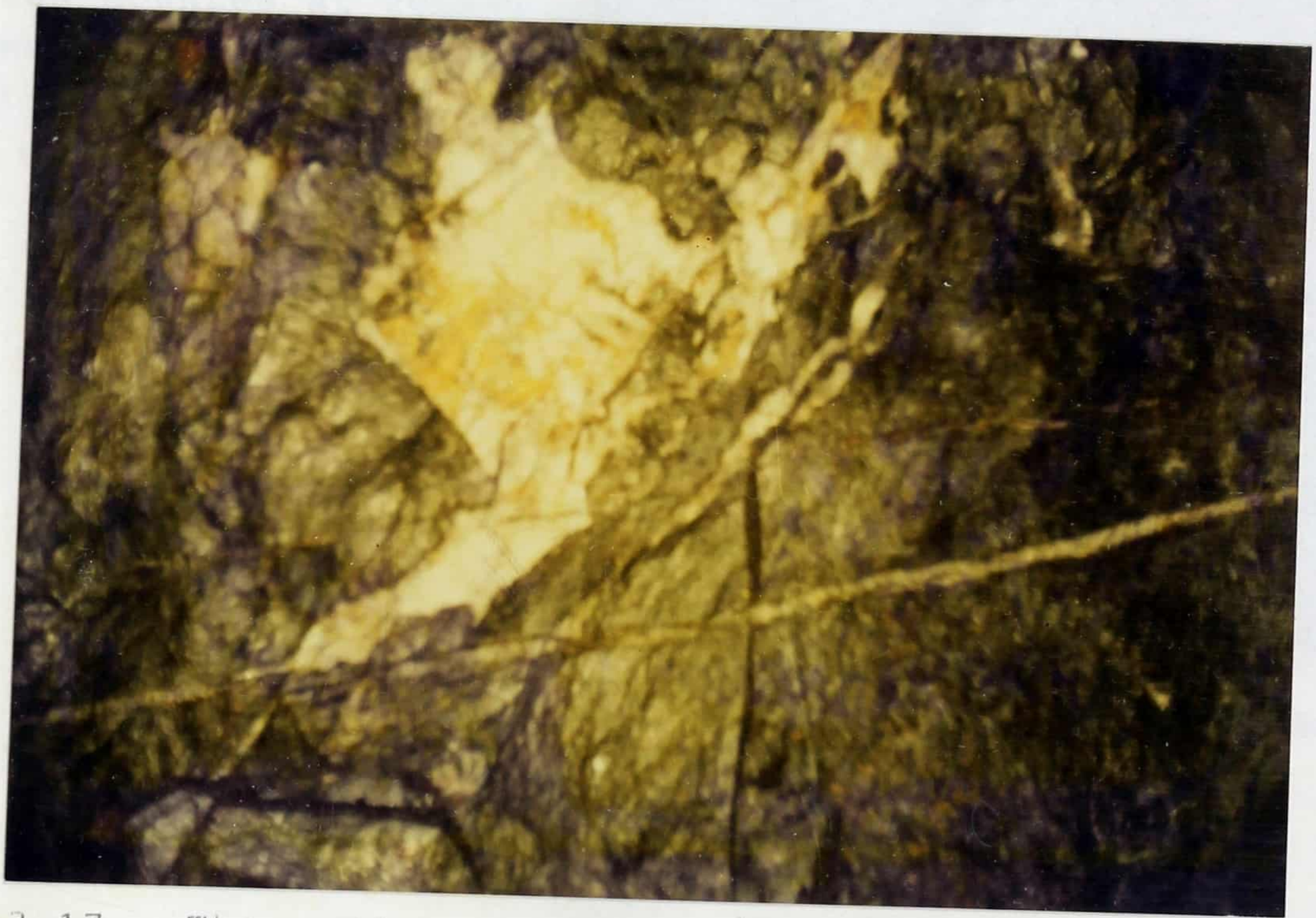

Fig.3.17. The adjacent rock matrix of 9Level (254 cross-cut),Prestea Goldfields. (i.e. at the time of collection).

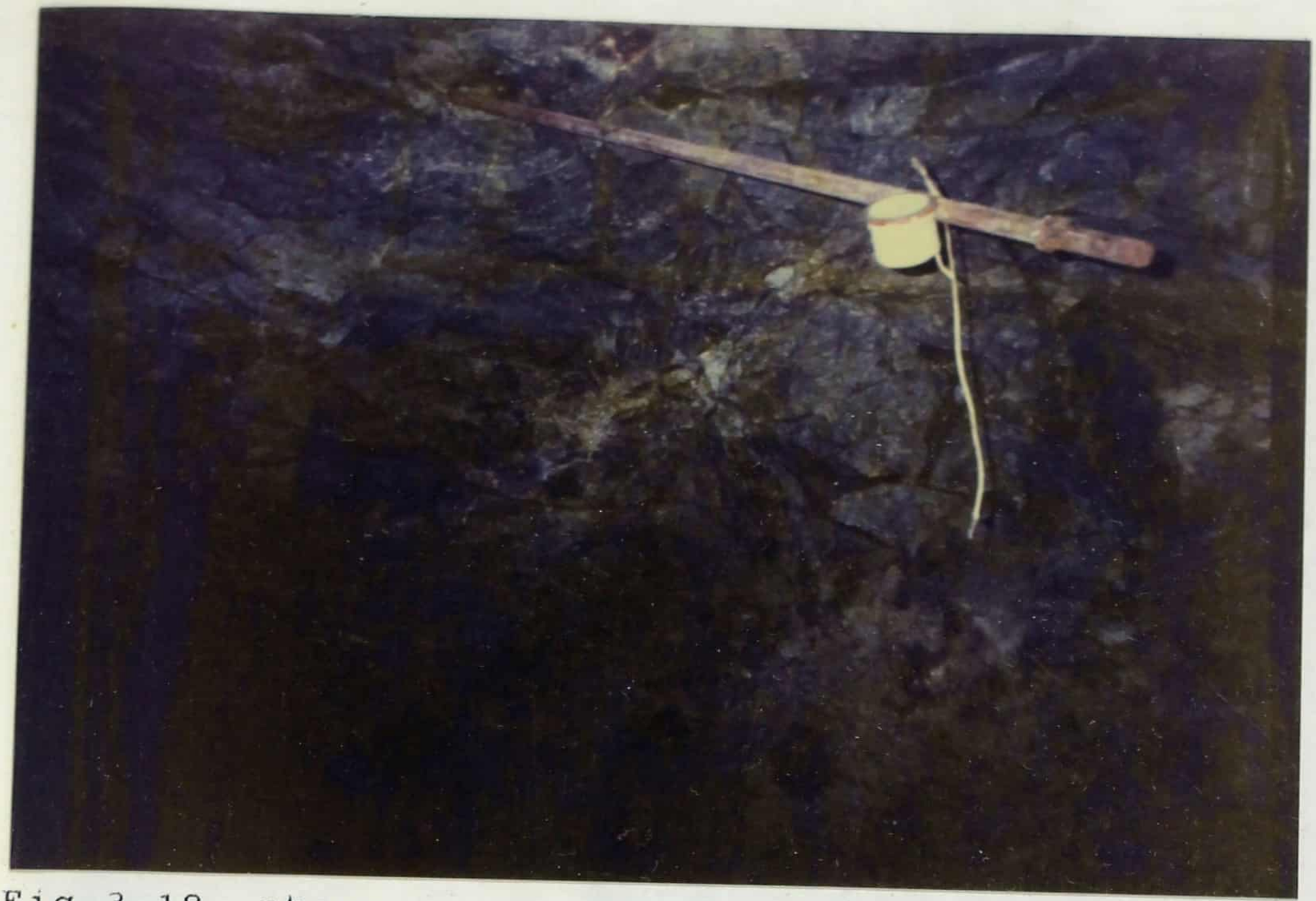

Fig.3.18, above,
the CR-39 stringed to an iron rod inside the sidewall in the 14Level drive, Tarkwa Goldfields.

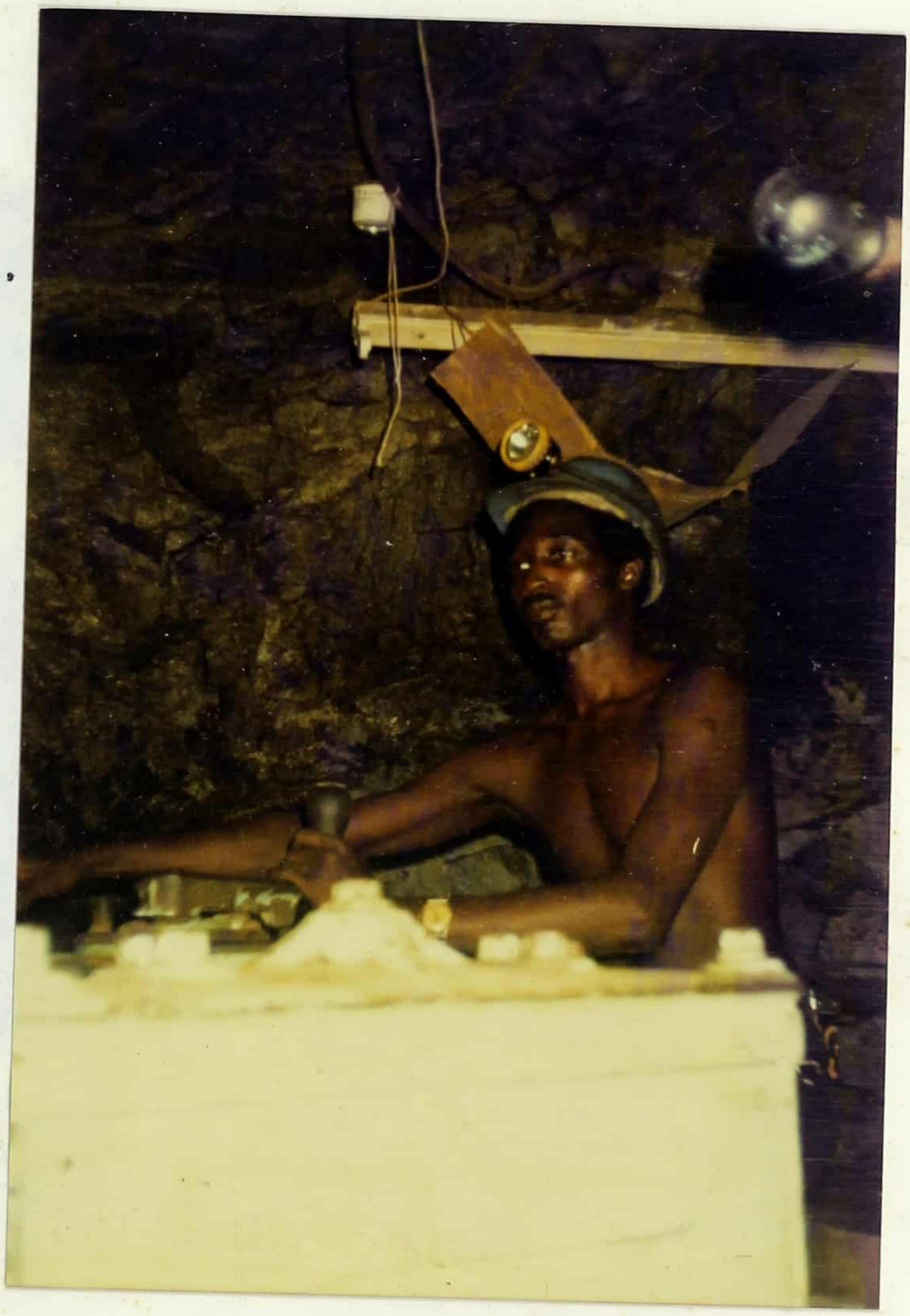

Fig.3.19, right,
the CR-39 plastic inside the can mounted at 20Level, winder house, Tarkwa Goldfields. This is the work place for this miner.

LIBRARY
UNIVERSITY OF SCIENCE AND TECHNOLOGY

Fig.3.20, The CR-39 in the can stringed to a cable in the 20Level drive at Tarkwa Goldfields.

LIBRARY
UNIVERSITY OF SCIENCE AND TECHNOLOGY

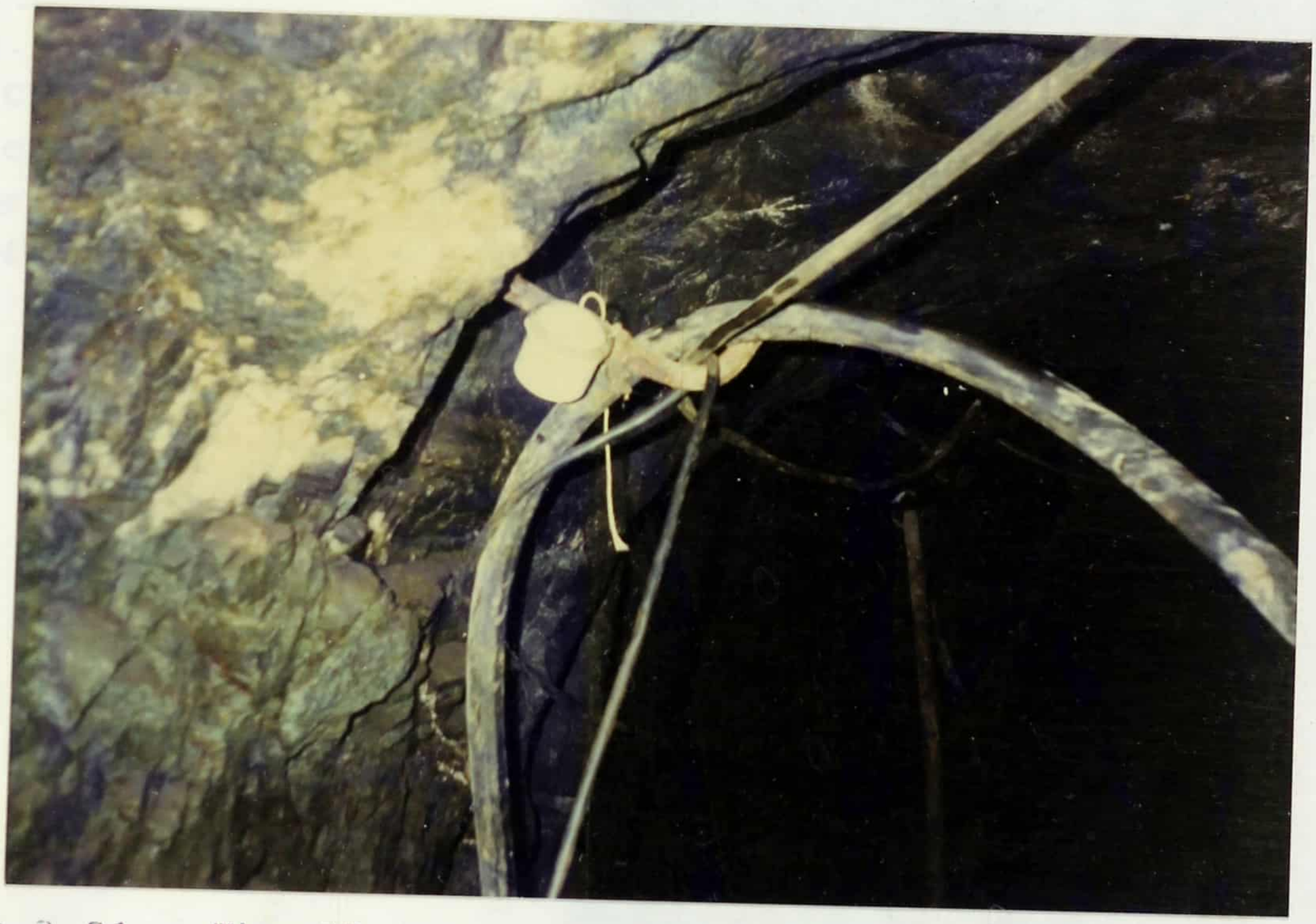

Fig.3.21, The CR-39 in the can stringed to a cable. in the 24Level incline at Tarkwa Goldfields.

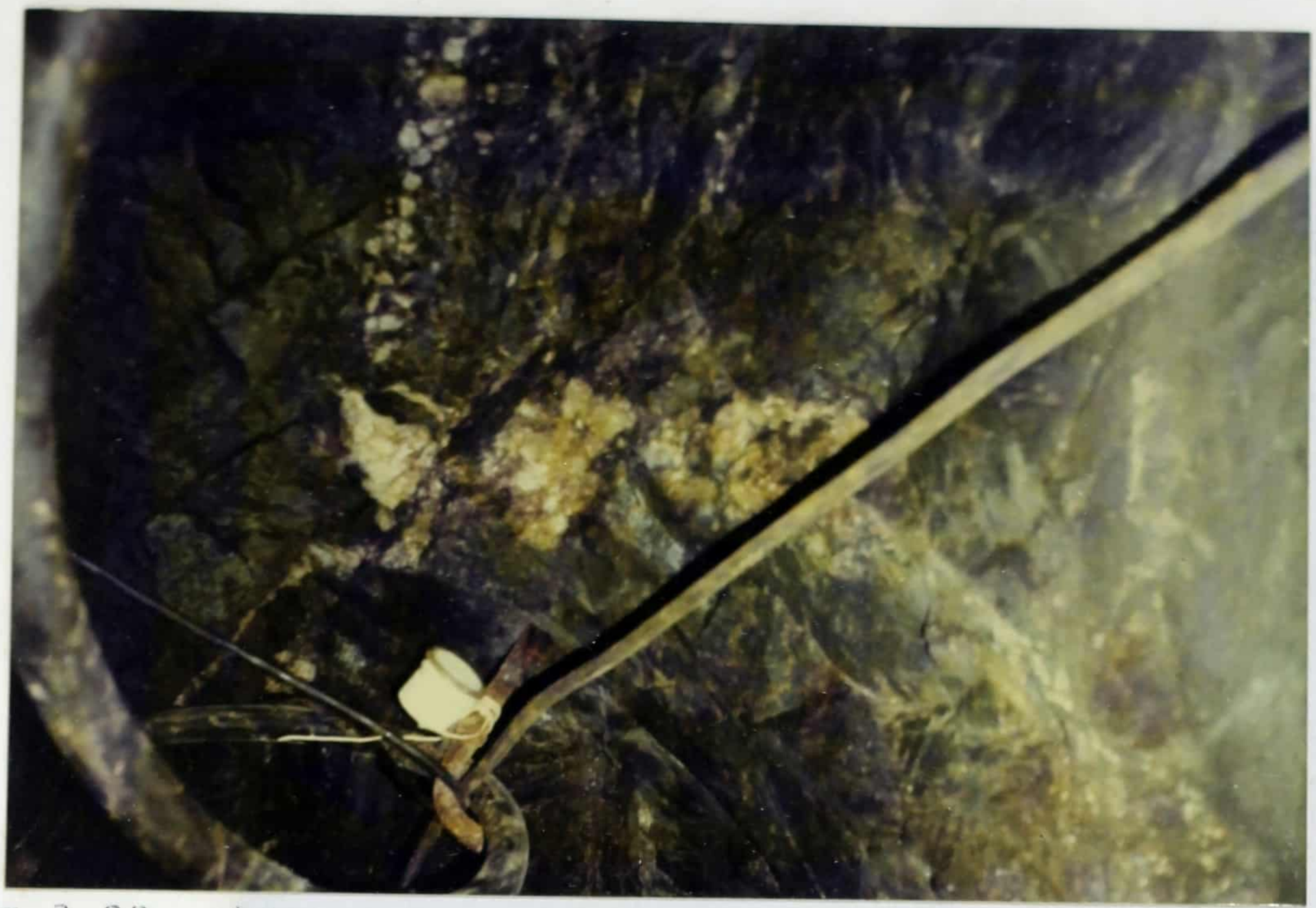

Fig.3.22, above,
the CR-39 stringed to an iron rod inside the side wall of the 14Level drive, Tarkwa Goldfields.

Fig.3.23, right,
the CR-39 plastic inside the can mounted at 17Level, winder house, Tarkwa Goldfields.

Fig.3.24, above,
the CB-29 stringed to an
iron rod inside the side
wall of the 25level drive,
Tarkwa Goldfields.

Fig.3.25, right,
the CB-29 plastic inside
the cab mounted at 25level,
sub-drive 2B, Tarkwa
Goldfields.

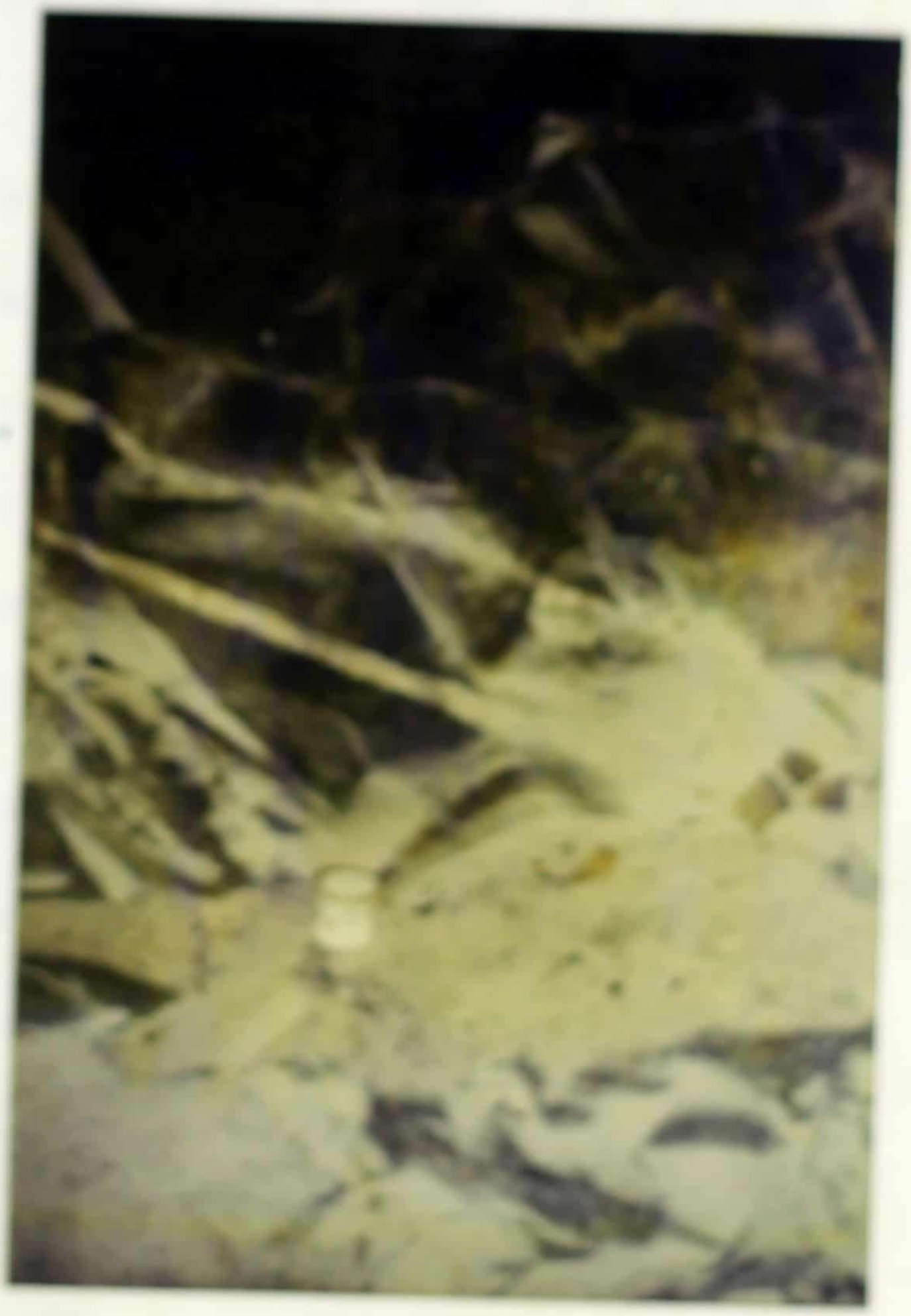

LIBRARY
UNIVERSITY OF SCIENCE AND TECHNOLOGY

Fig.3.24, above,
the CR-39 stringed to an iron rod inside the side wall of the 25Level drive, Tarkwa Goldfields.

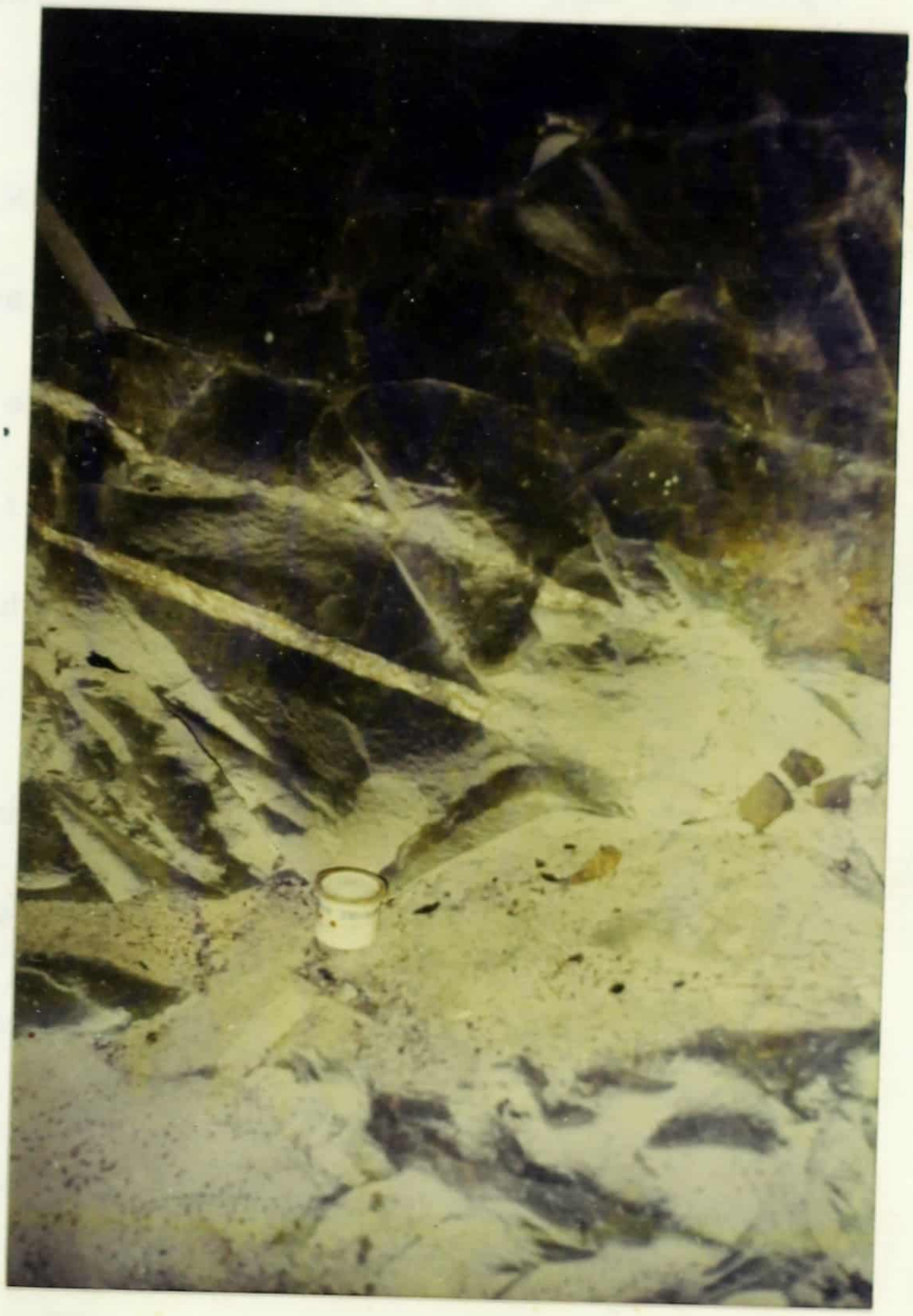

Fig.3.25, right,
the CR-39 plastic inside the can mounted at 25Level, sub-drive 2N, Tarkwa Goldfields.

UNIVERSITY OF SCIENCE AND TECHNOLOGY LIBRARY

## 3.2 MEASUREMENT OF THE PHYSICAL PARAMETERS

### 3.2.1 TECHNIQUES OF MEASURING THE AIR VELOCITY.

The vane anemometer, the standard instrument for general mine-ventilation work, was used. This is a classic device illustrating the mechanical effect of air in motion. It is a small windmill-like instrument consisting of a number of radial blades or impellers, a gearing mechanism, a clutch system and a pointer. In operation, it can be hand held with the blades oriented normal to the direction of air motion. The blades rotate at a speed proportional to the air velocity. The gearing mechanism translates the rotation directly into linear airflow in metres and the pointer integrates the flow on a marked dial. In Fig.3.26 the anemometer is incorporated with digital electronic device which takes only ten seconds to record the air velocity.

There are two methods of measuring the air velocity at a section of an airway in the drives. These are the fixed-point traversing and the continuous traversing methods. In the fixed-point traversing method, the airway cross section is first divided into a number of imaginary equal areas. This is followed by the measurement of the air velocity using the vane anemometer at the centre of each imaginary area so created. The average velocity for the areas is then found for the entire cross section. In the

continuous traversing the velocity measuring instrument is turned or started and the entire airway is traversed slowly, evenly and at a uniform speed. Here the average velocity for the cross section will then be the indicated reading on the instrument (Fig.3.27 and Fig.3.28).

The airflow rate Q of an airway is not measured directly but was calculated from the average velocity, V and the cross-sectional area of the airway, A, at the point of the measurement as Q = VA in cubic metres per second.

An average of four measurements was taken. See Tables 4.17 and 4.18 for the results at Tarkwa and Prestea Goldfields respectively.

Fig.3.26, The anemometer used for measuring the air velocity.

Fig.3.27, the continuous traversing method and

Fig.3.28, the fixed-point traversing method.

### 3.2.2 TEMPERATURE AND HUMIDITY MEASUREMENT

Ordinary laboratory mercury thermometer was used in the temperature measurements and this was made four times and the average taken.

In the humidity measurements, the sling psychrometer or the whirling hygrometer was used.

It consists of two identical thermometers; one measures the dry-bulb temperature, and the other with a cotton sleeve measures the wet-bulb temperatures. Both thermometers are mounted side by side in a rigid frame. A water reservoir, filled with tap water, keeps the wet-bulb sleeve wet at all times during the measurements. The frame is attached by a swivel connected to a handle for whirling. Fig.3.29.

By facing upstream and holding the handle of the instrument at arm's length in front of the body, the psychrometer was whirled for about 15 to 20 seconds and the readings were taken. Several of such measurements were made on four occasions and the mean found for the whole period. See Tables 4.19 and 4.20 for the results at Tarkwa and Prestea Goldfields respectively.

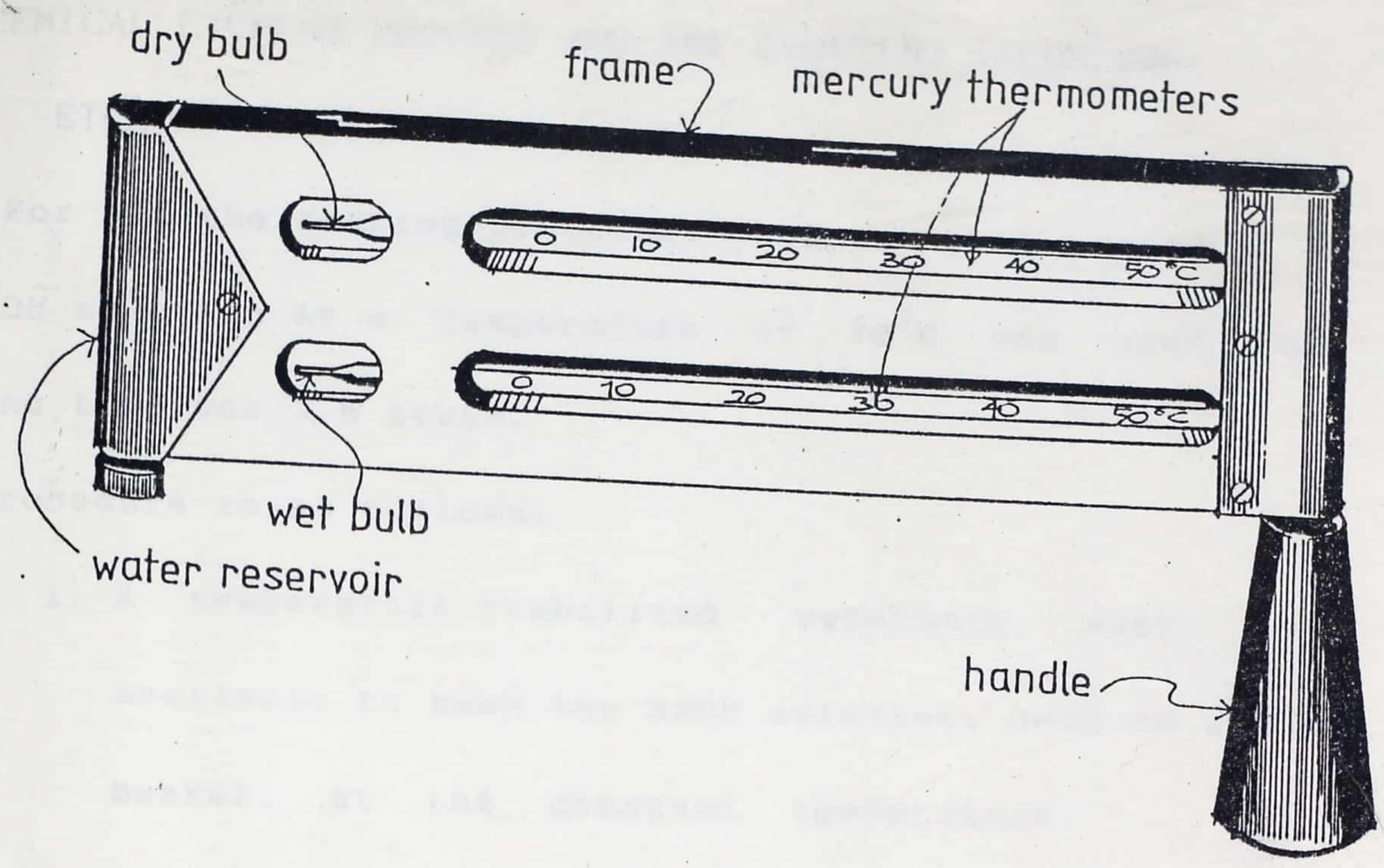

Fig.3.29. The sling psychrometer used in measuring the humidity.

## 3.3. CHEMICAL ETCHING PROCESS AND THE COUNTING TECHNIQUE.

### 3.3.1 ETCHING PROCEDURE

For all the etching processes done in this report, a 6M-NaOH solution at a temperature of 70°C was used The etching time was 3.5 hours.

The procedure is as follows;

i. A temperature-stabilized waterbath must be available to keep the NaOH solution, held in glass beaker, at the constant temperature.

ii. The plastics were removed from the cans and were then detached from the filter paper.

iii. The plastics were then fixed into a spiral spring and placed in the NaOH solution with a cover on the NaOH beaker in order to avoid quick change in the concentration through evaporation, as shown in Fig.3.30.

iv. After the etching process the plastics were rinsed in flowing cold water for some 10 to 30min.. The cold water quickly stops the etching of the left over - NaOH in the tracks. At the end of the rinsing, the plastics were then left hanging to air-dry in the laboratory overnight.

vi. The plastics now will be ready for counting under the optical microscope.

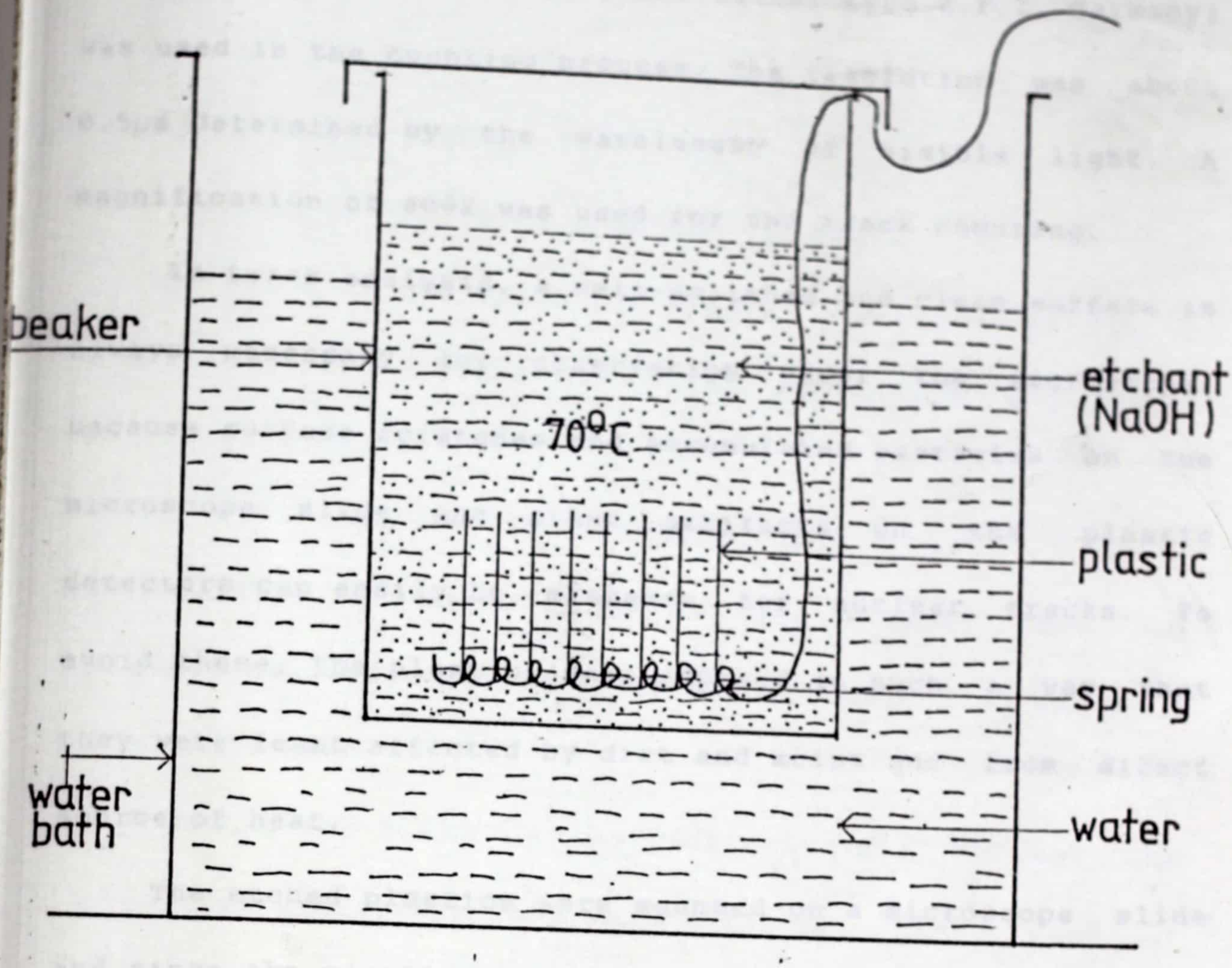


LIBRARY
UNIVERSITY OF SCIENCE AND TECHNOLOGY

Fig. 3.30 Experimental arrangement for the etching procedure.

### 3.3.2 THE COUNTING TECHNIQUE

An optical microscope (Carl Zeiss, type K.F.2, Germany) was used in the counting process. The resolution was about 0.5μm determined by the wavelength of visible light. A magnification of 400X was used for the track counting.

In track analysis, a well-polished and clean surface is always necessary for observation under the microscope, because surface scratches and accumulated particles on the microscope slide and other artifacts on the plastic detectors can easily be mistaken for nuclear tracks. To avoid these, the plastics were exposed in such a way that they were least affected by dirt and moist and from direct source of heat.

The etched plastics were mounted on a microscope slide and since the plastics were transparent a transmitted light was used in the scanning process. Most of the tracks appeared as regular shaped circular or elliptical dark patches against a general light background when the focal plane of the optical microscope coincided with the plastic surface. The number of tracks in the view was then counted. This process was repeated for the entire plastic surface for about 100 to 120 field of views and the mean number of tracks per field of view was obtained. This was followed by the calculation of the track density; which is the ratio of

the mean number of tracks per field of view to the area of view. (Appendix A)

## 3.4 EXPERIMENTAL ERRORS

### 3.4.1 ERRORS IN THE TRACK COUNTING TECHNIQUE

The error in the track counting of the tracks is due to the difficulties in using the optical microscope and these were the following;

i. One could not see tracks smaller than 0.5μm.

ii. The field of view to be counted was so small that the plastics needed, to be moved continuously to count a sizable area.

iii. Scanning the field of view with the eye through the optical microscope is a very difficult task. Some of the artifacts behave like the nuclear tracks so care was taken in trying to identify the tracks for counting

vi. In a situation where the number of tracks were many in a field of view, there is the possibility that one would not count number per field of view correctly.

v. Poor etching condition will also affect the number of tracks, because, the number of tracks increases with the temperature and concentration of the etchant.

Estimation of the error in the track density is based on the statistics of counting. (see appendix B)

### 3.4.2 ERRORS IN MEASURING THE RADON GAS

The error one encounters in the radon gas measurements is due to the exposure of the CR-39 plastics prior to the actual date of exposure. The plastics must be kept safe and from exposures to the environment (air) and must only be exposed at the time and place of investigation. To overcome this problem the plastics were kept in aluminium foil in self-sealed rubber envelopes and then in another thick paper envelope. After collection similar precaution is taken and the plastics kept in a refrigerator in the case where etching is not carried out directly after the end of the exposure time.

Some of the plastics were kept in the condition of the precaution above during the period of exposure as background measurements, but in most of these background plastics the observed track density was much less than the exposed plastics and therefore was neglected. The estimation of the error in the radon gas is based on the statistics of counting. (see appendix B)

### 3.4.3 ERRORS IN MEASURING THE PHYSICAL PARAMETERS.

The air velocity varies over the cross section of an opening because of the frictional resistance of the wall of the opening and the variations in the state of airflow The maximum velocity occurs at the geometric centres and

decreases gradually to a minimum at the walls of the opening, so if the instrument is not moved slowly and evenly there is bound to be an error in the measurements.

The airflow rate, Q is the product of the air velocity, V and the cross-sectional area, A and therefore error in Q will be a function of V and A. The error in V and A is a random one because of the irregular flow of the air velocity and the area of the opening walls. At a particular instant a number of measurements were made, some few metres away and from the opening with their corresponding areas and the mean taken. The standard error in V and in A is thus calculated.

The standard errors in the temperature and humidity measurements, were similarly treated. (See appendix C).

# CHAPTER FOUR

## 4.0 EXPERIMENTAL RESULTS

### 4.I THE TRACK DENSITY AND CALIBRATION FACTOR FOR CR-39 PLASTIC

To obtain the calibrated factor, six samples of the CR-39 plastics were irradiated in a controlled environment in the National Radiological Protection Board (NRPB, U.K.) radon chamber [35], described by Miles [40]. CR-39 plastics, attached to filter paper on the perspex lids of 5 x 6.5cm cans, were exposed to a known dose of radon gas for 40 hours. This was then sent to Kumasi for etching and counting. The average tracks per field of view for all the six plastics is 28.7±0.5 alpha tracks.

The track density is defined as the ratio of the average number of tracks to the area of field of view of the optical microscope. i.e

$$\text{Track density } (\rho) = \frac{\text{Ave. number of tracks}}{\text{Area of field of view}}$$

Area of field of view (see Appendix A)

$$= \pi\ (0.025)^2$$

$$= 1.96 \times 10^{-3} cm^2$$

Therefore, the average track density for the calibrated six plastics is $= 14643.0 \pm 273.3$ tracks $cm^{-2}$

LIBRARY
UNIVERSITY OF SCIENCE AND TECHNOLOGY

## 4.2 CALCULATION OF RADON EXPOSURE TERMS

### 4.2.1 THE BECQUEREL PER CUBIC METRE.

The activity of the radon dose given to the calibrated plastics is $55kBqm^{-3}$ for 40 hours, hence the radon concentration to the plastics is

$$C_{RN} = 55kBqm^{-3} \times 40hr$$

$$= 2.2\times10^{6}\ Bqm^{-3}hr$$

Since the track density obtained is proportional to the radon concentration, then,

$$\rho \propto C_{RN} \quad \text{or} \quad \rho = kC_{RN}$$

where k is the efficiency of the plastics, and

$$\frac{1}{k} = \frac{C_{RN}}{\rho} = \text{the calibrated factor}$$

$$= \frac{2.2\times 10^{6}\ Bqm^{-3}hr}{14643.0\ track/cm^{2}}$$

$$\boxed{tracks^{-1} = 150.2 \pm 2.8\ Bqm^{-3}hr\ tracks\ cm^{-2}}$$

From the above a factor of $150Bqm^{-3}hr\ tracks cm^{-2}$ was used to obtain the radon concentration in $Bqm^{-3}$ in a given environment. For example, in an environment with a track density of 3875 $tracks cm^{-2}$ in which the plastic was exposed for 106 days, will have a radon concentration given by;

$$\text{radon concn.} = \frac{(3875\ tracks cm^{-2}) \times (150\ \frac{Bqm^{-3}hr}{tracks/cm^{2}})}{106 \times 24hr}$$

$$= 228.5\ Bqm^{-3}$$

### 4.2.2 THE CALCULATION OF WORKING LEVEL, THE WORKING LEVEL MONTH AND THE SIEVERT

The working level can be calculated from the expression;

$$WL = \frac{F}{100} \text{ (radon concentration in pCi/l)}$$

where $F$ = equilibrium factor $F < 1.0$

$$= \frac{C_e}{C_o}$$

$C_e$ = equilibrium equivalent of a non-equilibrium mixture of the short-lived radon daughters in air.

$C_o$ = actual activity concentration of radon in air.

In the case where the equilibrium factor is not known, a value of 0.9 [36] is used, which is close to the theoretical maximum. [37] (See appendix E) for conversion tables.

a. RESULTS FROM THE RADON MEASUREMENTS AT TARKWA GOLDFIELDS

Table 4.1, Track density and radon concn., at Tarkwa Goldfields, (underground) the first period, with exposure time of $3^1/2$ months

| Location of cans in the Drives | | Track density track/cm$^2$ | Radon concn. (Bqm$^{-3}$) | |
|---|---|---|---|---|
| | | | | level's mean |
| 10L EVEL | Gangway | 2178.6±105.4 | 124.9±6.0 | 97.3± 7.5 |
| | Tramming drive (Bin) | 1214.3± 78.7 | 69.6±4.5 | |
| 12L EVEL | Gangway | 1816.3± 96.3 | 104.2±5.5 | 122.3± 8.4 |
| | Level's cross-cut | 2449.0±111.7 | 140.4±6.4 | |
| 14L EVEL | Gangway T'former s'tion | 1673.5± 92.4 | 96.0±5.3 | 145.4± 9.3 |
| | Level's cross-cut | 3398.0±131.7 | 194.8±7.6 | |
| 17L EVEL | Gangway | 3428.6±132.1 | 196.6±7.6 | 157.9± 9.6 |
| | Winder house | 2076.5±102.9 | 119.1±5.9 | |
| 18L EVEL | Gangway | 2173.5±108.6 | 124.7±6.2 | 127.3± 8.9 |
| | Level's cross-cut | 2265.3±110.9 | 129.9±6.4 | |
| 20L EVEL | Gangway | 1658.2± 92.0 | 95.1±5.3 | 95.7± 7.5 |
| | Winder house | 1678.6± 92.5 | 96.3±5.3 | |
| 24 LEVEL | 2416 incline | 1617.4± 90.8 | 92.7±5.2 | 92.7±5.2 |
| 25L EVEL | 2525 subdrive 2 north | 3806.1±139.4 | 218.2±8.0 | 217.9±11.0 |
| | 2525 subdrive 1 south | 3794.1±132.7 | 217.6±7.6 | |

Table 4.2, Track density and Radon concn. at Tarkwa Goldfields (underground) the second period, with exposure time of $3^1/2$ months.

| Location of cans in the Drives | | Track density (tracks/cm$^2$) | Radon concn. (Bqm$^{-3}$) | |
|---|---|---|---|---|
| | | | | level's mean |
| 10L E V E L | Gangway | 1476.6± 82.8 | 87.3±5.0 | 73.4± 6.4 |
| | Tramming drive (Bin) | 1006.5± 68.3 | 59.4±4.0 | |
| 12L E V E L | Gangway | 1316.3± 82.0 | 75.5±4.7 | 105.5± 7.9 |
| | Level cross-cut | 2295.9±108.2 | 135.4±6.4 | |
| 14L E V E L | Gangway T'former S'tion | 964.3± 70.1 | 56.9±4.1 | 118.7± 8.5 |
| | Level cross-cut | 3061.2±125.0 | 180.5±7.4 | |
| 17L E V E L | Gangway | 3438.8±120.3 | 202.8±7.1 | 157.8± 9.2 |
| | Winder house | 1913.3± 99.0 | 112.8±5.8 | |
| 18L E V E L | Gangway | 1903.1± 98.5 | 112.2±5.8 | 125.0± 8.6 |
| | Level cross-cut | 2336.7±109.2 | 137.8±6.4 | |
| 20L E V E L | Gangway | 1821.4± 96.4 | 107.4±5.7 | 107.6± 8.0 |
| | Winder house | 1828.5± 96.6 | 107.7±5.6 | |
| 24 LEVEL | 2416 incline | 1673.5± 92.4 | 98.7±5.5 | 98.7±5.5 |
| 25L E V E L | 2525 subdrive 2 north | 3403.0± 132.0 | 200.7±7.8 | 234.5±11.9 |
| | 2525 subdrive 1 south | 4551.0±152.6 | 268.3±9.0 | |

Table 4.3, Track density and Radon concn. at Tarkwa Goldfields (the mine offices), the first period of exposure for $3^1/2$ months.

| Location of cans in mine offices | Track density (track/$cm^2$ | Radon concn. ($Bqm^{-3}$) |
|---|---|---|
| Chief of Personnel | * | * |
| Personnel | 663.3±58.2 | 36.4±3.2 |
| Stores Department | 561.2±48.9 | 30.8±2.7 |
| Accounts | 561.2±48.9 | 30.8±2.7 |
| Akoon Shaft top | 673.5±58.6 | 36.9±3.2 |
| Electrical Shop | 561.2±48.9 | 30.8±2.7 |
| Carpentary Shop | * | * |
| Foundary | 756.8±56.7 | 41.5±3.1 |
| Assay Department | *** | *** |
| Mill Department | 566.3±45.5 | 30.3±2.4 |
| Security | 607.1±55.7 | 32.4±3.0 |

*** Plastic was destroyed by rodents
* Plastics got lost in the laboratory

Table 4.4, Track density and Radon concn. at Tarkwa Goldfields (the mine offices), the second period of exposure for $3^1/2$ month.

| Location of cans in the mine offices | Track density (tracks/$cm^2$) | Radon concn. ($Bqm^{-3}$) |
|---|---|---|
| Chief Personnel | 750.0±1.9 | 41.5± 3.4 |
| Personnel | 734.7±61.2 | 40.6±3.4 |
| Stores Department | 673.5±58.6 | 37.3±3.2 |
| Accounts | 720.0±63.9 | 39.8±3.5 |
| Akoon Shaft top | 617.4±56.1 | 34.2±3.1 |
| Electrical shop | 806.1±64.1 | 44.6±3.6 |
| Carpentary shop | 637.8±52.1 | 35.3±2.9 |
| Foundary | 672.5±55.9 | 37.2±3.1 |
| Assay Department | 785.7±63.3 | 49.1±4.0 |
| Mill Department | 709.2±60.2 | 39.2±3.3 |
| Security | 795.9±63.7 | 44.0±3.5 |

Table 4.5, Exposure units for the locations of cans at Tarkwa Goldfields (underground). for the first period.

| Location of plastic exposure in the drive | | Working Level (mWL) | Working Level Month (WLM) | Dose (μSv/hr) |
|---|---|---|---|---|
| 10L EVEL | Gangway | 30.4±1.6 | 0.468 | 0.697 |
| | Tramming Drive (Bin) | 16.9±1.2 | 0.260 | 0.388 |
| 12L EVEL | Gangway | 25.4±1.5 | 0.391 | 0.583 |
| | Level cross-cut | 34.2±1.7 | 0.526 | 0.784 |
| 14L EVEL | Gangway | 23.4±1.4 | 0.360 | 0.537 |
| | Level cross-cut | 47.4±2.1 | 0.729 | 1.087 |
| 17L EVEL | Gangway | 47.8±2.1 | 0.736 | 1.096 |
| | Winder house | 29.0±1.6 | 0.445 | 0.665 |
| 18L EVEL | Gangway | 30.3±1.7 | 0.466 | 0.695 |
| | Level drive | 31.6±1.7 | 0.486 | 0.725 |
| 20L EVEL | Gangway | 23.1±1.4 | 0.356 | 0.530 |
| | Winder house | 23.4±1.4 | 0.360 | 0.537 |
| 24 LEVEL | 2416 Incline | 22.6±1.4 | 0.348 | 0.518 |
| 25L EVEL | 2525 Subdrive 2 north | 53.1±2.2 | 0.817 | 1.218 |
| | 2525 Subdrive 1 south | 52.9±2.1 | 0.814 | 1.213 |

Table 4.6, Exposure units for the locations at Tarkwa Goldfields (underground), for the second period.

| LOCATION OF PLASTIC EXPOSURE IN THE DRIVE | | WORKING LEVEL (mWL) | WORKING LEVEL MONTH (WLM) | DOSE (μSv/hr) |
|---|---|---|---|---|
| 10L EVEL | Gangway | 21.2±1.4 | 0.317 | 0.500 |
| | Tramming drive (Bin) | 14.5±1.1 | 0.217 | 0.342 |
| 12L EVEL | Gangway | 18.4±1.3 | 0.275 | 0.434 |
| | Level cross-cut | 32.9±1.7 | 0.489 | 0.776 |
| 14L EVEL | Gangway | 13.9±1.1 | 0.208 | 0.328 |
| | Level cross-cut | 43.9±2.0 | 0.657 | 1.035 |
| 17L EVEL | Gangway | 49.3±1.9 | 0.738 | 1.163 |
| | Winder house | 27.5±1.6 | 0.412 | 0.649 |
| 18L EVEL | Gangway | 27.3±1.6 | 0.409 | 0.644 |
| | Level drive | 33.5±1.7 | 0.501 | 0.790 |
| 20L EVEL | Gangway | 26.1±1.5 | 0.391 | 0.616 |
| | Winder house | 26.3±1.5 | 0.394 | 0.620 |
| 24 LEVEL | 2416 Incline | 24.0±1.5 | 0.359 | 0.566 |
| 25L EVEL | 2525 Subdrive 2 north | 48.8±2.1 | 0.730 | 1.151 |
| | 2525 Subdrive 1 south | 65.3±2.4 | 0.977 | 1.540 |

Table 4.7, Exposure units for the location at Tarkwa Goldfields (the mine offices), the first period.

| LOCATION OF PLASTIC EXPOSURE IN OFFICE | WORKING LEVEL (mWL) | WORKING LEVEL MONTH (WLM) | DOSE (μSv/hr) |
|---|---|---|---|
| CHIEF PERSONNEL | * | * | * |
| PERSONNEL | 9.7±0.9 | 0.142 | 0.233 |
| STORES DEPARTMENT | 8.2±0.7 | 0.120 | 0.197 |
| ACCOUNTS | 8.4±0.7 | 0.123 | 0.202 |
| AKOON SHAFT TOP | 9.9±0.9 | 0.145 | 0.238 |
| ELECTRICAL SHOP | 8.1±0.7 | 0.119 | 0.195 |
| CARPENTARY SHOP | * | * | * |
| FOUNDARY | 11.1±0.8 | 0.163 | 0.267 |
| ASSAY DEPARTMENT | * | * | * |
| MILL DEPARTMENT | 8.3±0.7 | 0.122 | 0.200 |
| SECURITY | 8.9±0.9 | 0.131 | 0.214 |

* Lost plastics

b. RESULTS FROM RADON MEASUREMEMTS AT PRESTEA GOLDFIELDS

Table 4.9, Track density and Radon concn. at Prestea Goldfields (underground), the first period of exposure, for $3^1/2$ months

| Location of cans in the Drives | | Track density (tracks/cm$^2$) | Radon concn. (Bqm$^{-3}$) | |
|---|---|---|---|---|
| | | | | level's mean |
| 6L EVEL | Gangway | 989.8± 71.1 | 58.4±4.2 | 100.7± 7.8 |
| | 258 South cross-cut | 2423.5±111.2 | 142.9±6.0 | |
| 9L EVEL | Gangway | 1392.9± 84.3 | 82.1±5.0 | 155.2± 9.7 |
| | 254 South cross-cut | 3872.5±140.6 | 228.3±8.3 | |
| 12L EVEL | Gangway | 714.0± 60.4 | 42.6±3.6 | 347.6±14.5 |
| | 224 South cross-cut | 11066.3±237.6 | 652.5±14 | |
| 15L EVEL | Gangway | 1061.2± 73.6 | 62.6±4.3 | |
| | 235 South cross-cut | *** | *** | |
| 23L EVEL | Gangway | 1341.8± 82.7 | 79.1±4.9 | 138.6± 9.2 |
| | 224 South cross-cut | 3326.5±130.3 | 198.0±7.8 | |
| 30L EVEL | Gangway | *** | *** | 166.1± 7.1 |
| | Number 4 Shaft | 2816.3±119.9 | 166.1±7.1 | |

*** Plastics were destroyed by miners.

Table 4.10, Track density and Radon concn. at Prestea Goldfields, (underground) the second period with exposure time of $3^1/2$ months

| Location of cans in the Drives | | Track density (tracks/cm$^2$) | Radon concn. (Bqm$^{-3}$) | |
|---|---|---|---|---|
| | | | | level's mean |
| 6L EVEL | Gangway | 1173.5± 70.6 | 69.9±4.2 | 90.2± 7.2 |
| | 258 South cross-cut | 1857.1± 97.3 | 110.5±5.8 | |
| 9L EVEL | Gangway | 1867.4± 97.6 | 111.2±5.8 | 192.8±10.1 |
| | 254 South cross-cut | 4608.8±140.0 | 274.3±8.3 | |
| 12L EVEL | Gangway | 836.7± 65.3 | 49.8±3.9 | 463.8±16.8 |
| | 224 South cross-cut | 14744.9±274.3 | 877.7±16.3 | |
| 15L EVEL | Gangway | 1056.1± 67.0 | 62.9±4.0 | |
| | 235 South cross-cut | *** | *** | |
| 23L EVEL | Gangway | 1097.9± 67.8 | 64.3±4.0 | 110.7± 7.5 |
| | 224 South cross-cut | 2640.0±106.6 | 157.1±6.3 | |
| 30L EVEL | Gangway | *** | *** | 174.3± 7.3 |
| | Number 4 Shaft | 2928.6±122.2 | 174.3±7.3 | |

*** Plastics were destroyed by miners.

Table 4.11, Track density and Radon concn. at Prestea Goldfields (the mine offices) the first period with exposure time of $3^1/2$ months

| LOCATION OF THE CANS IN THE MINE OFFICE | TRACK DENSITY (tracks/cm$^2$) | RADON CONCN. (Bqm$^{-3}$) |
|---|---|---|
| CHIELF GEOLOGY | 612.3±51.0 | 32.7±2.7 |
| GENERAL MINES MANAGER | 760.2±62.3 | 40.6±3.3 |
| CHIELF MINING ENGINEER | 719.4±60.6 | 38.4±3.2 |
| TRANSPORT YARD | 678.6±58.8 | 36.3±3.1 |
| SECURITY | 591.8±55.0 | 31.6±2.9 |
| UNDERGROUND MANAGER | 846.9±65.7 | 45.2±3.5 |
| SHAFT COLLAR | 629.3±51.7 | 33.6±2.8 |
| SHAFT CONTROL ROOM | 1102.0±75.0 | 58.9±4.0 |
| CRUSHER HOUSE | 720.0±63.9 | 38.5±3.4 |
| BALL ROOM | 887.6±70.1 | 47.4±3.7 |
| ASSAY DEPARTMENT | 831.6±65.1 | 44.8±3.5 |
| OUTSIDE ASSAY DEPT. | 867.4±66.5 | 46.7±3.6 |
| ENGINEERING DEPARTMENT | 877.6±66.9 | 46.9±3.8 |
| CARPENTARY SHOP | 617.4±56.1 | 33.0±3.0 |
| ROASTER SECTION | ** | ** |

** No measurement was made

Table 4.12, Track density and Radon concn. at Prestea goldfields (the mine office) the second period with exposure time of $3^1/2$ months.

LIBRARY
UNIVERSITY OF SCIENCE AND TECHNOLOGY

| LOCATION OF CAN IN THE MINE OFFICE | TRACK DENSITY (tracks/cm$^2$) | RADON CONCN. (Bqm$^{-3}$) |
|---|---|---|
| CHIEF GEOLOGY | 1010.2±71.8 | 60.1±4.3 |
| GENERAL MINES MANAGER | 826.5±64.9 | 49.2±3.9 |
| CHIEF MINING ENGINEER | 816.3±64.5 | 48.6±3.8 |
| TRANSPORT YARD | 1051.0±73.2 | 62.6±4.4 |
| SECURITY | 933.7±69.0 | 55.6±4.1 |
| UNDERGROUND MANAGER | 780.6±63.1 | 46.5±3.8 |
| SHAFT COLLAR | 795.9±63.7 | 47.4±3.8 |
| SHAFT CONTROL ROOM | 1020.4±72.2 | 60.7±4.3 |
| CRUSHER HOUSE | 862.3±66.3 | 51.3±4.0 |
| BALL ROOM | 974.5±70.5 | 58.0±4.2 |
| ASSAY DEPARTMENT | 699.0±59.7 | 41.6±3.6 |
| OUTSIDE ASSAY DEPT. | 964.3±70.1 | 57.4±4.2 |
| ENGINEERING DEPARTMENT | 892.9±67.5 | 53.2±4.0 |
| CARPENTARY SHOP | 1280.6±80.8 | 76.2±4.8 |
| ROASTER SECTION | 1076.5±74.1 | 64.1±4.4 |

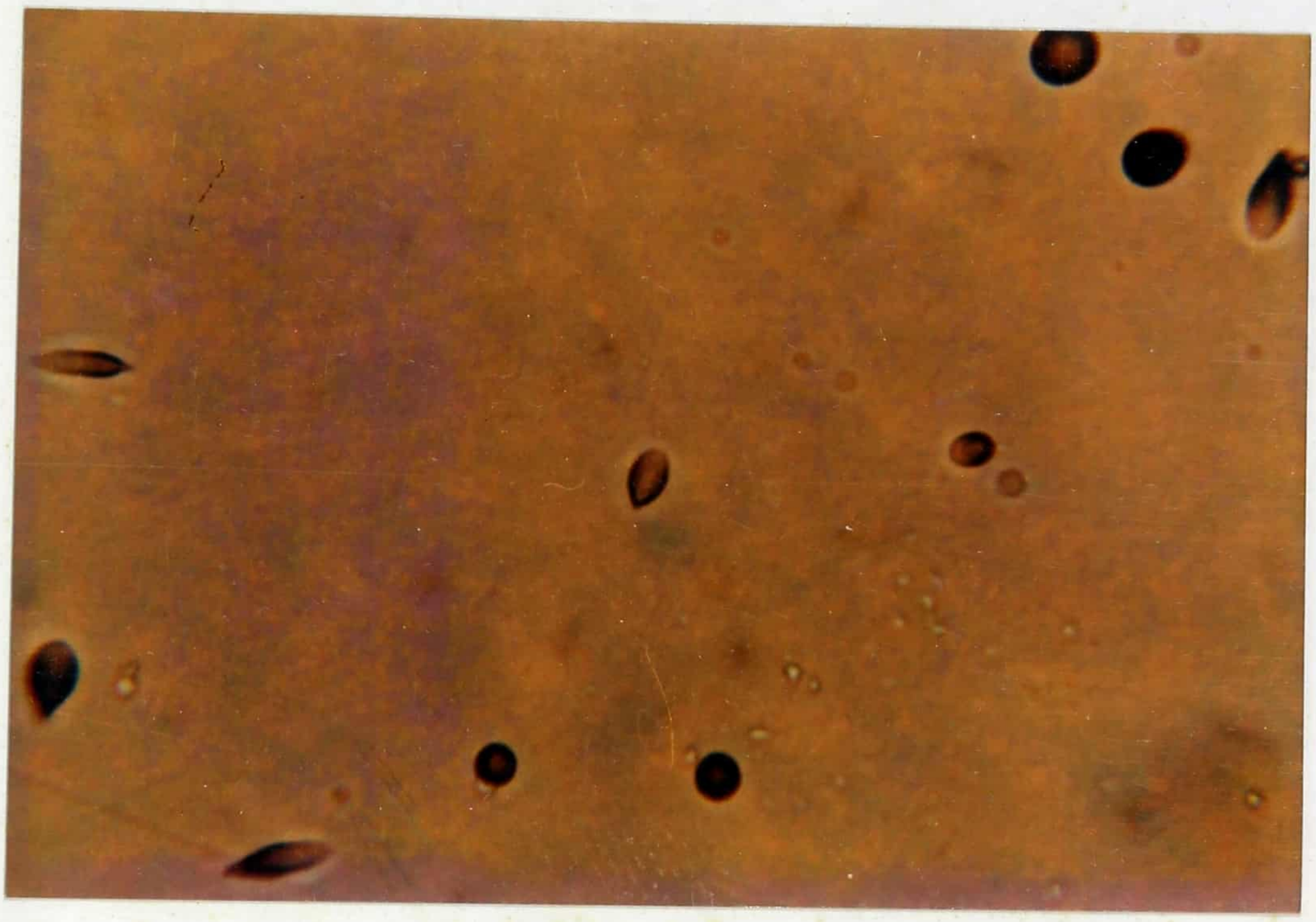

Fig.4.1 & 4.2 A section of the α-particle tracks in the CR-39 plastic exposed at 9Level (254 cross-cut), Prestea Goldields. Magnification 600X.

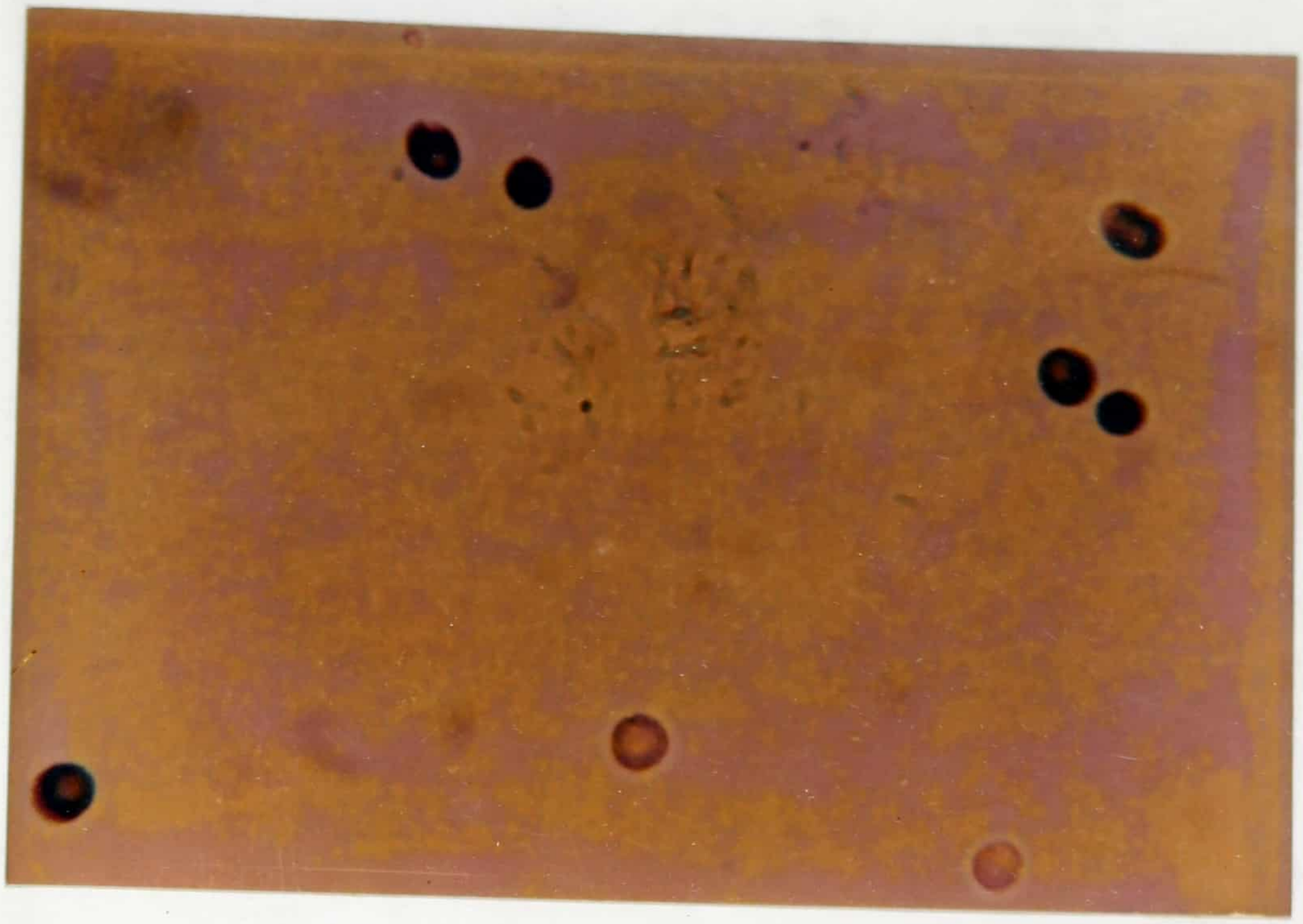

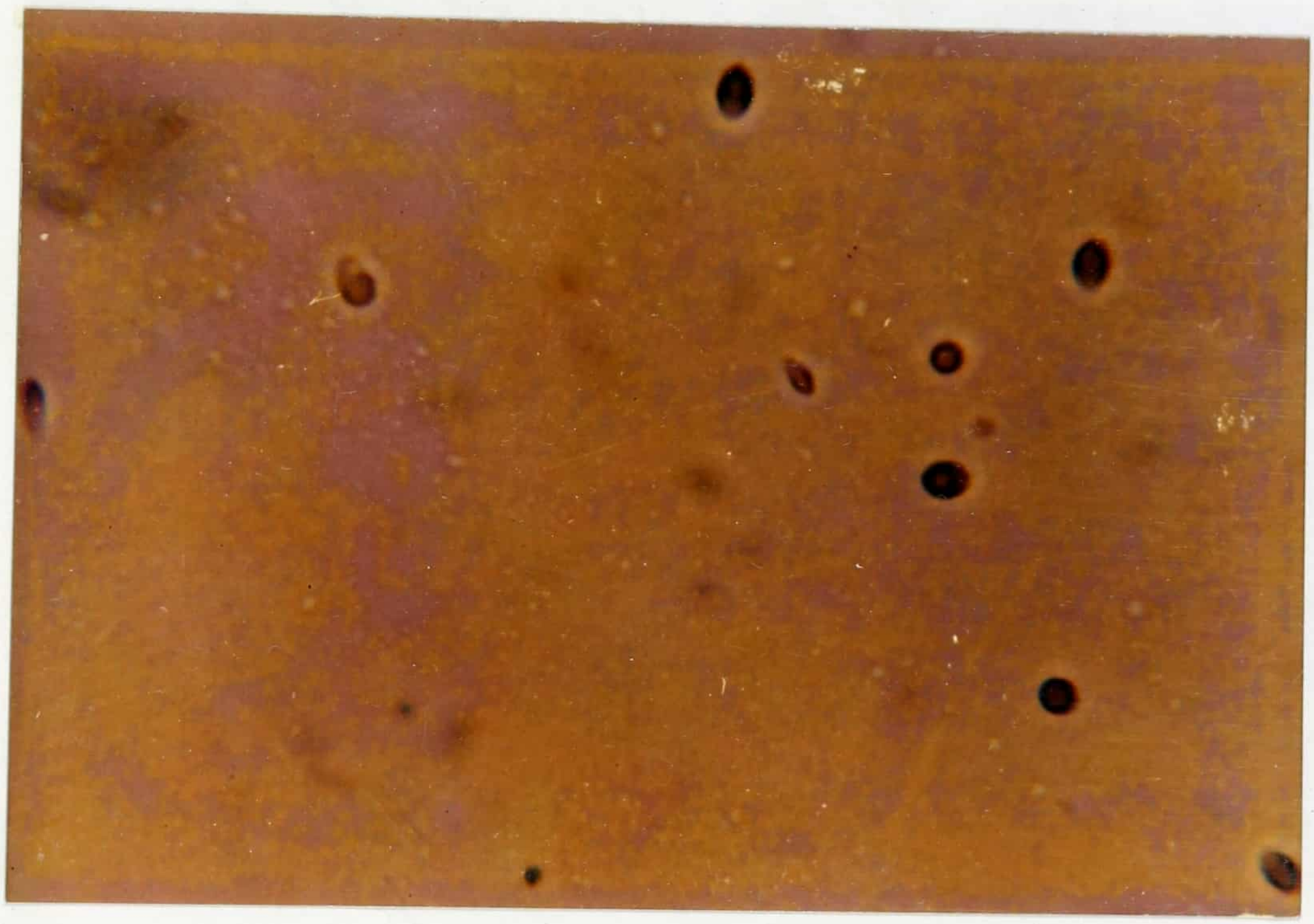

Fig.4.3 & 4.4 A section of the α-particle tracks in the CR-39 plastic exposed at 12Level (224 cross-cut), Prestea Goldields. Magnification 600X.

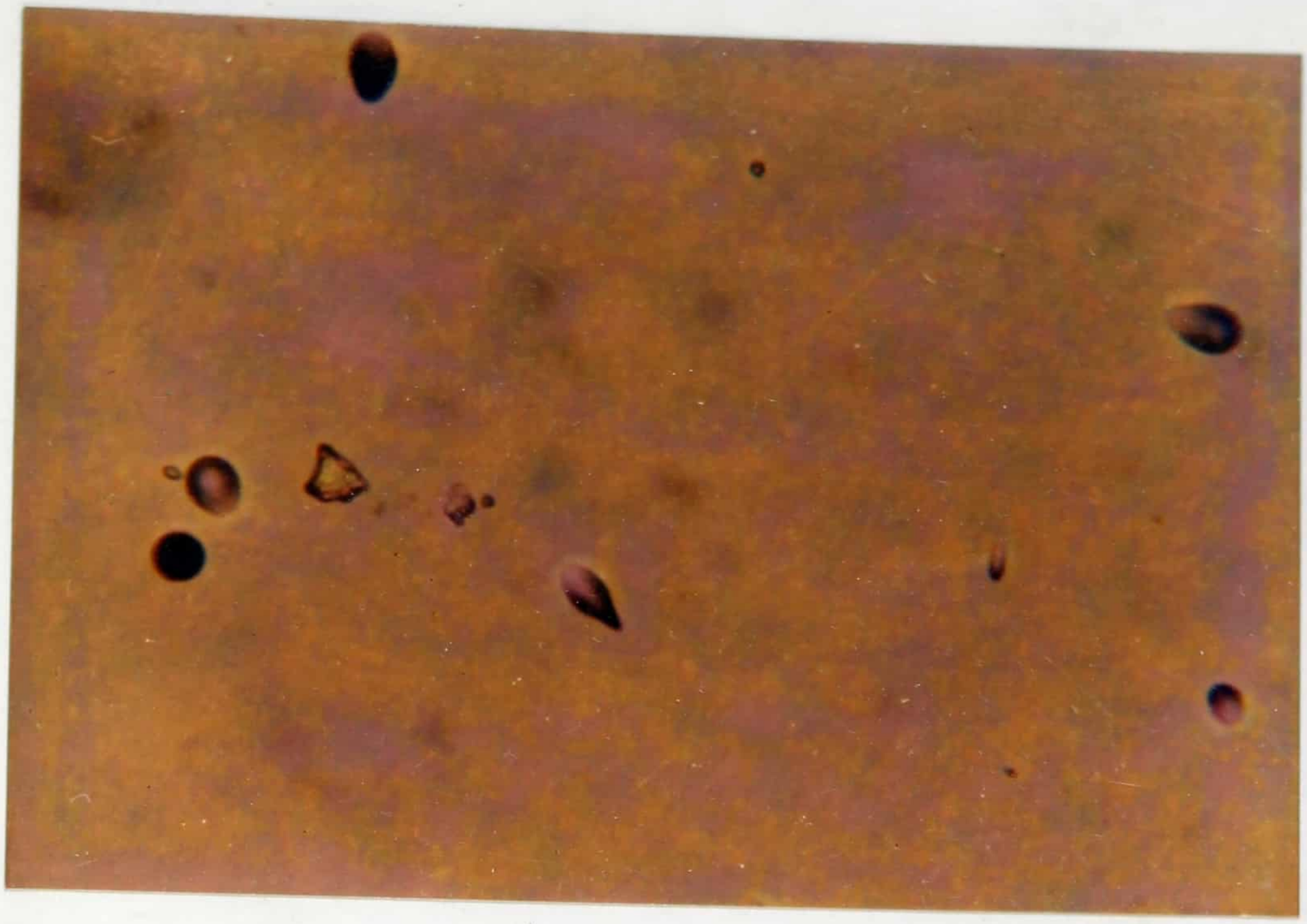

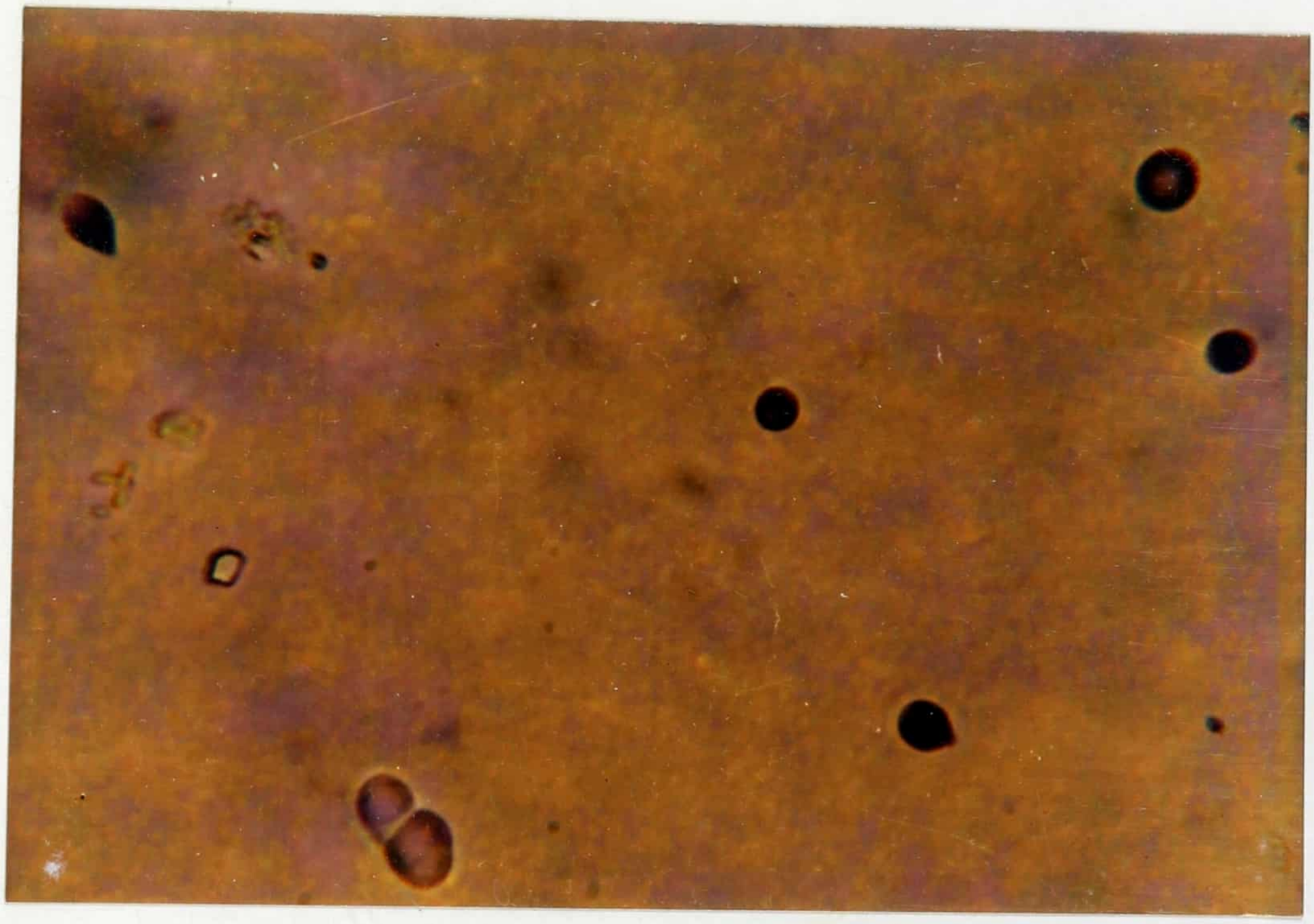

Fig.4.5 & 4.6 A section of the α-particle tracks in the CR-39 plastic exposed at 17Level (Gangway), Tarkwa Goldields. Magnification 600X.

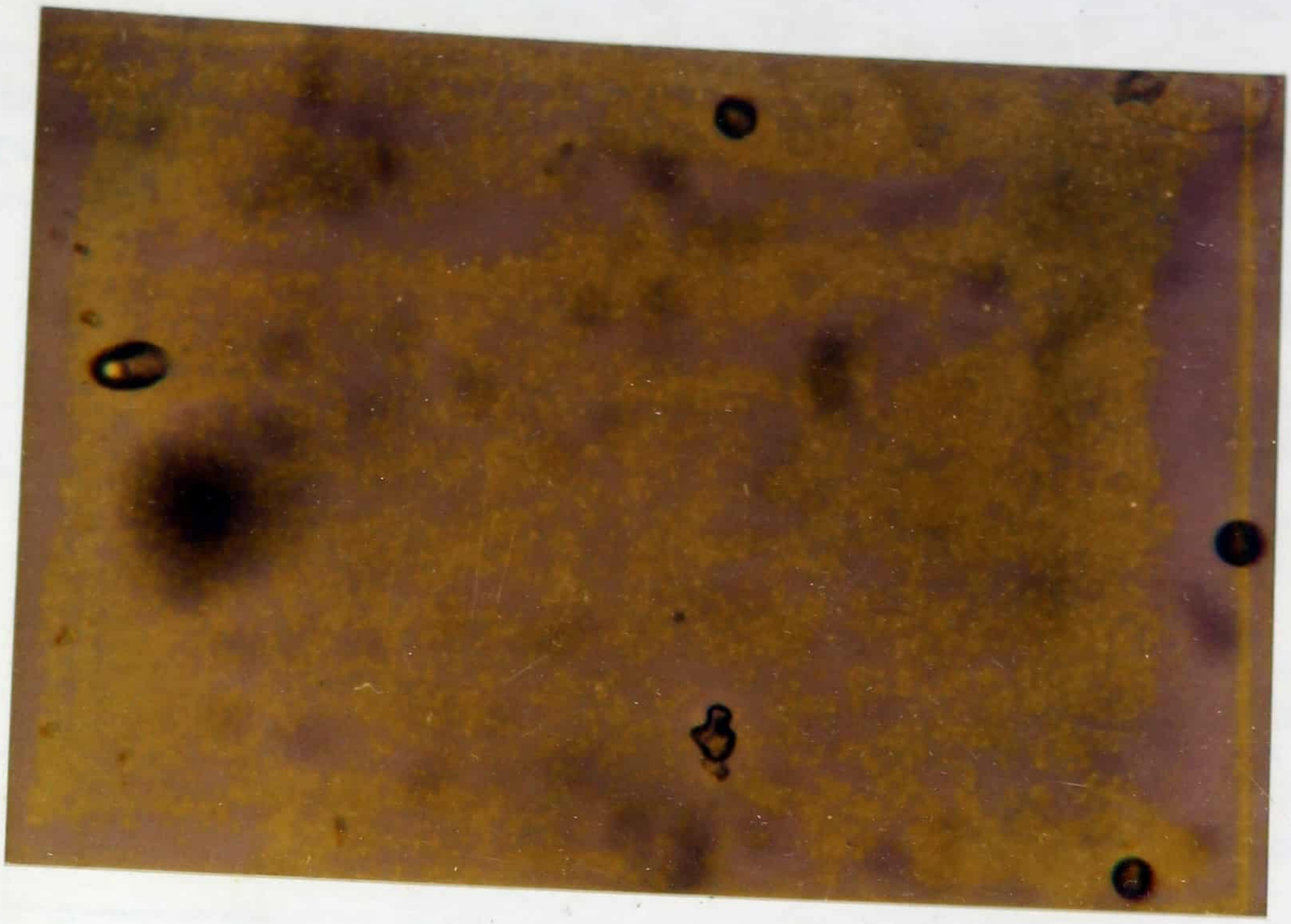

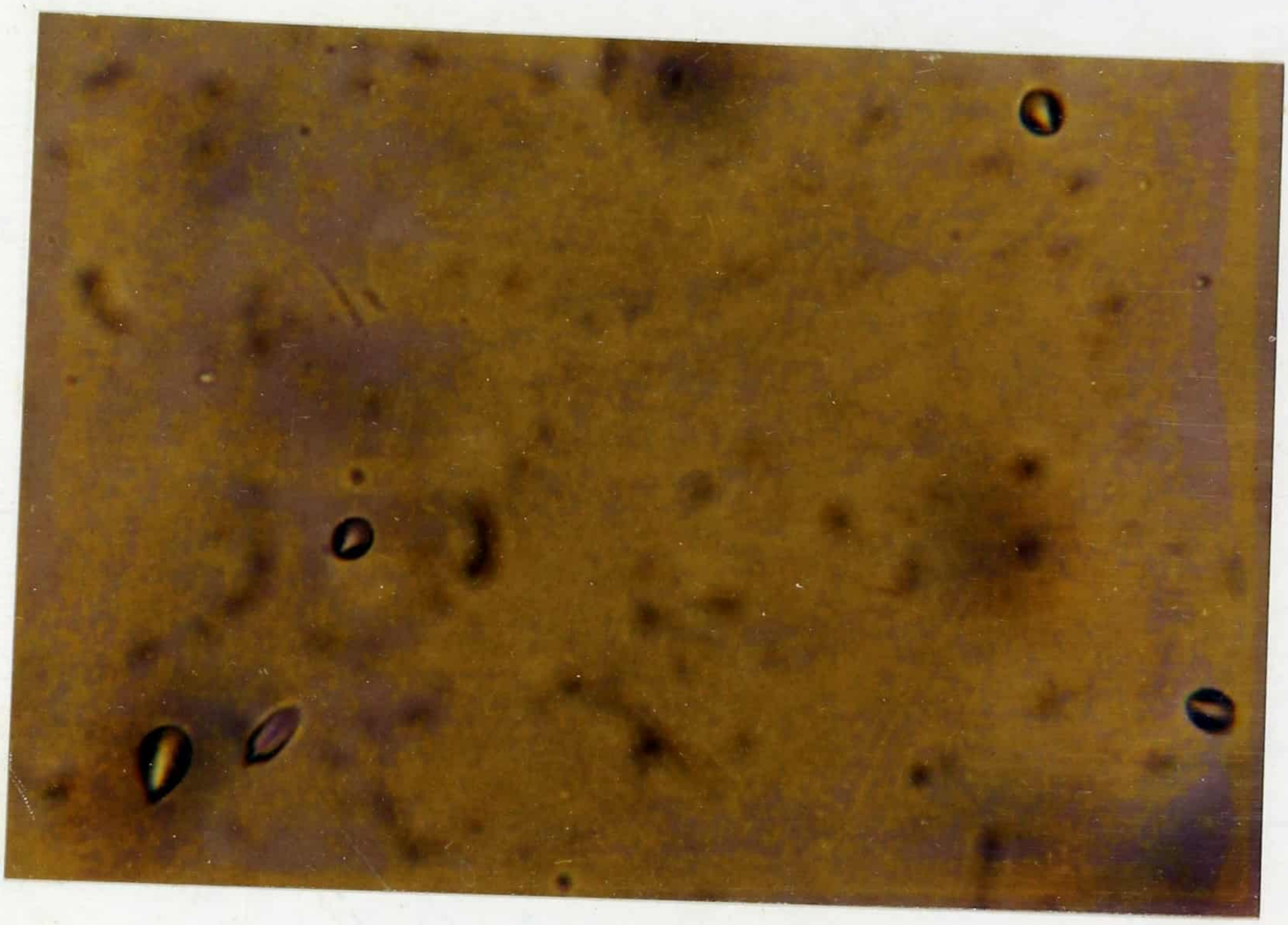

Fig.4.7 & 4.8 A section of the α-particle tracks in the CR-39 plastic exposed at 25Level (Subdrive 2N), Tarkwa Goldields. Magnification 600X.

Table 4.13, Exposure units for the locations of the cans at Prestea the Goldfields (underground). for the first period.

| Location of plastic exposure in the drive | | Working Level (mWL) | Working Level Month (WLM) | Dose (μSv/hr) |
|---|---|---|---|---|
| 6L EVEL | Gangway | 14.2±1.1 | 0.213 | 0.335 |
| | 258 South cross-cut | 34.8±1.8 | 0.521 | 0.821 |
| 9L EVEL | Gangway | 20.0±1.4 | 0.299 | 0.472 |
| | 254 South cross-cut | 55.5±2.2 | 0.831 | 1.309 |
| 12L EVEL | Gangway | 10.4±1.0 | 0.156 | 0.245 |
| | 224 South cross-cut | 158.7±3.8 | 2.375 | 3.743 |
| 15L EVEL | Gangway | 15.2±1.2 | 0.228 | 0.359 |
| | 235 South cross-cut | * | * | * |
| 23L EVEL | Gangway | 19.2±1.3 | 0.287 | 0.453 |
| | 224 South cross-cut | 48.2±2.1 | 0.721 | 1.137 |
| 30L EVEL | Gangway | * | * | * |
| | Number 4 Shaft | 40.4±1.9 | 0.605 | 0.953 |

* No measurements were made

Table 4.14, Exposure units for the locations of the cans.at Prestea Goldfields (underground), for the second period.

| Location of plastic exposure in the drive | | Working Level (mWL) | Working Level Month (WLM) | Dose (μSv/hr) |
|---|---|---|---|---|
| 6L EVEL | Gangway | 17.0±1.1 | 0.252 | 0.405 |
| | 258 South cross-cut | 26.9±1.6 | 0.399 | 0.641 |
| 9L EVEL | Gangway | 27.1±1.6 | 0.402 | 0.652 |
| | 254 South cross-cut | 66.7±2.2 | 0.989 | 1.588 |
| 12L EVEL | Gangway | 12.1±1.1 | 0.179 | 0.288 |
| | 224 South cross-cut | 213.5±4.4 | 3.157 | 5.083 |
| 15L EVEL | Gangway | 15.3±1.1 | 0.227 | 0.364 |
| | 235 South cross-cut | * | * | * |
| 23L EVEL | Gangway | 15.6±1.1 | 0.231 | 0.371 |
| | 224 South cross-cut | 38.2±1.7 | 0.566 | 0.910 |
| 30L EVEL | Gangway | * | * | * |
| | Number 4 Shaft | 42.4±2.0 | 0.629 | 1.010 |

* No measuremnets were made.

Table 4.15, Exposure units for the location at Prestea Goldfields (the mine offices), the first period,

| LOCATION OF PLASTIC EXPOSURE IN OFFICE | WORKING LEVEL (mWL) | WORKING LEVEL MONTH (WLM) | DOSE (μSv/hr) |
|---|---|---|---|
| CHIEF GEOLOGY | 8.0±0.7 | 0.121 | 0.187 |
| GENERAL MINES MANAGER | 9.9±0.8 | 0.150 | 0.231 |
| CHIEF MINING ENGINEER | 9.3±0.8 | 0.141 | 0.217 |
| TRANSPORT YARD | 8.8±0.7 | 0.133 | 0.206 |
| SECURITY | 7.7±0.7 | 0.116 | 0.180 |
| UNDERGROUND MANAGER | 11.0±0.9 | 0.166 | 0.257 |
| SHAFT COLLAR | 8.2±0.7 | 0.124 | 0.192 |
| SHAFT CONTROL ROOM | 14.3±1.0 | 0.216 | 0.334 |
| CRUSHER HOUSE | 9.4±0.8 | 0.142 | 0.220 |
| BALL ROOM | 11.5±0.9 | 0.174 | 0.269 |
| ASSAY DEPARTMENT | 10.9±0.9 | 0.165 | 0.255 |
| OUTSIDE ASSAY DEPT. | 11.4±0.9 | 0.172 | 0.266 |
| ENGINEERING DEPT | 11.4±0.9 | 0.172 | 0.266 |
| CARPENTARY SHOP | 8.0±0.7 | 0.121 | 0.187 |
| ROASTER SECTION | * | * | * |

* No measurement was made.

Table 4.16 Exposure units for the location at Prestea Goldfields (the mine offices), the second period.

| LOCATION OF PLASTIC EXPOSURE IN OFFICE | WORKING LEVEL (mWL) | WORKING LEVEL MONTH (WLM) | DOSE (μSv/hr) |
|---|---|---|---|
| CHIEF GEOLOGY | 14.6±1.1 | 0.216 | 0.348 |
| GENERAL MINES MANAGER | 12.0±1.0 | 0.178 | 0.286 |
| CHIEF MINING ENGINEER | 11.8±0.9 | 0.175 | 0.281 |
| TRANSPORT YARD | 15.2±1.1 | 0.225 | 0.362 |
| SECURITY | 13.5±1.0 | 0.200 | 0.321 |
| UNDERGROUND MANAGER | 11.3±1.0 | 0.168 | 0.269 |
| SHAFT COLLAR | 11.5±0.9 | 0.171 | 0.274 |
| SHAFT CONTROL ROOM | 14.8±1.1 | 0.219 | 0.352 |
| CRUSHER HOUSE | 12.5±1.1 | 0.185 | 0.298 |
| BALL ROOM | 14.1±1.1 | 0.209 | 0.336 |
| ASSAY DEPARTMENT | 10.1±0.9 | 0.150 | 0.241 |
| OUTSIDE ASSAY DEPT. | 14.0±1.0 | 0.208 | 0.333 |
| ENGINEERING DEPT | 12.9±1.0 | 0.191 | 0.307 |
| CARPENTARY SHOP | 18.5±1.2 | 0.274 | 0.404 |
| ROASTER SECTION | 15.6±1.2 | 0.231 | 0.371 |

## .3 RESULTS FROM THE MEASUREMENT OF THE PHYSICAL PARAMETERS

### 4.3.1 AIR FLOW RATE RESULTS.

a TARKWA MEASUREMENT

Table 4.17, The Average Air Velocity, the Average Area of the section and the calculated Airflow rate for Tarkwa.

| LOCATION OF PLASTIC EXPOSURE IN THE DRIVE | | AVE. AIR VEL. ($ms^{-1}$) | AVE. AREA ($m^2$) | AIRFLOW ($m^3s^{-1}$) |
|---|---|---|---|---|
| 10L LEVEL | Gangway | 0.33±0.09 | 7.74±0.22 | 2.58±0.78 |
| | Tramming drive (Bin) | 0.13±0.03 | 10.02±0.18 | 1.33±0.33 |
| 12L LEVEL | Gangway | 0.08±0.01 | 6.90±0.32 | 5.52±0.95 |
| | Level cross-cut | 0.58±0.04 | 8.23±0.35 | 4.77±0.53 |
| 14L LEVEL | Gangway | # | | |
| | Level cross-cut | # | | |
| 17L LEVEL | Gangway | 0.55±0.01 | 5.10±0.37 | 2.82±0.26 |
| | Winder house | 0.09±0.01 | 3.89±0.17 | 0.35±0.05 |
| 18L LEVEL | Gangway | 0.17±0.01 | 6.98±0.38 | 1.16±0.13 |
| | Level drive | 0.62±0.06 | 5.47±0.44 | 3.39±0.60 |
| 20L LEVEL | Gangway | 3.05±0.12 | 12.39±0.21 | 37.79±2.13 |
| | Winder house | 0.15±0.04 | 5.45±0.37 | 0.82±0.27 |
| 24 LEVEL | 2416 Incline | 0.41±0.02 | 7.81±0.60 | 3.21±0.40 |
| 25L LEVEL | 2525 Subdrive 2 north | 0.20±0.06 | 4.33±0.34 | 0.87±0.33 |
| | 2525 Subdrive 1 south | 0.20±0.06 | 4.33±0.34 | 0.87±0.33 |

LIBRARY
UNIVERSITY OF SCIENCE AND TECHNOLOGY

b. PRESTEA MEASUREMENT

Table 4.18, The Average Air Velocity, the Average Area of the section and the calculated Airflow rate for Prestea.

| LOCATION OF PLASTIC EXPOSURE IN THE DRIVE | | AVE. AIR VEL. ($ms^{-1}$) | AVE. AREA ($m^2$) | AIRFLOW ($m^3 s^{-1}$) |
|---|---|---|---|---|
| 6L E V E L | Gangway | 0.24±0.08 | 6.51±0.33 | 1.56±0.60 |
| | 258 South cross-cut | 0.11±0.01 | 7.02±0.26 | 0.77±0.01 |
| 9L E V E L | Gangway | 0.45±0.11 | 3.86±0.21 | 1.74±0.52 |
| | 254 South cross-cut | 0.11±0.01 | 5.91±0.13 | 0.65±0.07 |
| 12L E V E L | Gangway | 0.48±0.09 | 5.90±0.12 | 2.83±0.59 |
| | 224 South cross-cut | 0.12±0.02 | 3.23±0.36 | 0.39±0.11 |
| 15L E V E L | Gangway | 0.69±0.21 | 5.04±0.29 | 3.48±1.26 |
| | 235 South cross-cut | 0.44±0.11 | 6.89±0.22 | 3.03±0.85 |
| 23L E V E L | Gangway | 1.76±0.52 | 3.00±0.16 | 5.28±1.84 |
| | 224 South cross-cut | 0.93±0.10 | 6.30±0.15 | 5.86±0.77 |
| 30L E V E L | Gangway | @ | | |
| | Number 4 Shaft | 0.10±0.01 | 5.22±0.25 | 0.52±0.08 |

# dead end to air flow
@ the geometry of area does not permit air measurement

### 4.3.2 TEMPERATURE AND HUMIDITY RESULTS.

#### a. TARKWA MEASUREMENT

Table 4.19, Temperature and Humidity values at Tarkwa Goldfields for the entire period of exposure of the plastics.

| Location of cans in the Drives | | Temperature (°C) | Per'tage Humidity |
|---|---|---|---|
| 10L EVEL | Gangway | 26.9±0.8 | 95.8±0.8 |
| | Tramming drive (Bin) | 27.3±0.7 | 95.9±1.6 |
| 12L EVEL | Gangway | 27.1±0.6 | 97.9±1.9 |
| | Level cross-cut | 28.0±0.6 | 91.8±0.2 |
| 14L EVEL | Gangway T'former S'tion | 28.3±0.8 | 95.9±0.1 |
| | Level cross-cut | 29.1±0.9 | 93.8±2.0 |
| 17L EVEL | Gangway | 29.2±1.2 | 88.1±3.1 |
| | Winder house | 29.4±1.5 | 98.0±2.3 |
| 18L EVEL | Gangway | 29.5±1.2 | 95.9±3.2 |
| | Level cross-cut | 30.0±0.7 | 96.0±2.9 |
| 20L EVEL | Gangway | 31.0±1.2 | 98.0±1.8 |
| | Winder house | 30.4±0.3 | 92.3±2.2 |
| 24 LEVEL | 2416 incline | 31.6±0.8 | 96.0±2.8 |
| 25L EVEL | 2525 subdrive 2 north | 31.8±0.8 | 96.1±3.2 |
| | 2525 subdrive 1 south | 32.0±1.5 | 96.0±2.7 |

b. PRESTEA MEASUREMENT

Table 4.20, Temperature and Humidity values at Prestea Goldfields for the entire period of exposure of the cans.

| Location of cans in the Drives | | Temperature (°C) | Per'tage Humidity |
|---|---|---|---|
| 6L EVEL | Gangway | 29.2±0.8 | 91.7±3.3 |
| | 258 South cross-cut | 27.0±0.3 | 98.0±2.5 |
| 9L EVEL | Gangway | 29.6±0.9 | 95.9±3.5 |
| | 254 South cross-cut | 29.4±1.1 | 98.0±2.4 |
| 12L EVEL | Gangway | 30.5±0.7 | 91.7±2.0 |
| | 224 South cross-cut | 31.3±1.0 | 95.8±2.8 |
| 15L EVEL | Gangway | 30.3±0.8 | 92.1±3.1 |
| | 235 South cross-cut | 31.2±1.2 | 95.8±3.4 |
| 23L EVEL | Gangway | 31.5±1.1 | 86.5±2.6 |
| | 224 South cross-cut | 33.0±1.3 | 98.6±3.0 |
| 30L EVEL | Gangway | | |
| | Number 4 Shaft | 34.0±1.4 | 92.4±0.2 |

## 4.4 GRAPHICAL REPRESENTATION OF THE UNDERGROUND MEASUREMENTS.

### 4.4.1 THE VARIATION OF THE RADON CONCENTRATION WITH THE PHYSICAL PARAMETERS.

The following graphical representations were made of the results from the underground measurements in the two Goldfields:

i. Radon concentration with the depth below the surface, Note. Each level is separated from the next level by 150feet (45 metres) For example; 10Level is 10x45m below the ground surface and 17Level is 17x45m below the ground surface.

ii. The mean Radon concentration with average temperature recorded during the period of the experiment,

iii. The mean Radon concentration with the airflow rates in the underground for the period and

iv. The mean Radon concentration with the percentage humidity

These variations were made for each of the two Goldfields, the gangways and the drives. Figs.4.9 to Fig.4.24 show these variations as measured.

# THE VARIATIONS FOR THE GANGWAYS, TARKWA GOLDFIELDS.

Fig.4.9 Variation of Radon concn. at the Gangways with Depth below surface at Tarkwa, (for two different measurements).

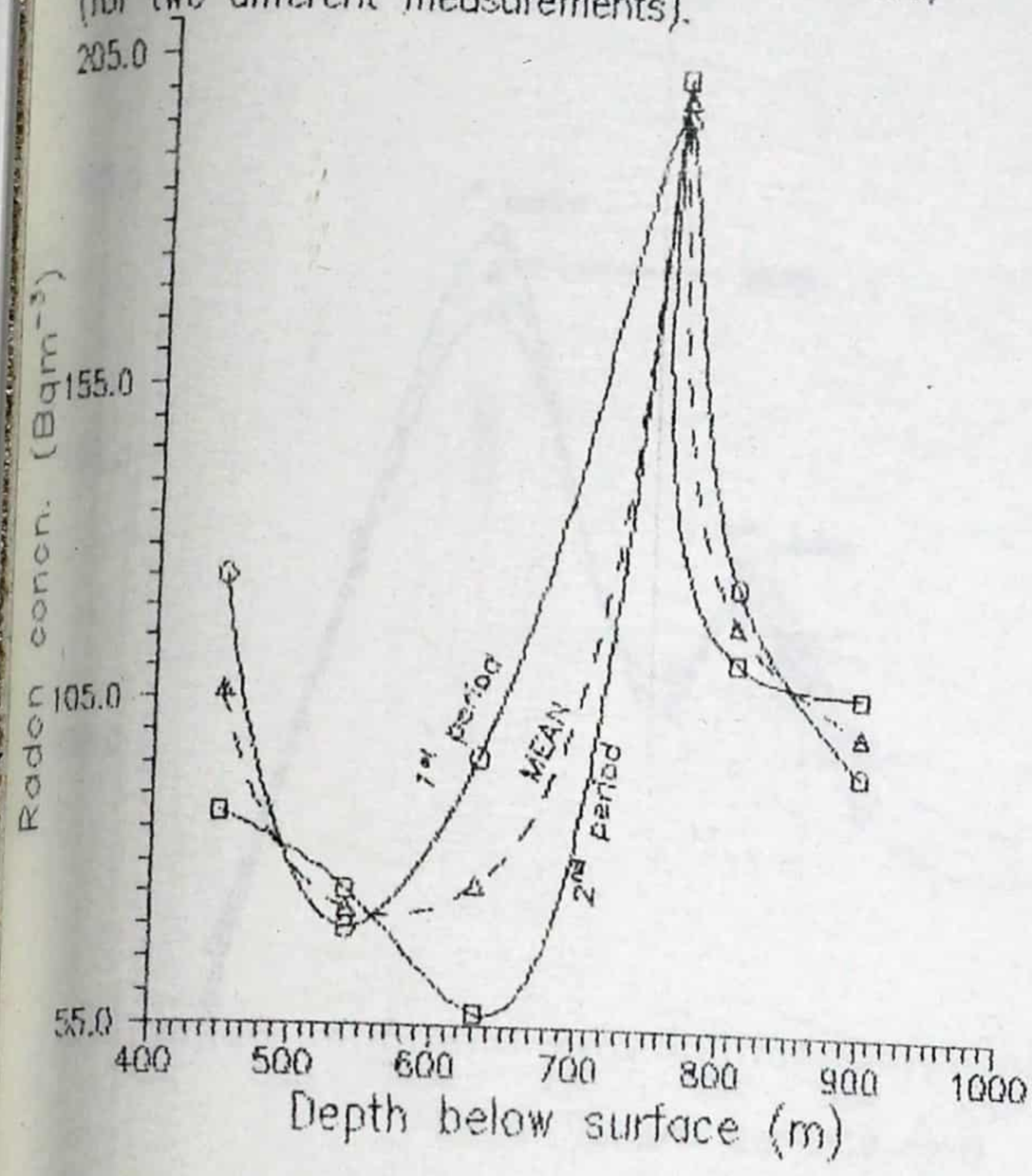


Fig. 4.11, A plot of Mean Radon concn. with the Av. airflow rates at the Gangways at Tarkwa Goldfields

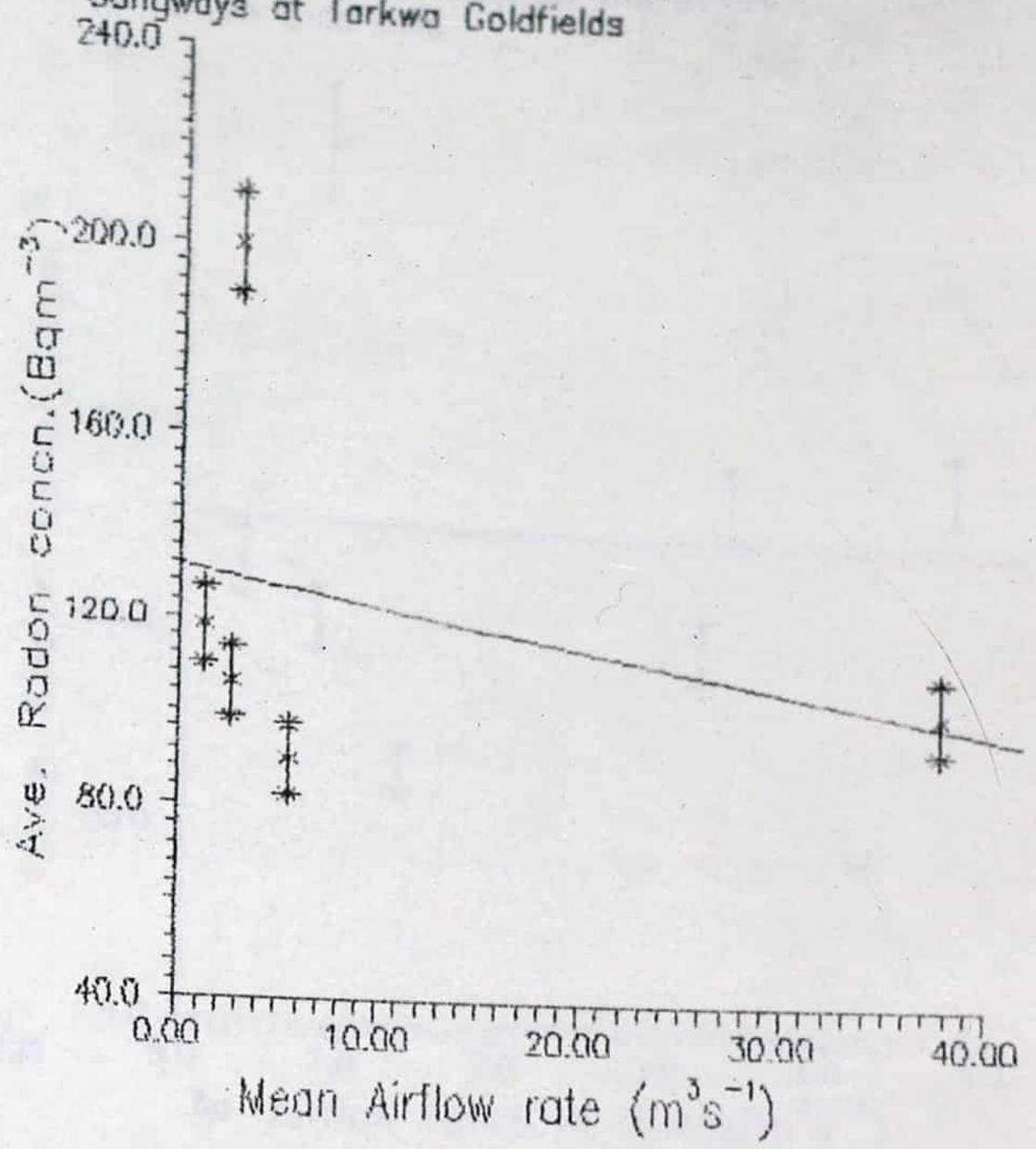


Fig.4.10 A plot of Mean Radon concn. with Ave. temp. at the Gangways at Tarkwa Goldfields

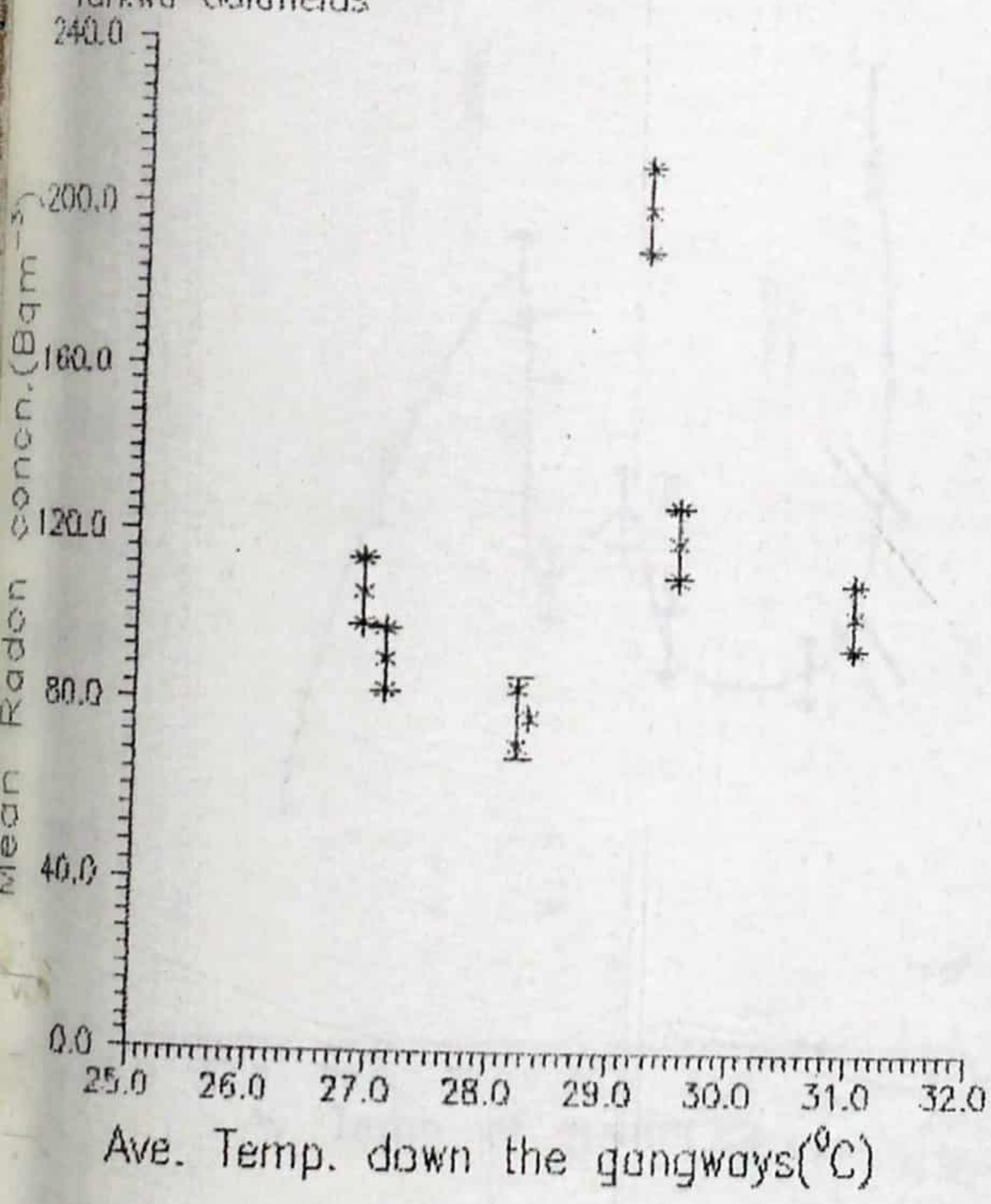


Fig.4.12, A plot of the mean Radon concn. with the Percentage Humidity at Gangways at Tarkwa Goldfields.

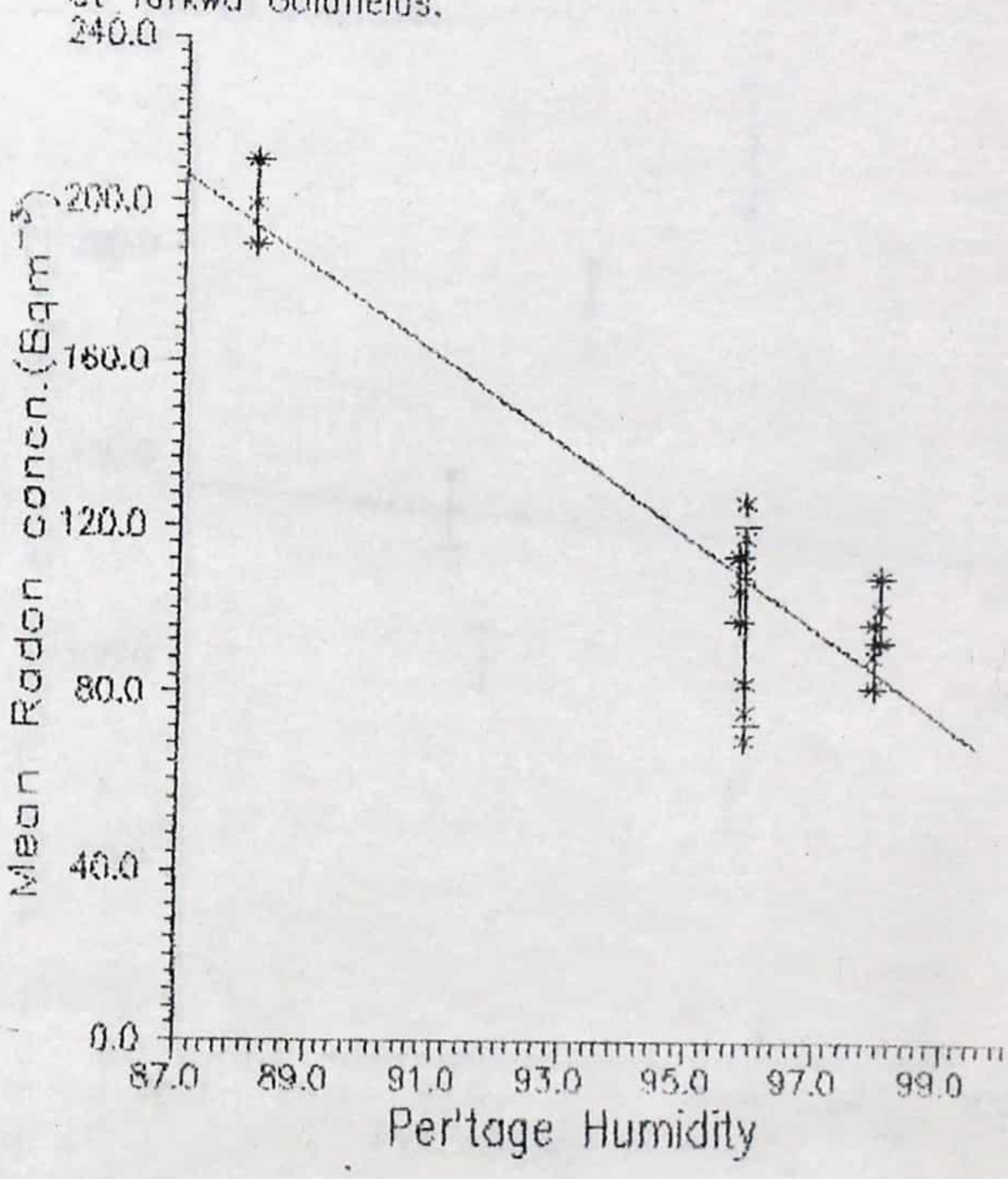

Fig 4.13 Variation of Radon concn. along the Drives with Depth below surface at Tarkwa, (for two different measurements).

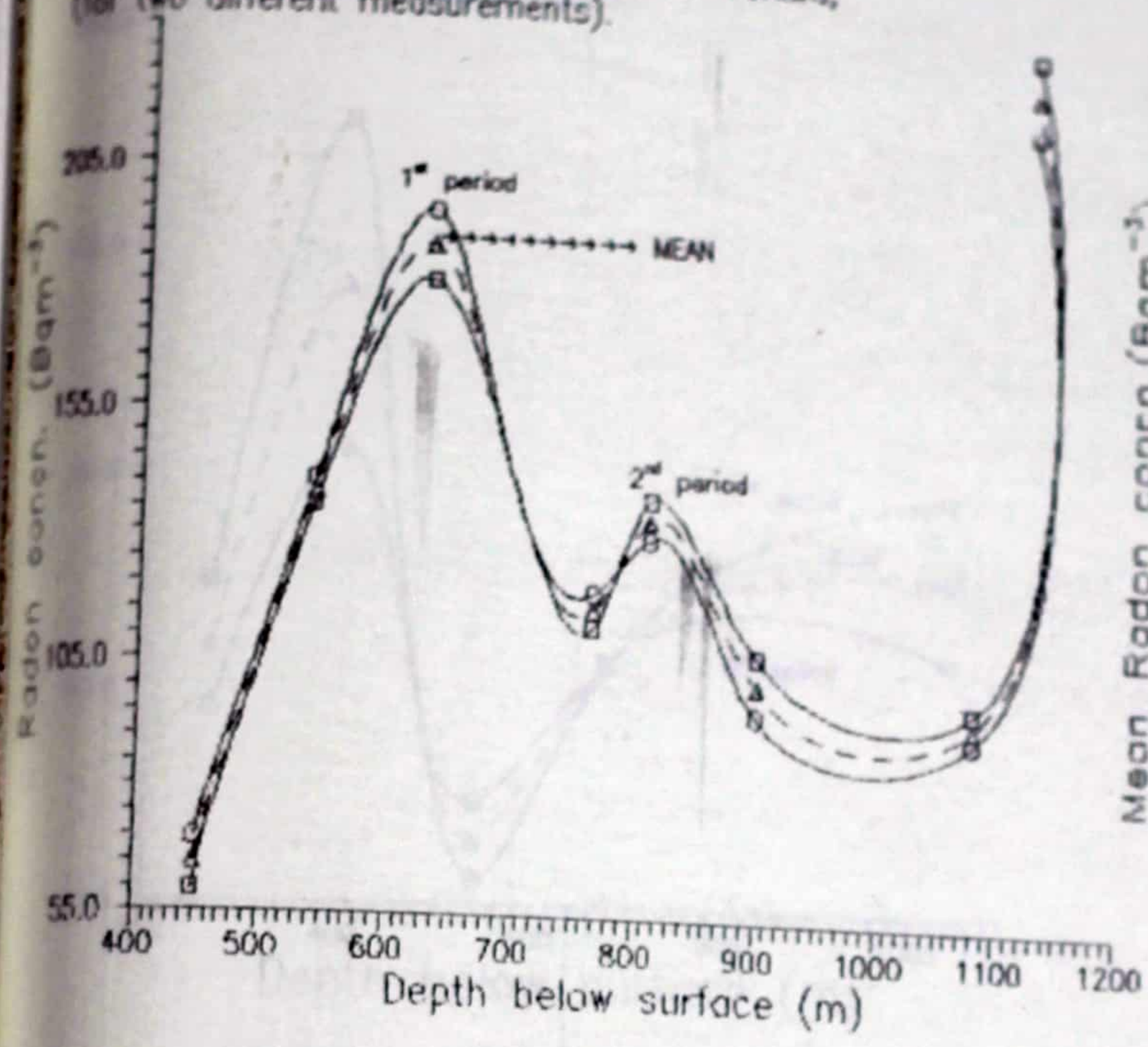


Fig.4.15. A plot of Mean Radon concn. with the Av. Airflow rate of the drives at Tarkwa Goldfields.

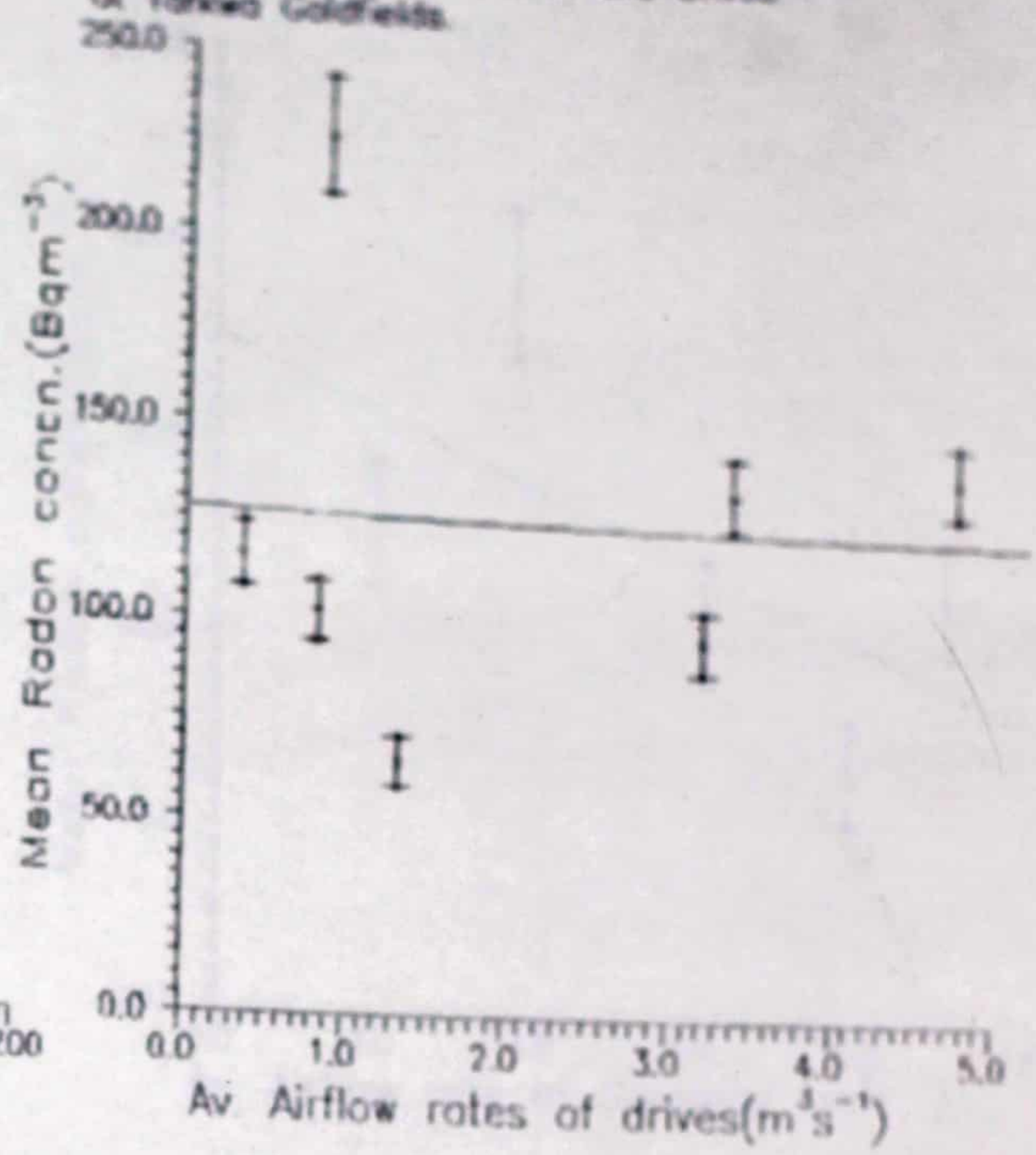


Fig. 4.14 Variation of Mean Radon concn. with Av temp. in the drives at Tarkwa Goldfields.

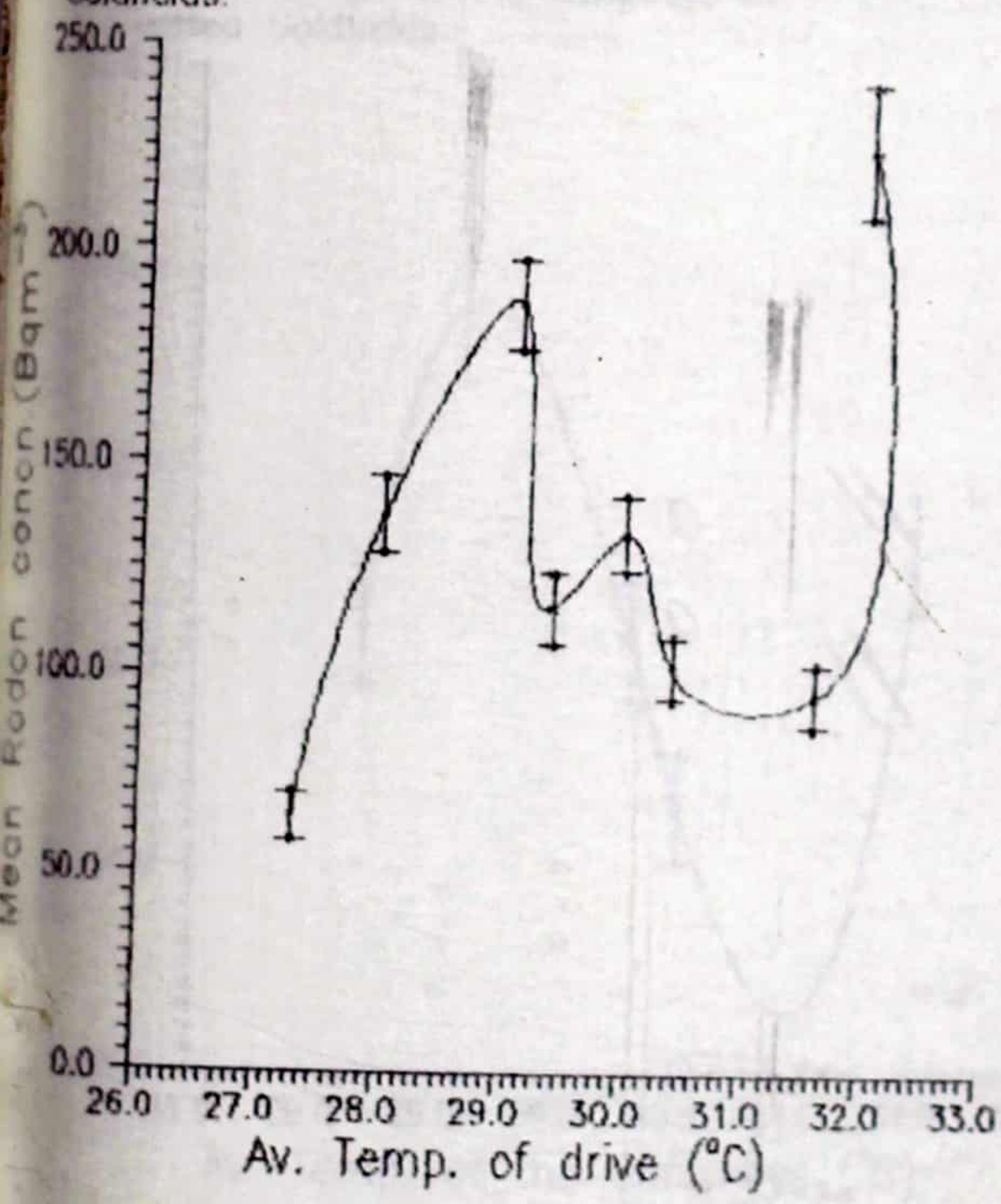


Fig.4.16, A plot of Mean Radon concn. with Percentage Humidity of the drives at Tarkwa Goldfields.

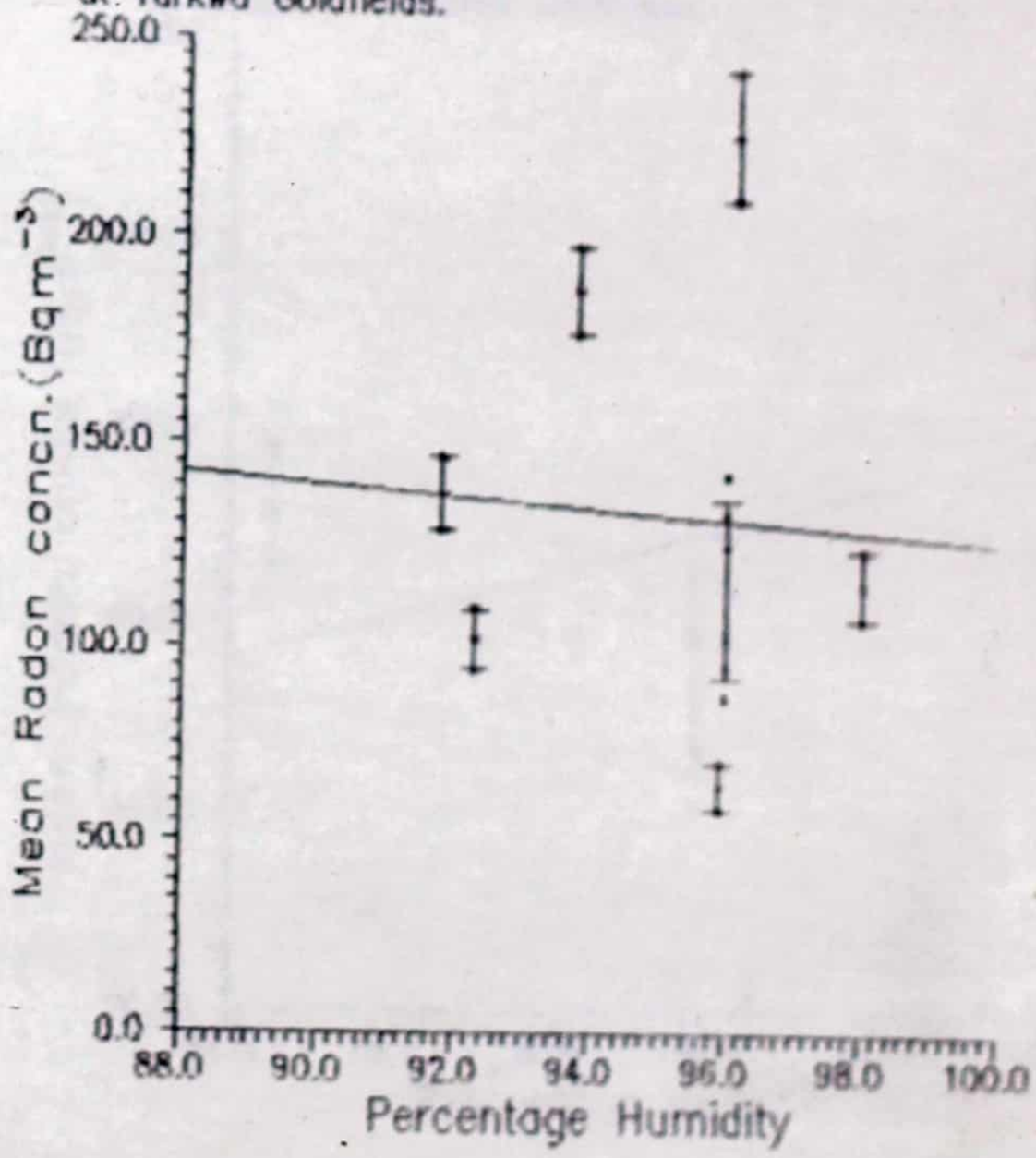

# THE VARIATIONS FOR THE GANGWAYS, PRESTEA GOLDFIELDS.

Fig.4.17, Variation of Radon concn. at the Gangways with Depth below surface at Prestea (for two different measurements).

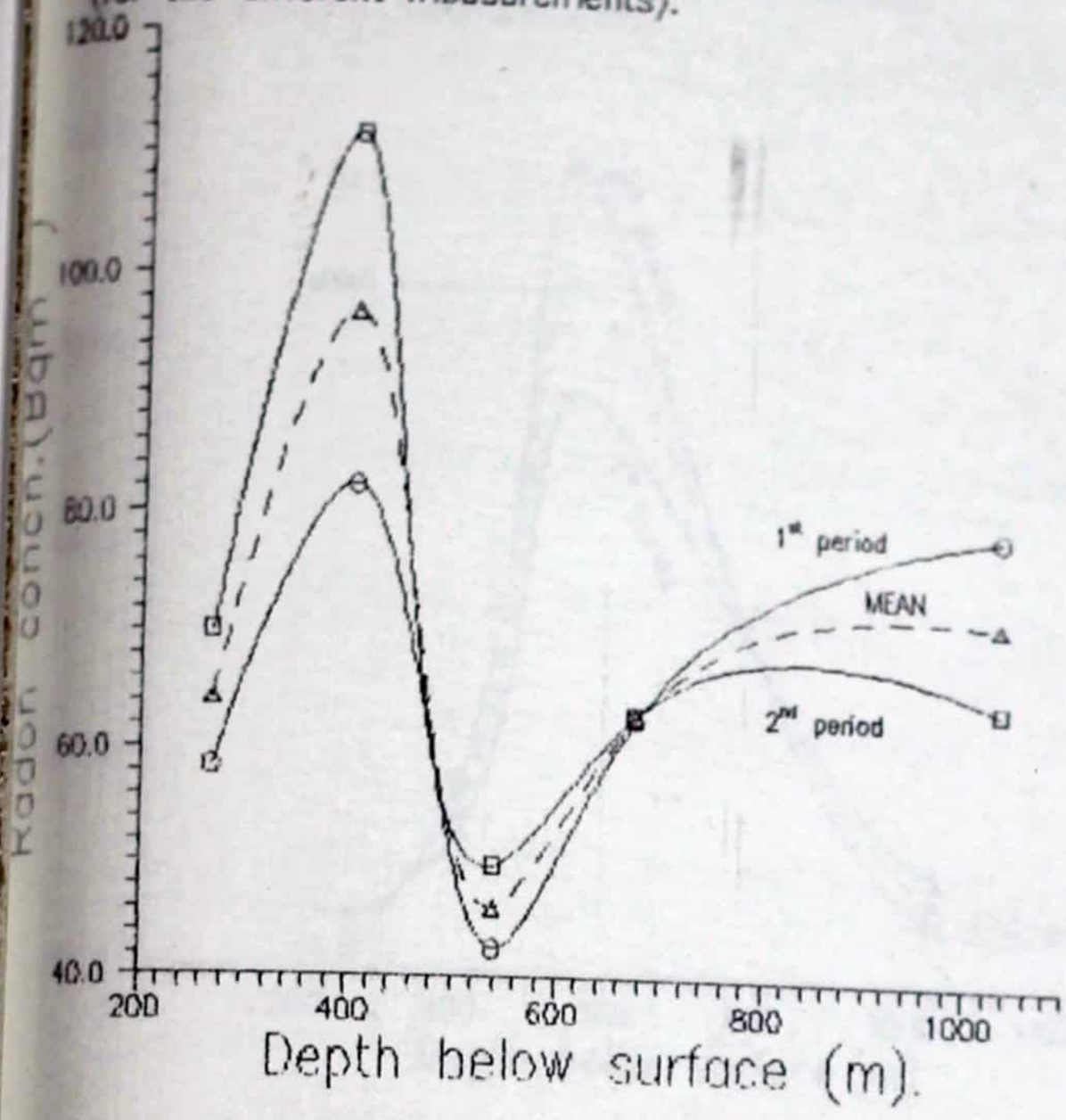


Fig.4.19, A plot of Mean Radon concn. with the Av. Airflow rates at the Gangways at Prestea Goldfields.

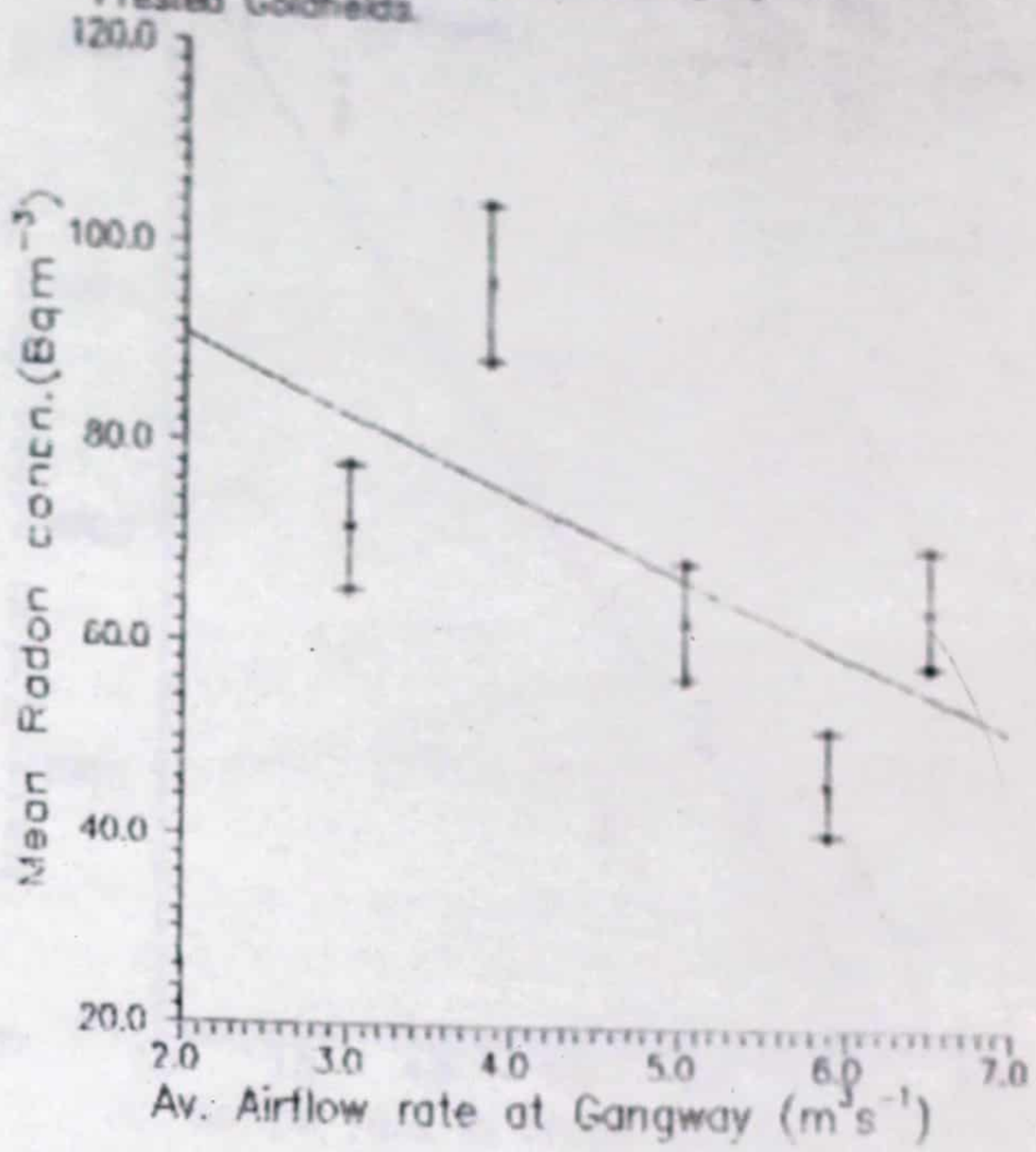


Fig.4.18, A plot of Mean Radon concn. with Av. Temp. at the Gangways at Prestea Goldfields

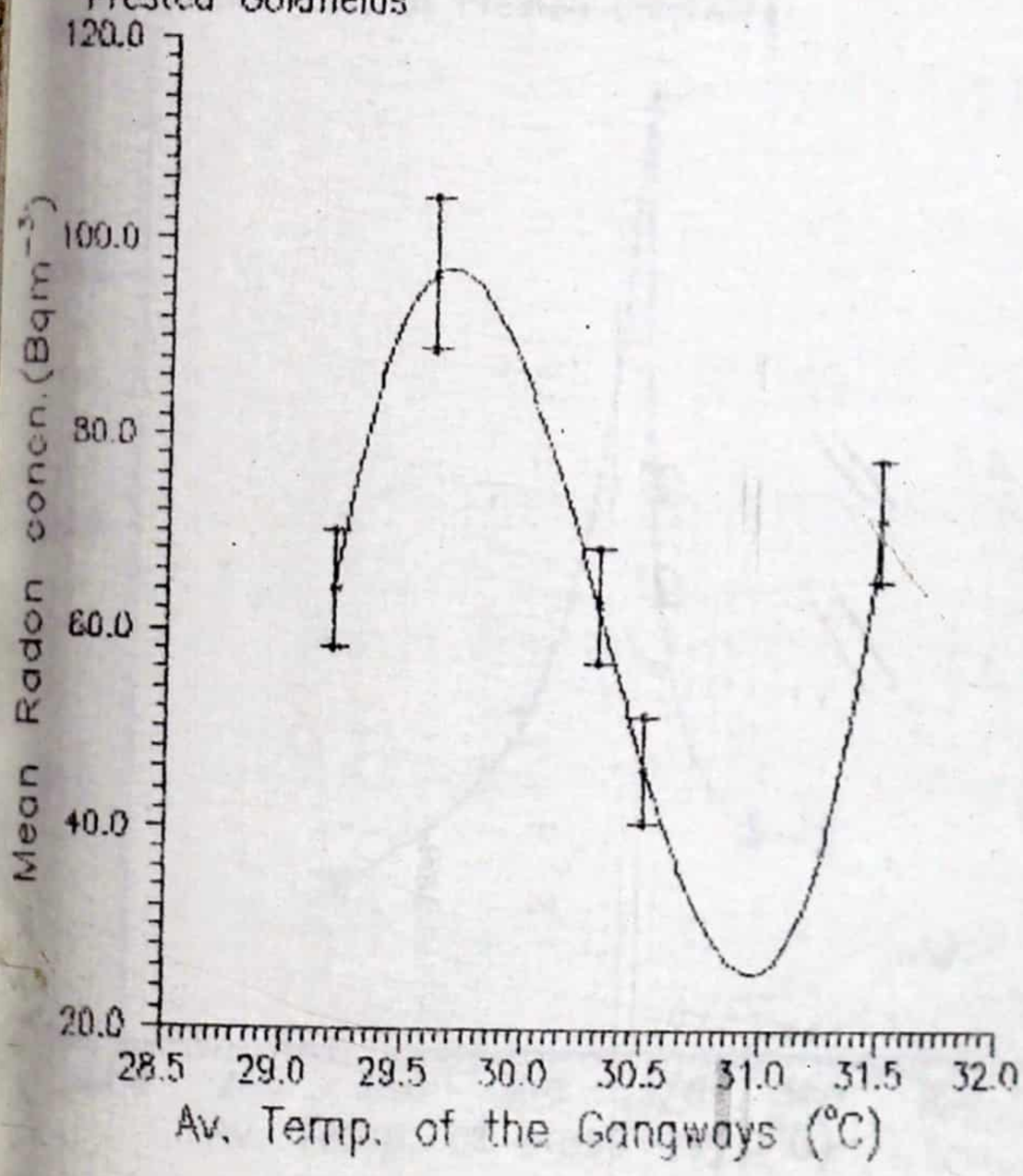


Fig.4.20, A plot of Mean Radon concn. with the Percentage Humidity at the Gangways at Prestea Goldfields.

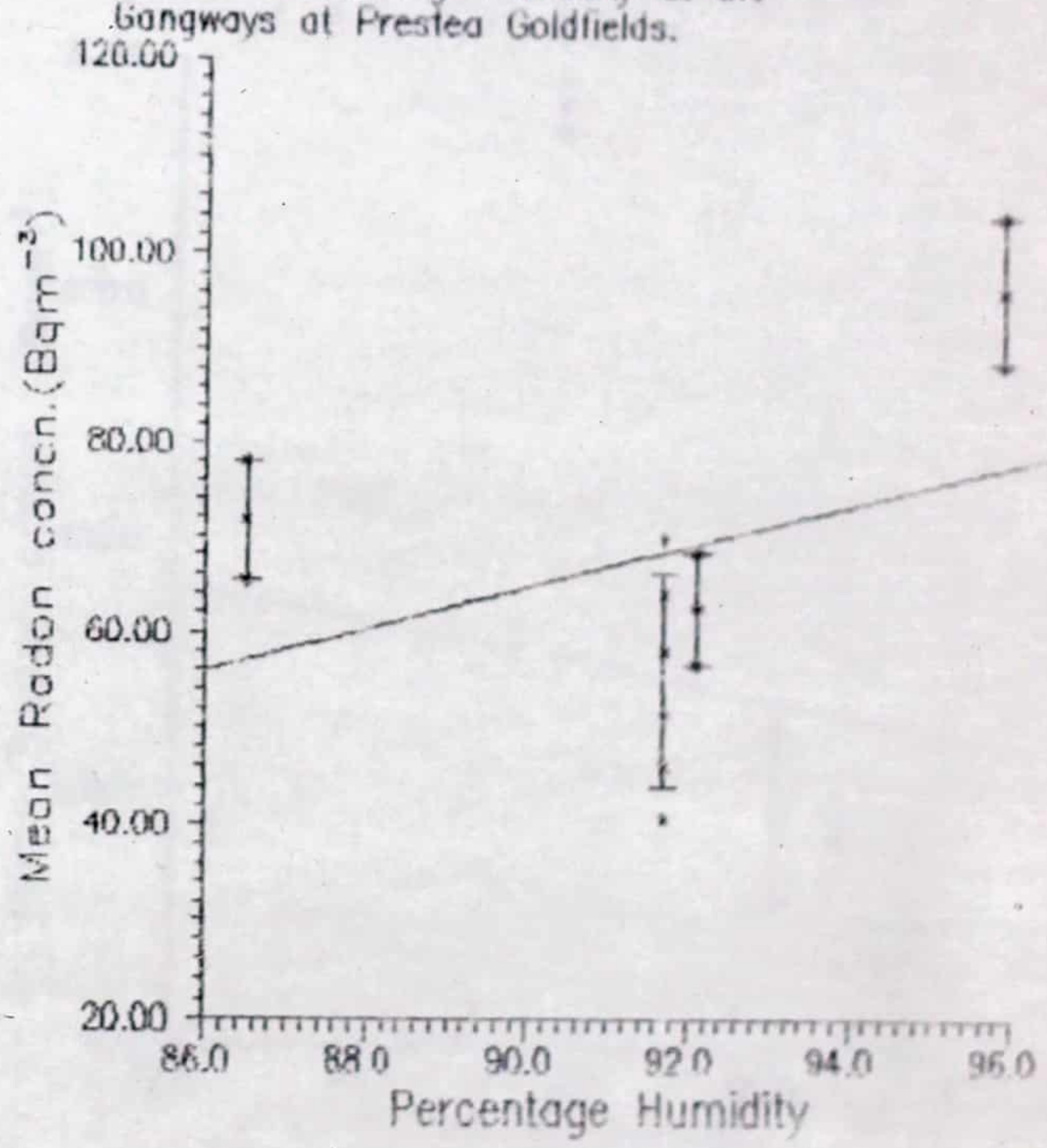

# THE VARIATIONS FOR THE CROSS-CUT, FOR PRESTEA GOLDFIELDS

Fig.4.21, Variation of Radon concn. the cross-cuts with Depth below surface at Prestea, (for two different measurements).

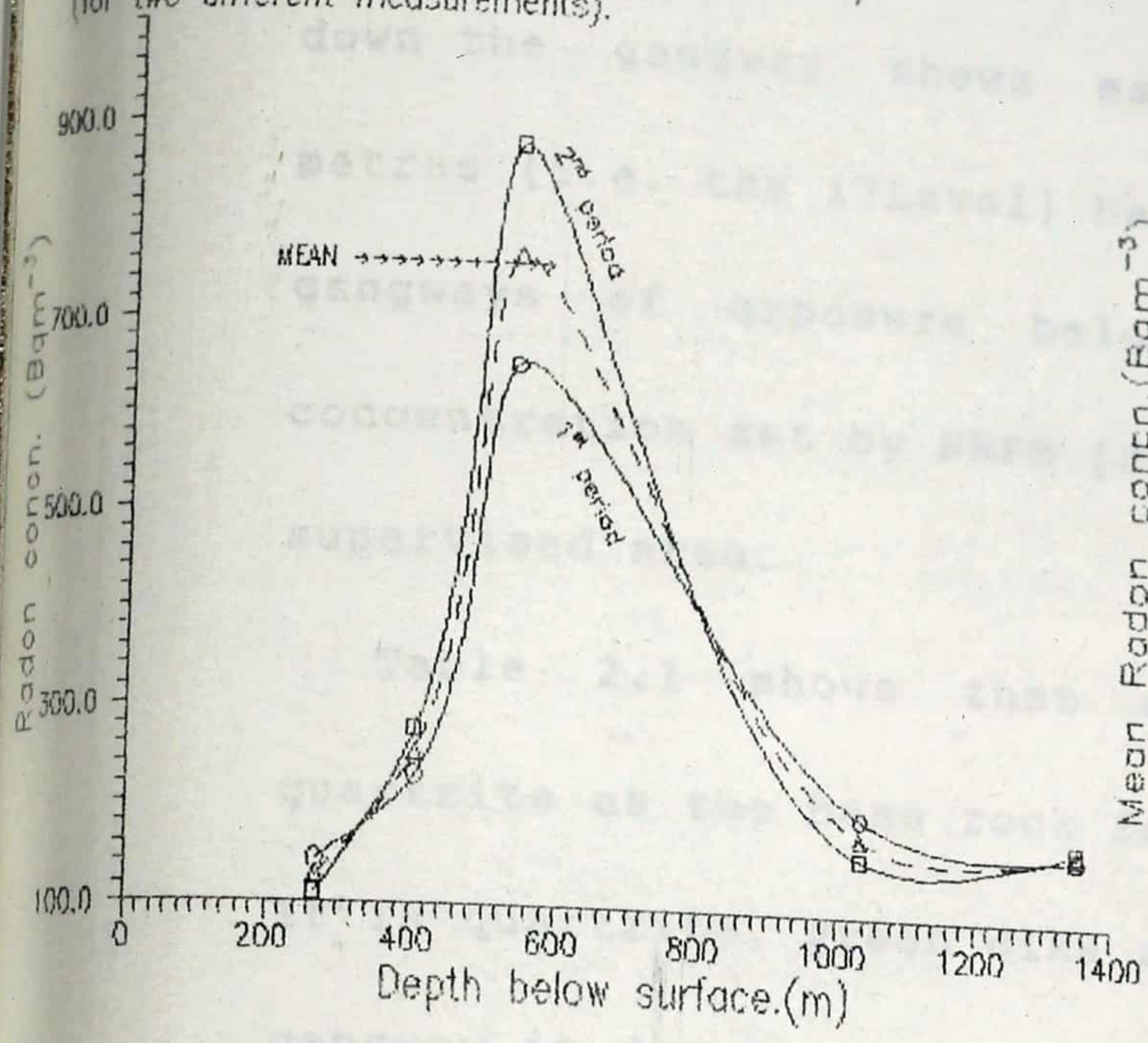


Fig.4.23, A plot of the Mean Radon concn. with Av. Airflow rates in the cross-cuts at Prestea Goldfields.

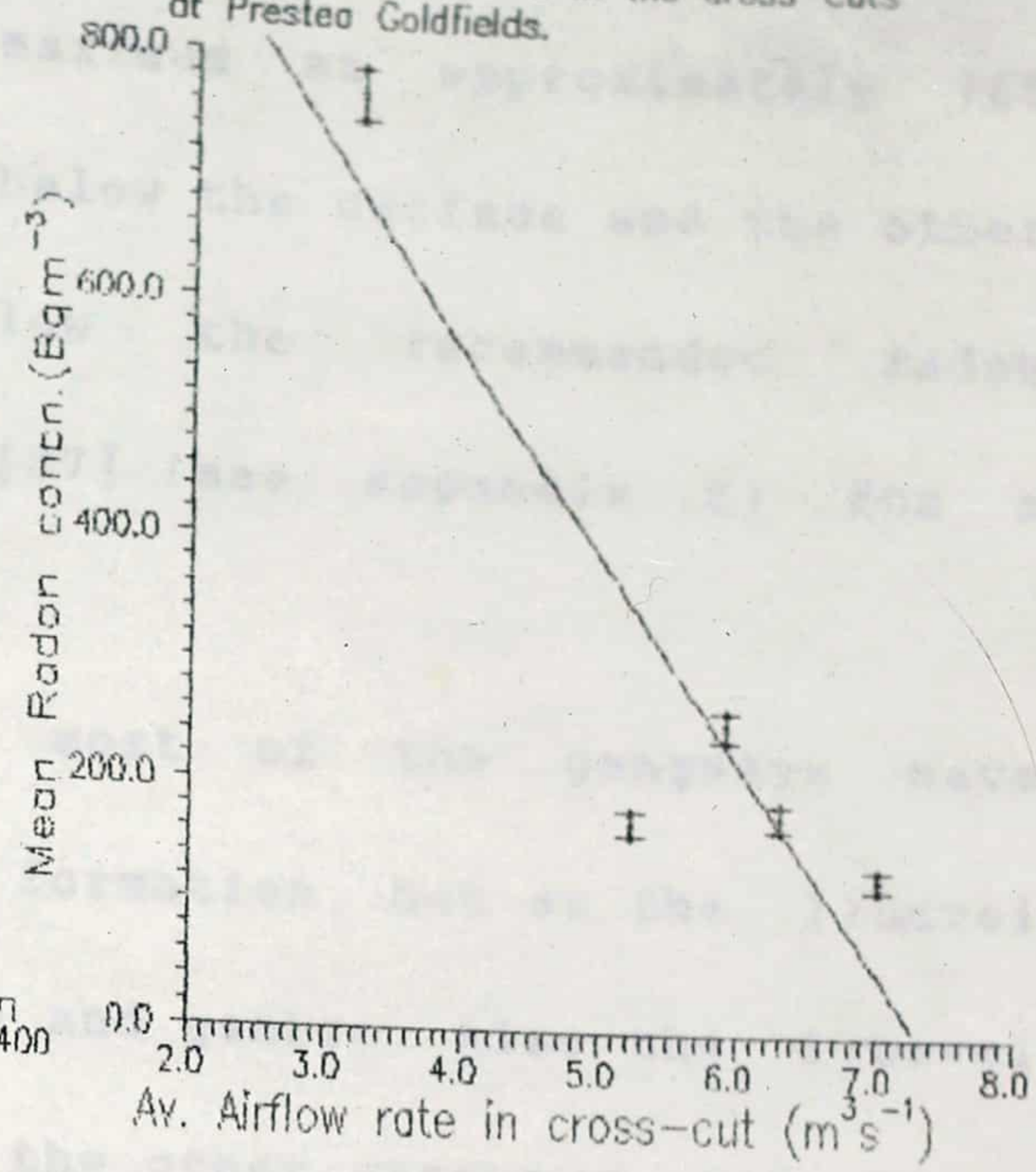


LIBRARY
UNIVERSITY OF SCIENCE AND TECHNOLOGY

Fig.4.22 A plot of the Mean Radon concn. with the Av.Temp. in the drives (cross-cut) at Prestea Goldfields.

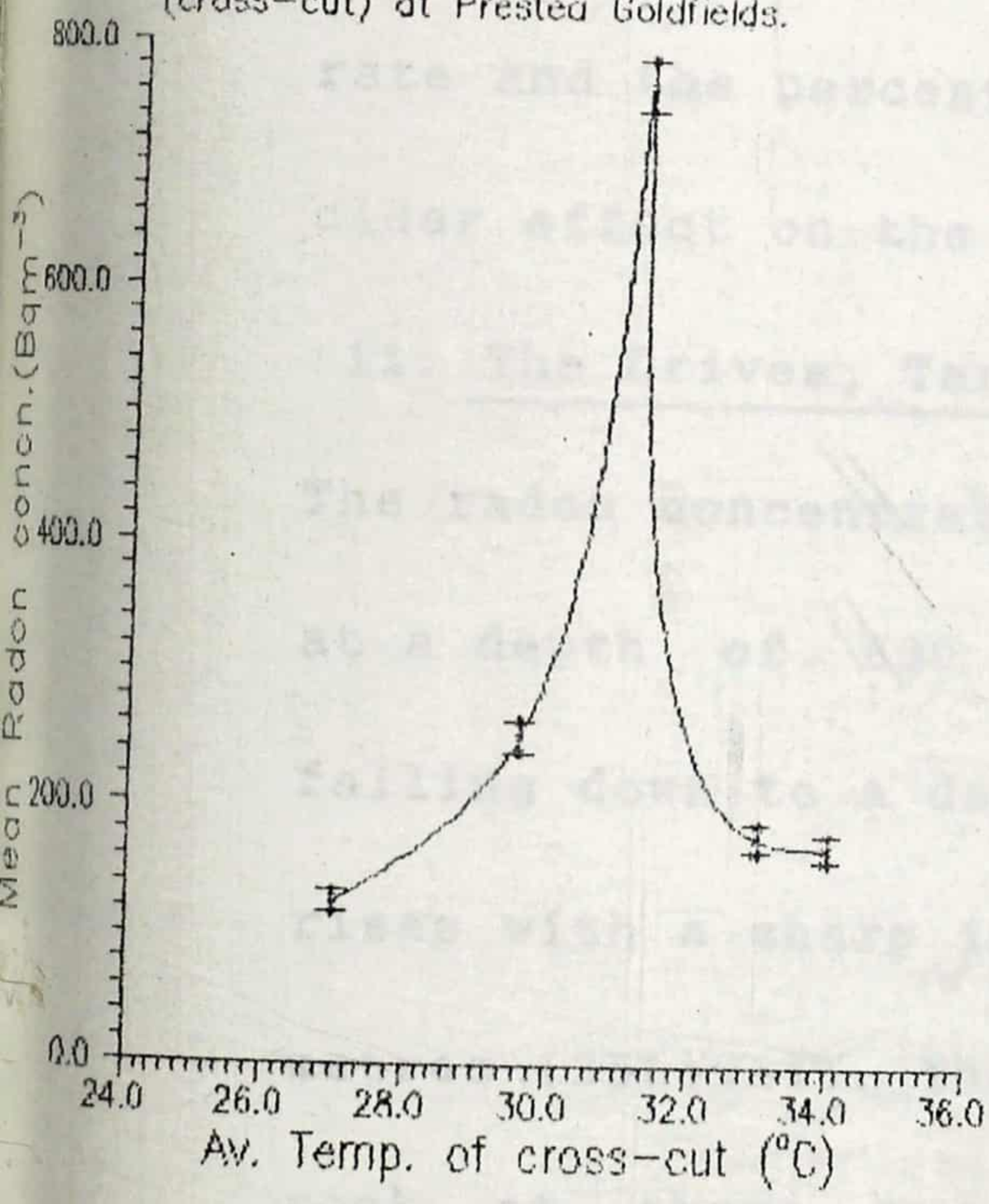


Fig.4.24, A plot of the Mean Radon concn. with the Percentage Humidity of the cross-cut at Prestea Goldfields.

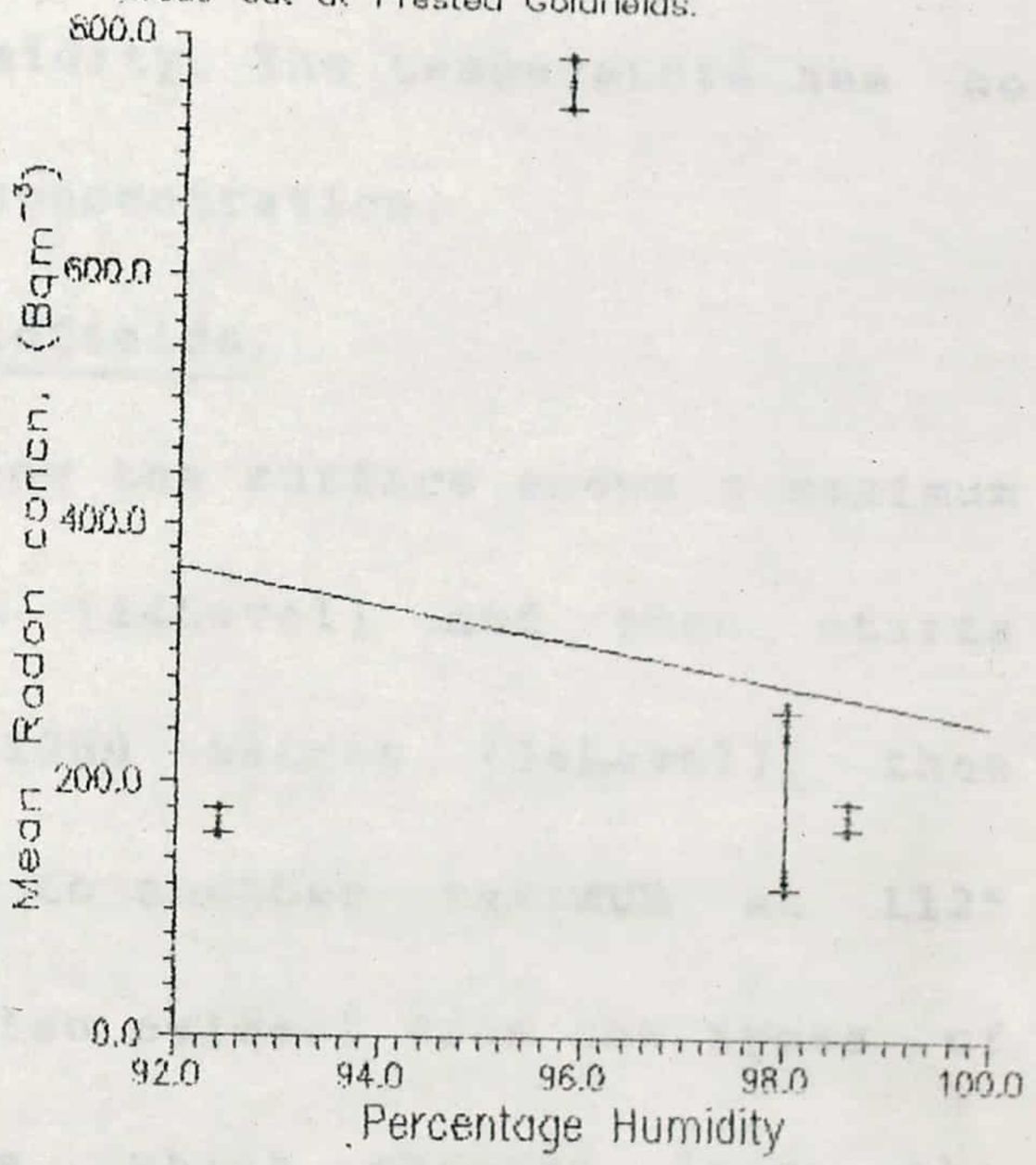

### 4.4.2 DEDUCTION FROM THE GRAPHS.

i. The Gangway, Tarkwa Goldfields.

The variation of the radon concentration as one moves down the gangway shows maximum at approximately 765 metres (i.e. the 17Level) below the surface and the other gangways of exposure below the recommended radon concentration set by NRPB [37] (see appendix F) for a supervised area.

Table 2.1 shows that most of the gangways have quartzite as the base rock formation, but at the 17Level it is quartzite, green dike and gabbro. Also the 17Level gangway is dry compared to the other gangways and these factors may account for the maximum.

From the graphs (Figs.4.11 and 4.12) the radon concentration is expected to decrease with the airflow rate and the percentage humidity. The temperature has no clear effect on the radon concentration.

ii. The Drives, Tarkwa Goldfields.

The radon concentration below the surface shows a maximum at a depth of 630 metres (14Level) and then starts falling down to a depth of 1080 metres (24Level), then rises with a sharp increase to another maximum at 1125 metres (25Level). This is also evident from the types of rock at these two places, which changes from the

quartzite formation to different formation (Table 2.1). It is expected that the radon concentration will decrease with increasing airflow rate and percentage humidity. (See Figs.4.15 and 4.16)

iii. The Gangways, Prestea Goldfields.

The radon concentration down the gangway shows a slight increase at the depth of 405 metres (9Level), but drops to lower values down the shaft. These radon concentrations are below the recommendation set by NRPB, UK.[37]

The rock formations are similar along the shaft, except at the 15Level (675m) where the vertical shaft intercepts a fault line or a fissure zone running from the north-west to south-east of the Goldfield. Table 4.18, shows that the airflow rate increases down the shaft together with carbonaceous nature of the rocks might account for the low radon concentrations. Here the radon concentration increases with the percentage humidity. There is no clear variation between the radon concentration and the temperature here, considering the shapes of the two graphs in Figs.4.17 and 4.18 which appear almost similar.

iv. The Cross-cut in the Drives, Prestea Goldfields.

The radon concentration with the depth indicates the highest maxima at 540 metres down the shaft (i.e. the 12Level 224 cross-cut). This is above the 370Bqm$^{-3}$ specified by NRPB, UK.,[37] for a controlled area in the mines. The other cross-cuts have radon concentration levels above the 110Bqm$^{-3}$ of a supervised area. A glance through Table 4.18 shows that the cross-cuts have the lowest air velocity. The direction of the air is from the gangway into the drive and the way the cross-cuts have been opened indicates that there is little exchange of air between the drive and the cross-cuts. Here the rock formation is not telling much about the radon variation and it is expected that the radon concentration will decrease as both the airflow rates and the humidity values increase. There is no clear variation between the radon concentration and the temperature as shown by the two graphs in Figs.4.21 and 4.22.

# CHAPTER FIVE

# 5.0 DISCUSSION AND CONCLUSION

## 5.1 DISCUSSION

Measurements of the radon gas in the two goldfields beginning with the surface environment have shown that the radon concentrations on the surface are lower than those of underground environment. This is contrary to my initial expectation that the processing of the ore from the underground on the surface might an have effect on the surface environment. The results obtained are just like those of background measurements. Places like the crusher house, the mill house and the assay department where the main processing of the ore is done, have radon concentrations below the 110Bqm$^{-3}$ as recommended by NRPB, UK [37] (see appendix F). Most of these places have been sited on hill tops and are well ventilated.

The underground measurements show a different pattern. The results obtained show some variation between the radon concentration the and geological formation of mine, airflow values and the percentage humidity of the location of the measurements. In general, it will be expected that the radon concentration will decrease with the airflow rates and the percentage humidity as one goes deep down into the mines.

There was no clear variation of the radon concentration with the surrounding temperature, which was evident from the plots. (See the graphs).

In Tarkwa, low radon concentrations were recorded in quartzite rock formation and high in composite rock formation. In Prestea, low radon concentrations were recorded along the gangways which have carbon phyllite as the main rock formation. The highest values were recorded in the cross-cuts of the drives in Prestea Goldfields. Here the ventilation is from the shaft gangway into the drives with bolsters to places where air is essential. There are no means where air can be exchanged between the drives and the cross-cuts and most of them intercept a fissure zone. If the seepage of gas which is predominantly through these fault lines, will have a longer hold-up time, there will be high radon concentration in some of these cross-cuts. Therefore, in measuring radon in the underground the nature of the rock system should be given priority attention which will then determine how the working areas should be protected from radon and its daughters.

LIBRARY
UNIVERSITY OF SCIENCE AND TECHNOLOGY

Past studies done on the exhalation rates of underground tailings from the two Goldfields by the department, has shown that Tarkwa tailings have higher radon concentration than that of Prestea tailings, [32,38] but the

results obtained from this work have shown that Tarkwa underground environment has the lower radon concentration compared to Prestea underground environment. As mentioned in chapter two, the Tarkwaian rock system, which Tarkwa Goldfield is mining, is strong and well compacted clastic sediments compared to the loose Birrimain sediment of overthrust faults and shear zones of the Prestea belt. From the studies on the exhalation rates, [32,38] it is reasonable to assumed that tailings in their loose form will have high radon concentration, but the strength and compactness of the Tarkwa rock formation is curtailing the release of the radon gas in its environment.

Another important aspect to talk about is the ventilation. The average airflow rates measured at Tarkwa and Prestea over the period are $5.04 m^3 s^{-1}$ and $2.37 m^3 s^{-1}$ respectively. Tarkwa has better ventilation than Prestea. This could also be a factor that has made Tarkwa to have lower radon concentrations than Prestea, because if the air circulation is effective, radon concentration will be low [3,12].

In order to specify the miners' exposure to radon and its daughters the estimation of the working level month is necessary. This was based on the reference working period of 170 hours per month, assuming 8 hours per day for 21 working

days in a month.

Radon concentration, however, is not simply related to radon decay product concentration. It is necessary to know the appropriate value of the equilibrium factor, F < 1.0, for the calculation of the working level. A value of 0.9 [32] (the theoretical maximum) was used and it is possible that this will be less for the mine environments in consideration.

The concentration of radon and its daughter products may vary widely with the location within a mine, and there may also be a temporal variation. It is difficult, therefore, to estimate reliably workers' exposure from area measurements. In Prestea for example, at the 12Level (224 south cross-cut), the cumulative exposure is 5.53WLM for 7 months which exceeds the 4.0WLM annually as specified by NRPB [37]. A miner may not work in this place (224 south cross-cut) throughout the seven months to receive this cumulative exposure, therefore, individual monitoring is necessary. Most of the miners enter these places without respiratory protection which is very dangerous if the daughter products are present in large quantities.

## 5.2 CONCLUSION AND SUGGESTION FOR FURTHER WORK

Setting standards to provide remedial actions to protect the mine workers from exposure of radon and its daughters requires judgement based on the best scientific evidence — which now exists in the underground mine environment in this country. However, in Ghana the body charged with such responsibilities is silent about radon gas emissions into the mines. Presumably, this could be due to the fact that there is no radioactive mining in this country. The results have clearly demonstrated the need to determine the precise level of standards to ensure the safety of the miners from the exposure to radon gas. There have been reports of Lung disease prevalent among mine workers at Tarkwa Goldfields. The disease is silicosis which occurs as a result of inhalation of dust particulates. It is possible that the extreme form of this disease will be lung cancer associated with the inhalation of radon and its daughter products if they are in large excess and are attached to these dust particulates.

These results show that the radon concentrations at the offices at Tarkwa and Prestea are below the maximum safe of $110 Bqm^{-3}$ as recommended by National Radiological Protection Board, (NRPB) UK. However, sixteen (16) out of the twenty five (25) underground locations monitored in the two gold

mines have radon concentrations above the recommended limit.

The results show that Tarkwa underground environment has lower radon concentrations than that of Prestea due to two reasons: first, there is the strong rock formation and secondly, there is better ventilation system put in place in Tarkwa than in Prestea.

Several measures must be taken to protect employees in the mine where radon and its daughters are present. The following control measures can be put in place:

i. First, it is necessary that intensive area and individual exposure concentrations be monitored and recorded.

ii. Secondly, in active working areas like the 25Level subdrives at Tarkwa, where radon and daughters are present in high concentrations, respirators for protection against the gas must be provided.

iii. Thirdly, where inactive working areas like the cross-cuts in the drives of the Prestea Goldfields, contain the gas in excess, these areas must be posted against unauthorised entry with signs specifying that they are areas where respirators must be worn.

iv. Finally, there should be sufficient ventilation to dilute and render harmless, and to carry away the gas.

From the discussion and the conclusion come the following suggestions for further work:

i. In collaboration with the Ghana Chamber of Mines (the custodians of the Ghana Mining Regulations) to determine the precise radon concentration for standards. These must include the equilibrium factor for each of the mines.

ii. Individual monitoring on the mine workers be made using the simple diffusion cup with SSNTDs developed at NRPB by Miles and Dew.[6]

iii. Gamma ray survey must also be made since this work is primarily made on alpha radiations.

iv. Neutron activation or X-ray fluorescence analysis be made on the underground rocks to determines the elements, whether they contain Uranium or Radium the for-runner of Radon gas.

v. Since the measurements of the gas in working levels can be used to estimate lung cancer deaths per million of the population per year that would occur from the inhalation of radon daughters, I will finally suggest that these studies be done among other for all the existing goldmines in Ghana for compilation of national data base.

# APPENDIX A

## AREA OF FIELD OF VIEW OF THE OPTICAL MICROSCOPE

Total magnification of the microscope is given by

$$M_T = \frac{\text{Limit of resolution of eye}}{\text{Limit of resolution of the objective}}$$

$$= \frac{\text{Numerical aperture of the objective}}{\text{Numerical aperture of the eye}}$$

$$= \frac{\text{Diameter of eyepiece x eyepiece magnification}}{\text{Diameter of objective lens}}$$

but $M_T$ = objective x eyepiece magnifications

= 40 x 10 =400X

and Diameter of eyepiece = 2cm

hence,

LIBRARY
UNIVERSITY OF SCIENCE AND TECHNOLOGY

$$400 = \frac{2 \times 10}{\text{Diameter of objective (field of view)}}$$

and

Diameter of field of view = 0.05cm

Radius of field of view = 0.025cm

therefore Area of field of view = $\pi(0.025)^2 cm^2$

Hence,

$$\text{Track density} = \frac{\text{Mean number of tracks}}{\text{Area of field of view}}$$

$$= \frac{\text{Mean number of tracks}}{\pi(0.025)^2 cm^2}$$

## APPENDIX B

ERROR CALCULATION FOR THE TRACK DENSITY AND THE RADON CONCENTRATION

If the total number of tracks counted for n field of views is N, then the error in the count is $\sqrt{N}$, and the error in the track density is

$$\rho_e = \frac{\sqrt{\overline{N}}}{\text{Area of field of view}}$$

where $\overline{N}$ is the mean number of count per field of view = N/n

The error in estimating the radon concentration will be

$$\Delta_{RN} = \frac{\rho_e \times \text{calibrated factor}}{\text{period of exposure of plastic}}$$

For a example, sum for 110 field of views for a particular plastic which was exposed for 109 days is 818. The in the count is $\sqrt{818} = 28.6$

the error in the track density $\rho_e = \dfrac{28.6/110}{1.96 \times 10^{-3}}$

$$= 132.7 \text{ tracks}\,\text{cm}^{-2}$$

therefore, the error in the radon concentration will be;

$$\Delta_{RN} = \frac{(132.7 \text{ tracks}\,\text{cm}^{-2}) \times \dfrac{(150 \text{ Bqm}^{-3}\text{hr})}{\text{tracks/cm}^2}}{109 \times 24 \text{ hr}}$$

If two quantities X and Y have error $\rho_x$ and $\rho_y$ respectively then the error for X + Y is $\sqrt{\rho_x^2 + \rho_y^2}$ .

## APPENDIX C

ERROR CALCULATION FOR THE PHYSICAL PARAMETERS

i. The standard deviation for n number of observation is

$$\sigma = \left[ \frac{\Sigma(x - \bar{x})^2}{n} \right]^{1/2}$$

where x represent the quantity investigated

$\bar{x}$ represent the arithmetic mean

and the standard deviation has been called the standard error of an individual observation.

ii. The quantity Q of air is a function of the air velocity V and the area of the section A, i.e.

$$Q = VA$$

$$\ln Q = \ln V + \ln A$$

differentiating, we have

$$\frac{\delta Q}{Q} = \frac{\delta V}{V} + \frac{\delta A}{A}$$

and the error in calculating Q is

$$\delta Q = \left[ \frac{\delta V}{V} + \frac{\delta A}{A} \right] Q$$

where $\delta V$ and $\delta A$ are the errors in measuring the air velocity and the area of section respectively.

# APPENDIX D

Table A Definition of the Working Level (WL) unit. [2,12]

| Nuclide | α-energy (MeV) | Half-life | No. of atoms/ 100pCi | Total α-energy (MeV/100pCi) | Fraction of total α-energy |
|---|---|---|---|---|---|
| Rn ($Rn^{222}$) | 5.49 | 3.82days | $1.77 \times 10^{6}$ | none | none |
| RaA ($Po^{218}$) | 6.00 | 3.05mins | 977 | $0.134 \times 10^{5}$ | 0.10 |
| RaB ($Pb^{214}$) | 0 | 26.80mins | 8580 | $0.659 \times 10^{5}$ | 0.52 |
| RaC ($Bi^{214}$) | 0 | 19.70mins | 6310 | $0.485 \times 10^{5}$ | 0.38 |
| RaC' ($Po^{214}$) | 7.68 | $10^{-6}$min | 0.0008 | $0.000 \times 10^{5}$ | 0.00 |
| | | | Total | $1.278 \times 10^{5}$ | 1.00 |
| | | | $\cong$ | $1.30 \times 10^{5}$ | |

# APPENDIX E

## able B UNITS CONVERSION FACTORS

| ty | Units | Conversion factor |
|---|---|---|
| red | | |
| cy | picoCuries | 1Ci = $10^{12}$pCi |
| | Curies | 1Ci = $3.7x10^{10}$dis. per. sec. |
| | Becquerels(Bq) | 1pCi = 0.037Bq |
| | | 1Bq = 27pCi |
| | | 1Bq = 1 disintegration/sec. |
| y | pCi/l, Bq/$m^3$ | 1pCi/l = 37Bq/$m^3$ |
| al | Working Level | $1.30x10^5$MeV/l = 1WL |
| | (WL) | 100pCi/l = 1WL |
| y | | 1WL = 6Rems |
| | Roentgen | 100Rems = 1Sv |
| ent | equivalent | 1Rem = 1/6WL |
| | man (Rem) | 1WL = $6x10^{-2}$Sv |
| | Sievert (Sv) | |

UNIVERSITY OF SCIENCE AND TECHNOLOGY LIBRARY

# REFERENCES


[1] Source, Effects and Risk of Ionizing Radiation
United Nation Scientific Committee on the Effects of Atomic Radiation, Report to the U.N. General Assembly New York (1988)

[2] Gonzales, A.J. and Anderer, J.
"Radiation verses Radiation Nuclear Energy in Perspective."
Quarterly Journal of the International Atomic Energy Agency, Vienna, Austria Vol.31 (2) (1989) pp21-31

[3] Abu-Jarad F.A.N
"A Study of the Activity of Radon and its Daughters inside Houses and from Building Materials using Solid State Nuclear Track Detectors." (PhD Thesis)
Department of Physics, University of Birmingham (1980)

[4] Rock, R.L. et al
"Evaluation of Radioactivity Aerosols in United States Underground Coal Mining."
MESA. I.R (1025) U.S.A (1975)

[5] Amoo D.N.
"Environmental Monitoring of Radon Gas in and around Kumasi using Solid State Nuclear Track Detection."
(B.Sc Project Report

Dept. of Physics, University of Science and Technology, Kumasi. (1990)

[6] Sackey, T.A.

"Measurements of Radon in Deep Mines" (B.Sc Project Report) Dept. of Physics, University of Science and Technology, Kumasi. (1991)

[7] Sherry, S.P and Petschek, A.G

"Exhalation of Radon and Thoron; The Question of the effect of Thermal Gradient in Soil." Earth and Planetary Science letters Vol. 64, pp 56-60 (1983)

[8] Pearson, J.E.

"Natural Environmental Radioactivity from Radon-222." U.S. Department of Health, Education and Welfare, (999) RH-26 (1967)

[9] Rock, R.L and Walker, D.K.

"Controlling Employee Exposure to Alpha Radiation in Underground Uranium Mines."

USBM, Handbook Vol.1 pp 7-10 (1970)

[10] U.S Environmental Protection Agency

"Health Risk Due to Radon in Structures: A Strategy and Management Plan for Assessment and Mitigation" USEPA (1985)

UNIVERSITY OF SCIENCE AND TECHNOLOGY LIBRARY

[11] UNSCEAR

" Ionizing Radiation; Source and Biological Effects". United Nation Scientific Committee on the Effect of Atomic Radiation, Report to the General Assembly with annexes New York. (1982)

[12] Mueller Association Inc., SYSCON Corp. and Brookhaven National Laboratory.

"Handbook of Radon in Buildings: Detection, Safety and Control". U.S. Dept of Energy office of Environmental Analysis pp30 - 40 (1988).

[13] Levitt, P.M., et al with Drs. A.R., Kagan and H. Gilbert.

"The Cancer Reference Book", Facts on File, Inc. New York. pp287. (1983)

[14] Weiffenbach, C. V., (University of Maine at Orono) "Radon, Water, and Air Pollution: Risk and Control", Technology Transfer Project, Annual Cooperative Program, U.S Dept. of Interior, pp17, (1982).

[15] Land and Water resources Centre (University of Maine at Orono) and Division of Health Engineering (Maine Dept. of Human Services).

"Radon in Water and Air: Health Risk and Control Measures:, The Resources Highlights series U.S. pp12 (1983)

[16] Holaday, D.A., Rushing, D.E., Coleman, R.D., Woolrich, P.F., Kusnetz, H.C., and Bale, W.F.,
"Control of Radon and Daughters in Uranium Mines and Calculations on Biological Effects",
U.S. Dept. of Health, Education and Welfare. Public Health service Publication (494), Wash. D.C. (1975).

[17] Shirokov, Yu. M., Yudin, N.P.,
"Nuclear Physics, Volume one"
pp260-261 (Mir) Moscow (1982).

[18] Young, D.A.,
"Etching of Radiation Damage in Lithium Fluoride"
Nature 182, pp375- 377 (1958).

[19] Silk, E.C.H., and Barne, R.S.,
"Examination of Fission Fragment Tracks with an electron Microscope",
Phil. Mag. 4. pp970-972 (1959).

[20] Fleischer, R.L., Price, P.B., and Walker, R.M.,
"Solid State Track Detectors: Applications to Nuclear Science and Geophysics".
Ann. Rev. Nucl. Sci. 15 pp1-28 (1959).

[21] Enge, W.,
"Introduction to Plastic Nuclear Track Detectors",
J. Nucl. Tracks Vol.4 (4) pp238-308 (1980).

[22] Seitz, F.,

"The Disordering of Solids by the Action of Fast Massive Particles",

J. Disc. Faraday Soc. 5, pp271-282 (1949).

[23] Benton, E.V.,

"A Study of Charged Particles Tracks in Cellulose Nitrate (PhD. Thesis)", University of California.

U.S. Naval Radiological Defense Laboratory, San Francisco, Calif. USNDRL Report TR-68-14. (1968).

[24] Fleischer, R.L., Price, P.B., and Walker, R.M.,

"The Ion-Explosion Spike Mechanism for Formation of Charged Particle Tracks in Solids".

J. Appl. Phys. 36 pp3645-3652 (1962).

[25] Durrani, S.A., and Bull, R.K.,

Solid State Nuclear Tracks Detector: Principles, Methods and Application",

Int. Series in Nat. Phil. Vol. 111 pp48-54 Pergamon Oxford. (1987).

[26] Beth, M., Enge, W., and Sermund, G.,

"Some New Aspects of Etching of CR-39 Plastics Detector"

Contribution to the 13th Int. Conf. on SSNTDs Rome, Italy pp5-11 Sept. (1985).

[27 Adadey, E., and Mintah, G.B.,

Geology of Prestea Goldfields

State Gold Mining Corporation, Prestea, Ghana. (1983)

[28] Hess, C.T., Michel, J., Horton, T.R., Pirchard, H.M., and Coniglio, W.A.,
"The Occurrence of Radioactivity in Public Water Supplies in the United States" Health Physics Vol. 48, No.5 May (1985).

[29] Junner, N.J.
"Gold in the Gold Coast"
Geological Survey Department, Ghana Memoir No.4 pp13-20 (1973).

[30] Stranden, E., Kolstad, A.K., and Lind, B.,
"Radon Exhalation, Moisture and Temperature Dependence"
Health Physics Vol 47, No. 3 Sept. (1984).

[31] Auxier, J.A., Christian, D.J., Jones, T.D., Kerr, G.D., Perdue, P.T., Shinpaugh, W.H., and Thorngate, J.H.,
"Contribution of Natural Terrestrial Sources to the Total Radiation Dose Man"
Oak Ridge National Laboratory, U.S.A. ORNL-TM-4323 Sept (1973).

[32] Asamoah, E.Y.,
"Radon Exhalation Rates of Gold Mine Gangue" (BSc. Project Report), Department of Physics, University of Science and Technology, Kumasi pp22 (1993).

[33] "The List of Code of Federal Regulation Sections Affected", Federal Register, Vol. 45, (69).
The Mine Safety and Health Administration (MSHA).
Department of Labour, Wash. D.C. (1980).

[34] Ghana Mining Regulation
Ministry of Mines and Energy, Ghana.
Legislative Instrument 665 , Part II Sect.142. pp53 (1970).

[35] Andam, A.A.B.,
Private Communication, (1991)

[36] Dixon, D.W., Miles, J.C.H., and Wrixon, A.D.,
"A Comparison of Method for Monitoring the Exposure of Miners to Radon Decay Products"
Proc. of the Int. Conf. on Occupational Radiation Safety in Mining, Toronto, Canada. (1984).

[37] Bartlett, D.T, Gilvin, P.J., Dixon, D.W., Miles, J.C.H.
"The NRPB Radon Personal Dosimetry Service",
J. Radiol. Prot. Vol. 8 (1) pp19-24 UK, (1988).

[38] Kusi-Appiah, G.,
"The Study of the Radon Exhalation Rates of Gold Mine Gangue" (B.Sc. Project Report),
Department of Physics, University of Science and Technology, Kumasi, (1992).

[39] Miles, J.C.H., and Dew, E.J.,

"A Passive Radon Gas Detectors for Use in Homes",

Proc. 11th Int. Conf., Solid State Nuclear Tracks

Detectors, Bristol and Supplement 3, Nuclear Tracks.

(Pergamon) Oxford. (1982).

[40] Miles, J.,

"The NRPB Radon Environmental Chamber and its Use in

International Comparisons",

Paper presented at the Workshop on Radon Monitoring in

Radioprotection, Environmental Radioactivity, and Earth

Science. ICTP, Trieste, Italy. (1989).

[41] International Commission on Radiological Protection

"Radiation Protection of Workers in Mines",

ICRP Publication 47 (Pergamon), Oxford, (1985).

[33] "The List of Code of Federal Regulation Sections Affected", Federal Register, Vol. 45, (69).

The Mine Safety and Health Administration (MSHA). Department of Labour, Wash. D.C. (1980).

[34] Ghana Mining Regulation

Ministry of Mines and Energy, Ghana.

Legislative Instrument 665 , Part II Sect.142. pp53 (1970).

[35] Andam, A.A.B.,

Private Communication, (1991)

[36] Dixon, D.W., Miles, J.C.H., and Wrixon, A.D.,

"A Comparison of Method for Monitoring the Exposure of Miners to Radon Decay Products"

Proc. of the Int. Conf. on Occupational Radiation Safety in Mining, Toronto, Canada. (1984).

[37] Bartlett, D.T, Gilvin, P.J., Dixon, D.W., Miles, J.C.H.

"The NRPB Radon Personal Dosimetry Service",

J. Radiol. Prot. Vol. 8 (1) pp19-24 UK, (1988).

[38] Kusi-Appiah, G.,

"The Study of the Radon Exhalation Rates of Gold Mine Gangue" (B.Sc. Project Report),

Department of Physics, University of Science and Technology, Kumasi, (1992).

[39] Miles, J.C.H., and Dew, E.J.,

"A Passive Radon Gas Detectors for Use in Homes",

Proc. 11th Int. Conf., Solid State Nuclear Tracks

Detectors, Bristol and Supplement 3, Nuclear Tracks.

(Pergamon) Oxford. (1982).

[40] Miles, J.,

"The NRPB Radon Environmental Chamber and its Use in

International Comparisons",

Paper presented at the Workshop on Radon Monitoring in

Radioprotection, Environmental Radioactivity, and Earth

Science. ICTP, Trieste, Italy. (1989).

[41] International Commission on Radiological Protection

"Radiation Protection of Workers in Mines",

ICRP Publication 47 (Pergamon), Oxford, (1985).